Table S1 Pearson correlation between $-\log_{10}(p)$ and |SS-H12| for uncorrected p-values (see *Materials and Methods*) assigned to genomic analysis windows across all 1000 Genome Project Auton *et al.* (2015) human study population pairs. All correlations are significant, yielding $p_{\text{Pearson}} < 2.2 \times 10^{-16}$.

Populations	|SS-H12|
CEU-GBR	0.9600019
CEU-GIH	0.9969635
CEU-JPT	0.9881075
CEU-YRI	0.9889807
LWK-YRI	0.9832174
GIH-YRI	0.9759596
JPT-YRI	0.9928664
JPT-GIH	0.9985984
JPT-KHV	0.9953857

Table S2 Mean |SS-H12| cutoffs for 1% false discovery rate (FDR) across `smc++`-derived neutral and sweep models for all empirical study population pairs. Cutoffs were determined from 10^6 neutral replicates and 1000 random resamples of 10^6 sweep replicates drawn from the simulations used to infer the most probable ν (see *Materials and Methods*). Also included are the standard deviation of cutoffs across the resamples, the proportion of genic analysis windows exceeding the cutoff, and the proportion of non-genic windows exceeding the cutoff (both proportions computed after filtering steps).

Populations	1% FDR cutoff	Standard deviation	Genic exceeding	Non-genic exceeding
CEU-GBR	0.38960	2.339×10^{-4}	6.637×10^{-4}	7.991×10^{-5}
CEU-GIH	0.09769	3.413×10^{-5}	3.173×10^{-2}	1.736×10^{-2}
CEU-JPT	0.07526	2.398×10^{-5}	2.872×10^{-2}	1.652×10^{-2}
CEU-YRI	0.12570	2.409×10^{-5}	3.409×10^{-3}	2.091×10^{-3}
LWK-YRI	0.05320	6.952×10^{-6}	1.775×10^{-1}	1.299×10^{-1}
GIH-YRI	0.10540	1.798×10^{-5}	6.756×10^{-3}	4.096×10^{-3}
JPT-YRI	0.08830	2.556×10^{-5}	1.160×10^{-2}	7.900×10^{-3}
JPT-GIH	0.05543	2.663×10^{-5}	7.739×10^{-2}	4.997×10^{-2}
JPT-KHV	0.20650	1.259×10^{-4}	1.536×10^{-2}	7.395×10^{-3}

Table S3 Spearman correlation (ρ) between maximum |SS-H12| and local recombination rate across all studied genes for 1000 Genomes Project (Auton *et al.* 2015) sampled population pairs.

Populations	Spearman's ρ	p-value
CEU-GBR	-0.6193003	$< 2.2 \times 10^{-16}$
CEU-GIH	-0.5737725	$< 2.2 \times 10^{-16}$
CEU-JPT	-0.4968813	$< 2.2 \times 10^{-16}$
CEU-YRI	-0.4025128	$< 2.2 \times 10^{-16}$
LWK-YRI	-0.5875197	$< 2.2 \times 10^{-16}$
GIH-YRI	-0.397393	$< 2.2 \times 10^{-16}$
JPT-YRI	-0.4113872	$< 2.2 \times 10^{-16}$
JPT-GIH	-0.5135683	$< 2.2 \times 10^{-16}$
JPT-KHV	-0.6124639	$< 2.2 \times 10^{-16}$

Table S4 Top 40 SS-H12 sweep candidates at RNA- and protein-coding genes shared between the Central and Western European CEU and GBR populations. Candidates presented are those that remained after application of a mappability and alignability filter to data (see *Materials and Methods*). Target genes that pass the significance threshold are colored in gold in the "*P*-value" column. Genes whose sweeps are assigned as hard ($\nu = 1$) are shaded in red in the "Inferred ν" column, while soft sweeps ($\nu \geq 2$) are colored in blue.

	Top gene	Chromosome	Maximum SS−H12	H2tot/H1tot	*P*−value	Inferred ν
1	*ZRANB3*	2	0.6138516	0.005253369	4.88×10^{-8}	1
2	*SLC12A1*	15	0.5964931	0.007102656	8.10×10^{-8}	1
3	*R3HDM1*	2	0.5907587	0.005776011	9.58×10^{-8}	1
4	*DARS*	2	0.5605804	0.012398870	2.30×10^{-7}	1
5	*MCM6*	2	0.5604343	0.010608920	2.31×10^{-7}	1
6	*LCT*	2	0.5097962	0.009314534	1.01×10^{-6}	1
7	*LOC100507600*	2	0.5097962	0.009314534	1.01×10^{-6}	1
8	*AC093391.2*	2	0.4822492	0.008069683	2.23×10^{-6}	1
9	*RAB3GAP1*	2	0.4788360	0.016863240	2.46×10^{-6}	1
10	*UBXN4*	2	0.4709547	0.008006012	3.09×10^{-6}	1
11	*BCAS3*	17	0.4342505	0.024135620	8.91×10^{-6}	1
12	*KAT6B*	10	0.4063248	0.010954180	1.99×10^{-5}	1
13	*PPM1D*	17	0.4043315	0.013758900	2.10×10^{-5}	1
14	*MYO9A*	15	0.3919436	0.014969490	3.00×10^{-5}	1
15	*FAM149B1*	10	0.3841613	0.013332280	3.7×10^{-5}	1
16	*ZNF546*	19	0.3824392	0.053683500	3.94×10^{-5}	1
17	*MAP3K19*	2	0.3807448	0.175652800	4.13×10^{-5}	3
18	*PRMT9*	4	0.3782229	0.030300370	4.44×10^{-5}	1
19	*KITLG*	12	0.3772852	0.023892210	4.56×10^{-5}	1
20	*MLLT3*	9	0.3756959	0.085799300	4.78×10^{-5}	1
21	*LAMA3*	18	0.3749289	0.327190100	4.88×10^{-5}	3
22	*TMEM116*	12	0.3716065	0.023778920	5.37×10^{-5}	1
23	*KMT2A*	11	0.3684665	0.034335420	5.87×10^{-5}	1
24	*ADRBK2*	22	0.3648397	0.029916410	6.51×10^{-5}	1
25	*ACMSD*	2	0.3628647	0.058329770	6.89×10^{-5}	1
26	*CCNT2−AS1*	2	0.3628647	0.058329770	6.89×10^{-5}	1
27	*PLAGL2*	20	0.3588937	0.315722400	7.71×10^{-5}	3
28	*DIRC3*	2	0.3560424	0.021817340	8.36×10^{-5}	1
29	*POLN*	4	0.3534160	0.101220900	9.01×10^{-5}	1
30	*AC005592.1*	5	0.3518146	0.018718710	9.43×10^{-5}	1
31	*PRKDC*	8	0.3491810	0.262222100	1.02×10^{-4}	4
32	*BVES−AS1*	6	0.3486739	0.277810700	1.03×10^{-4}	4
33	*PVRL3−AS1*	3	0.3470860	0.045461390	1.08×10^{-4}	1
34	*ECD*	10	0.3464802	0.201522500	1.10×10^{-4}	3
35	*CLK3*	15	0.3446577	0.022635880	1.16×10^{-4}	1
36	*C4orf22*	4	0.3430783	0.034845850	1.21×10^{-4}	1
37	*EPN2*	17	0.3405261	0.099649860	1.30×10^{-4}	1
38	*NR6A1*	9	0.3385413	0.412935900	1.38×10^{-4}	4
39	*CUX2*	12	0.3370432	0.466497500	1.44×10^{-4}	4
40	*MIR548O2*	8	0.3367965	0.120149300	1.45×10^{-4}	1

Table S5 Top 40 SS-H12 sweep candidates at RNA- and protein-coding genes shared between the Western European CEU and South Asian GIH populations. Candidates presented are those that remained after application of a mappability and alignability filter to data (see *Materials and Methods*). Target genes that pass the significance threshold are colored in gold in the "*P*-value" column. Genes whose sweeps are assigned as hard ($\nu = 1$) are shaded in red in the "Inferred ν" column, while soft sweeps ($\nu \geq 2$) are colored in blue.

	Top gene	Chromosome	Maximum SS−H12	H2tot/H1tot	*P*−value	Inferred ν
1	*SLC12A1*	15	0.4687775	0.01928730	2.40×10^{-8}	1
2	*PRMT9*	4	0.3592987	0.02846361	1.29×10^{-6}	1
3	*ZNF546*	19	0.3543484	0.01440592	1.54×10^{-6}	1
4	*RNU6−28P*	15	0.3328967	0.14154430	3.37×10^{-6}	2
5	*PPIP5K1*	15	0.3328967	0.14154430	3.37×10^{-6}	2
6	*CUX2*	12	0.3244117	0.01913100	4.59×10^{-6}	1
7	*RUNX1T1*	8	0.3239634	0.02660100	4.67×10^{-6}	1
8	*HDAC1*	1	0.3000066	0.02793417	1.12×10^{-5}	1
9	*KIAA0947*	5	0.2985386	0.09924729	1.18×10^{-5}	1
10	*LINC00478*	21	0.2978392	0.03430060	1.21×10^{-5}	1
11	*P4HA1*	10	0.2940247	0.02457430	1.39×10^{-5}	1
12	*BCAS3*	17	0.2928297	0.01725947	1.46×10^{-5}	1
13	*HS2ST1*	1	0.2925146	0.02843537	1.47×10^{-5}	1
14	*USP37*	2	0.2841170	0.26690330	2.00×10^{-5}	2
15	*EXOC6B*	2	0.2839310	0.03022084	2.02×10^{-5}	1
16	*TRMT11*	6	0.2823063	0.09785459	2.14×10^{-5}	1
17	*MYO9A*	15	0.2807536	0.02811068	2.27×10^{-5}	1
18	*TFAP2E*	1	0.2788397	0.19573280	2.43×10^{-5}	2
19	*PPM1D*	17	0.2780563	0.01891077	2.50×10^{-5}	1
20	*METTL25*	12	0.2774661	0.02117459	2.56×10^{-5}	1
21	*CCDC178*	18	0.2756744	0.08725221	2.73×10^{-5}	1
22	*USP25*	21	0.2754877	0.01694058	2.75×10^{-5}	1
23	*KIAA0825*	5	0.2741257	0.04268183	2.89×10^{-5}	1
24	*CELSR3*	3	0.2722865	0.04291467	3.09×10^{-5}	1
25	*LOC100188947*	10	0.2716363	0.03509440	3.16×10^{-5}	1
26	*HECTD2*	10	0.2716363	0.03509440	3.16×10^{-5}	1
27	*GNA14*	9	0.2715994	0.03925893	3.17×10^{-5}	1
28	*DNAH6*	2	0.2696911	0.02045324	3.40×10^{-5}	1
29	*FBN1*	15	0.2693902	0.04027675	3.44×10^{-5}	1
30	*LYRM7*	5	0.2668650	0.04480839	3.77×10^{-5}	1
31	*KCNQ5*	6	0.2646294	0.01399575	4.09×10^{-5}	1
32	*OSBPL9*	1	0.2636045	0.04380993	4.25×10^{-5}	1
33	*OTUD6B*	8	0.2635197	0.16525760	4.26×10^{-5}	2
34	*C8orf44−SGK3*	8	0.2629975	0.02040620	4.34×10^{-5}	1
35	*SGK3*	8	0.2629975	0.02040620	4.34×10^{-5}	1
36	*FAM69A*	1	0.2622265	0.06324476	4.47×10^{-5}	1
37	*UNC5D*	8	0.2610994	0.03623753	4.65×10^{-5}	1
38	*KITLG*	12	0.2607259	0.05006524	4.72×10^{-5}	1
39	*PSMB2*	1	0.2596058	0.02267442	4.92×10^{-5}	1
40	*MAP2K5*	15	0.2586188	0.33523410	5.10×10^{-5}	2

Table S6 Top 40 SS-H12 sweep candidates at RNA- and protein-coding genes shared between the Western European CEU and East Asian JPT populations. Candidates presented are those that remained after application of a mappability and alignability filter to data (see *Materials and Methods*). Target genes that pass the significance threshold are colored in gold in the "*P*-value" column. Genes whose sweeps are assigned as hard ($\nu = 1$) are shaded in red in the "Inferred ν" column, while soft sweeps ($\nu \geq 2$) are colored in blue.

	Top gene	Chromosome	Maximum SS−H12	H2tot/H1tot	*P*−value	Inferred ν
1	*SPIDR*	8	0.4841559	0.13789160	3.49×10^{-11}	2
2	*MRAP2*	6	0.3577093	0.05691596	1.68×10^{-8}	1
3	*BVES−AS1*	6	0.3550710	0.35553100	1.91×10^{-8}	2
4	*BCAS3*	17	0.3003483	0.01124741	2.78×10^{-7}	1
5	*RUNX1T1*	8	0.2911443	0.01286325	4.37×10^{-7}	1
6	*DIRC3*	2	0.2846624	0.02342707	6.00×10^{-7}	1
7	*LINC00478*	21	0.2845995	0.04674953	6.02×10^{-7}	1
8	*CASC4*	15	0.2817489	0.28631390	6.92×10^{-7}	2
9	*ZNF546*	19	0.2775094	0.01187426	8.52×10^{-7}	1
10	*C16orf70*	16	0.2759704	0.15519460	9.19×10^{-7}	2
11	*CUX2*	12	0.2711322	0.07265968	1.17×10^{-6}	1
12	*C4orf22*	4	0.2676980	0.04613398	1.38×10^{-6}	1
13	*HDAC1*	1	0.2613163	0.01923077	1.89×10^{-6}	1
14	*EXOC6B*	2	0.2550717	0.02907524	2.56×10^{-6}	1
15	*NCAPG*	4	0.2540412	0.47979580	2.70×10^{-6}	3
16	*DENND1A*	9	0.2502850	0.03534972	3.24×10^{-6}	1
17	*LRRC29*	16	0.2498870	0.01559488	3.31×10^{-6}	1
18	*ZNF780B*	19	0.2453862	0.01894595	4.12×10^{-6}	1
19	*C12orf4*	12	0.2413896	0.05908229	5.02×10^{-6}	1
20	*MRPS11*	15	0.2379901	0.04262436	5.93×10^{-6}	1
21	*USP25*	21	0.2354323	0.03030037	6.72×10^{-6}	1
22	*EPB41L1*	20	0.2351457	0.05879280	6.82×10^{-6}	1
23	*LCORL*	4	0.2345143	0.49844510	7.03×10^{-6}	3
24	*NR6A1*	9	0.2344024	0.41874140	7.07×10^{-6}	3
25	*FOXP2*	7	0.2320563	0.06177330	7.94×10^{-6}	1
26	*PRKDC*	8	0.2316219	0.02158066	8.11×10^{-6}	1
27	*CELSR3*	3	0.2282892	0.03061224	9.55×10^{-6}	1
28	*C2CD5*	12	−0.2282773	0.40252750	9.56×10^{-6}	1
29	*LOC100130987*	11	0.2266829	0.03103294	1.03×10^{-5}	1
30	*EPS8*	12	0.2262990	0.03675885	1.05×10^{-5}	1
31	*C5orf42*	5	0.2258946	0.23871430	1.07×10^{-5}	2
32	*SGCD*	5	0.2248583	0.04520540	1.13×10^{-5}	1
33	*PHF20*	20	0.2247397	0.03888761	1.14×10^{-5}	1
34	*KIAA1324L*	7	0.2246612	0.05278810	1.14×10^{-5}	1
35	*SPIN1*	9	0.2244122	0.02988283	1.16×10^{-5}	1
36	*KCND2*	7	0.2238942	0.03960568	1.19×10^{-5}	1
37	*DNAH6*	2	0.2228843	0.04768519	1.25×10^{-5}	1
38	*CCBL2*	1	0.2220159	0.38969610	1.30×10^{-5}	2
39	*DBT*	1	0.2211143	0.02032617	1.36×10^{-5}	1
40	*CLCF1*	11	0.2209926	0.03304531	1.37×10^{-5}	1

Table S7 Top 40 SS-H12 sweep candidates at RNA- and protein-coding genes shared between the Central European CEU and West African YRI populations. Candidates presented are those that remained after application of a mappability and alignability filter to data (see *Materials and Methods*). Target genes that pass the significance threshold are colored in gold in the "*P*-value" column. Genes whose sweeps are assigned as hard ($\nu = 1$) are shaded in red in the "Inferred ν" column, while soft sweeps ($\nu \geq 2$) are colored in blue.

	Top gene	Chromosome	Maximum SS−H12	H2tot/H1tot	*P*−value	Inferred ν
1	*RP11−554F20.1*	9	0.404033	0.011758	7.98×10^{-11}	1
2	*SPRED3*	19	0.349570	0.008281	2.01×10^{-9}	1
3	*CASC4*	15	0.344882	0.018257	2.65×10^{-9}	1
4	*KIAA0825*	5	0.344536	0.023952	2.71×10^{-9}	1
5	*ERLIN2*	8	0.331350	0.020023	5.91×10^{-9}	1
6	*DEDD*	1	0.326073	0.060158	8.07×10^{-9}	1
7	*PHKB*	16	0.323691	0.034042	9.29×10^{-9}	1
8	*CPNE1*	20	0.317672	0.029957	1.33×10^{-8}	1
9	*NNT*	5	0.317165	0.017918	1.37×10^{-8}	1
10	*ATP6V1A*	3	0.313268	0.142126	1.72×10^{-8}	2
11	*DDHD2*	8	0.308964	0.058368	2.22×10^{-8}	1
12	*GLRX2*	1	0.305354	0.233674	2.74×10^{-8}	3
13	*DANCR*	4	0.303997	0.040780	2.97×10^{-8}	1
14	*PIGV*	1	0.303657	0.025363	3.03×10^{-8}	1
15	*USP46*	4	0.299556	0.079339	3.86×10^{-8}	1
16	*RALGAPA2*	20	0.299108	0.025898	3.97×10^{-8}	1
17	*GRIK5*	19	0.298155	0.029954	4.20×10^{-8}	1
18	*PLEKHA8*	7	0.297591	0.086840	4.34×10^{-8}	1
19	*MIR548H3*	6	0.296110	0.037196	4.73×10^{-8}	1
20	*PAWR*	12	−0.290466	0.440909	6.60×10^{-8}	3
21	*ENTHD1*	22	0.288627	0.085943	7.36×10^{-8}	1
22	*GRIA2*	4	0.284654	0.121846	9.30×10^{-8}	1
23	*DKK2*	4	0.282323	0.022480	1.07×10^{-7}	1
24	*C2orf69*	2	0.279331	0.144744	1.27×10^{-7}	1
25	*ATF2*	2	0.272288	0.046900	1.93×10^{-7}	1
26	*PPAPDC1B*	8	0.271310	0.048928	2.04×10^{-7}	1
27	*CNNM2*	10	0.269927	0.042493	2.22×10^{-7}	1
28	*KIAA1244*	6	0.259040	0.023619	4.21×10^{-7}	1
29	*GABRA4*	4	0.258726	0.254621	4.28×10^{-7}	3
30	*SLC4A10*	2	0.258345	0.033468	4.38×10^{-7}	1
31	*TGFBR1*	9	0.258316	0.097025	4.39×10^{-7}	1
32	*CDK6*	7	0.258091	0.019577	4.45×10^{-7}	1
33	*PHF20*	20	0.256049	0.024958	5.02×10^{-7}	1
34	*SEMA3C*	7	0.249090	0.038386	7.55×10^{-7}	1
35	*SPG11*	15	0.247412	0.038899	8.33×10^{-7}	1
36	*EXOC4*	7	0.246085	0.068343	9.01×10^{-7}	1
37	*ABHD17B*	9	0.244367	0.067034	9.97×10^{-7}	1
38	*SYT1*	12	0.242758	0.071155	1.10×10^{-6}	1
39	*ITFG1*	16	0.241579	0.064650	1.17×10^{-6}	1
40	*WHSC1L1*	8	0.241159	0.091198	1.20×10^{-6}	1

Table S8 Top 40 SS-H12 sweep candidates at RNA- and protein-coding genes shared between the East African LWK and West African YRI populations. Candidates presented are those that remained after application of a mappability and alignability filter to data (see *Materials and Methods*). Target genes that pass the significance threshold are colored in gold in the "*P*-value" column. Genes whose sweeps are assigned as hard ($\nu = 1$) are shaded in red in the "Inferred ν" column, while soft sweeps ($\nu \geq 2$) are colored in blue.

	Top gene	Chromosome	Maximum SS−H12	H2tot/H1tot	*P*−value	Inferred ν
1	*GRIK5*	19	0.4257102	0.04258992	4.70×10^{-6}	1
2	*RGS18*	1	0.3987118	0.05121985	9.70×10^{-6}	1
3	*RP11−554F20.1*	9	0.3888096	0.03007582	1.27×10^{-5}	1
4	*SPIDR*	8	0.3877237	0.47505840	1.30×10^{-5}	2
5	*KIAA0825*	5	0.3792208	0.06521739	1.64×10^{-5}	1
6	*ARID1A*	1	0.3696765	0.05678665	2.12×10^{-5}	1
7	*PPAPDC1B*	8	0.3677224	0.02213772	2.23×10^{-5}	1
8	*MIR548AE2*	16	0.3602984	0.01837085	2.72×10^{-5}	1
9	*LONP2*	16	0.3602984	0.01837085	2.72×10^{-5}	1
10	*NNT*	5	0.3578539	0.01703393	2.91×10^{-5}	1
11	*ATF2*	2	0.3566302	0.10607440	3.01×10^{-5}	1
12	*CASC4*	15	0.3498801	0.02336532	3.61×10^{-5}	1
13	*PIGV*	1	0.3469070	0.01980346	3.91×10^{-5}	1
14	*BRIP1*	17	0.3454437	0.05989424	4.07×10^{-5}	1
15	*FLJ46284*	8	0.3335889	0.34581390	5.60×10^{-5}	2
16	*FER1L6*	8	0.3319929	0.36210560	5.84×10^{-5}	2
17	*FER1L6−AS1*	8	0.3319929	0.36210560	5.84×10^{-5}	2
18	*PSMD14*	2	0.3302383	0.21238350	6.13×10^{-5}	2
19	*EHBP1*	2	0.3301406	0.04231345	6.14×10^{-5}	1
20	*SYT1*	12	0.3268402	0.02131281	6.72×10^{-5}	1
21	*MAGI3*	1	0.3234881	0.03887382	7.35×10^{-5}	1
22	*DDHD2*	8	0.3230242	0.03319609	7.45×10^{-5}	1
23	*TCF4*	18	0.3221087	0.04095041	7.63×10^{-5}	1
24	*FGFR1*	8	0.3219437	0.11190390	7.67×10^{-5}	1
25	*DANCR*	4	0.3217441	0.02757380	7.71×10^{-5}	1
26	*DDX19B*	16	0.3201310	0.05961249	8.05×10^{-5}	1
27	*PHKB*	16	0.3199744	0.14290570	8.09×10^{-5}	2
28	*RRN3P3*	16	0.3192156	0.12601100	8.26×10^{-5}	2
29	*ANK3*	10	0.3168877	0.41411630	8.79×10^{-5}	2
30	*CNNM2*	10	0.3157693	0.04354118	9.06×10^{-5}	1
31	*DKK2*	4	0.3148797	0.02507450	9.28×10^{-5}	1
32	*UCHL5*	1	0.3148279	0.23817200	9.30×10^{-5}	2
33	*GRIA4*	11	0.3093281	0.06513791	1.08×10^{-4}	1
34	*HEMGN*	9	0.3087151	0.03213826	1.10×10^{-4}	1
35	*RNLS*	10	0.3086794	0.05394666	1.10×10^{-4}	1
36	*TMC1*	9	0.3059124	0.05989460	1.18×10^{-4}	1
37	*FAM172A*	5	0.3046091	0.36377590	1.23×10^{-4}	2
38	*NANS*	9	0.3022555	0.14421540	1.31×10^{-4}	2
39	*SPRED3*	19	0.3006544	0.01691324	1.36×10^{-4}	1
40	*CCDC178*	18	0.3005286	0.06074190	1.37×10^{-4}	1

Table S9 Top 40 SS-H12 sweep candidates at RNA- and protein-coding genes shared between the South Asian GIH and West African YRI populations. Candidates presented are those that remained after application of a mappability and alignability filter to data (see *Materials and Methods*). Target genes that pass the significance threshold are colored in gold in the "*P*-value" column. Genes whose sweeps are assigned as hard ($\nu = 1$) are shaded in red in the "Inferred ν" column, while soft sweeps ($\nu \geq 2$) are colored in blue.

	Top gene	Chromosome	Maximum SS−H12	H2tot/H1tot	*P*−value	Inferred ν
1	*RP11−554F20.1*	9	0.3771248	0.011770770	5.11×10^{-10}	1
2	*ATP6V1A*	3	0.3639640	0.099682930	1.10×10^{-9}	1
3	*DDHD2*	8	0.3602952	0.013720550	1.36×10^{-9}	1
4	*CDK6*	7	0.3578316	0.071008260	1.57×10^{-9}	1
5	*KIAA0825*	5	0.3525741	0.027694560	2.13×10^{-9}	1
6	*SYT1*	12	0.3492609	0.012266520	2.58×10^{-9}	1
7	*PSMD14*	2	0.3412286	0.135670300	4.12×10^{-9}	1
8	*WHSC1L1*	8	0.3283306	0.043503220	8.70×10^{-9}	1
9	*PHKB*	16	0.3232317	0.042223410	1.17×10^{-8}	1
10	*NNT*	5	0.3223767	0.017984340	1.23×10^{-8}	1
11	*PPAPDC1B*	8	0.3196440	0.032132440	1.44×10^{-8}	1
12	*FBXW4*	10	0.3196397	0.031138790	1.44×10^{-8}	1
13	*CASC4*	15	0.3150844	0.009182066	1.88×10^{-8}	1
14	*PLEKHA8*	7	0.3142622	0.083226860	1.97×10^{-8}	1
15	*PIGV*	1	0.3115851	0.031716870	2.30×10^{-8}	1
16	*ZNF451*	6	0.3085450	0.029623300	2.74×10^{-8}	1
17	*MIR548AE2*	16	0.3065668	0.025105820	3.08×10^{-8}	1
18	*LONP2*	16	0.3065668	0.025105820	3.08×10^{-8}	1
19	*SLC4A10*	2	0.3062220	0.024992630	3.14×10^{-8}	1
20	*DEDD*	1	0.2978007	0.043610860	5.11×10^{-8}	1
21	*USP46*	4	0.2930645	0.043401900	6.73×10^{-8}	1
22	*ATF2*	2	0.2890980	0.042325940	8.47×10^{-8}	1
23	*C10orf76*	10	0.2791604	0.241891000	1.51×10^{-7}	2
24	*GRIK5*	19	0.2789334	0.026200520	1.53×10^{-7}	1
25	*FRYL*	4	0.2770178	0.124549800	1.70×10^{-7}	1
26	*ABHD17B*	9	0.2761729	0.019974820	1.79×10^{-7}	1
27	*CPNE1*	20	0.2749730	0.053890870	1.92×10^{-7}	1
28	*RALGAPA2*	20	0.2742919	0.031716870	2.00×10^{-7}	1
29	*COL7A1*	3	0.2710832	0.030527860	2.40×10^{-7}	1
30	*PAWR*	12	−0.2695280	0.500033000	2.63×10^{-7}	5
31	*ERLIN2*	8	0.2694367	0.032420110	2.64×10^{-7}	1
32	*TYW5*	2	0.2662606	0.079070670	3.18×10^{-7}	1
33	*KCNIP2*	10	0.2654300	0.188650300	3.33×10^{-7}	2
34	*ENTHD1*	22	0.2648954	0.059516600	3.44×10^{-7}	1
35	*CADM1*	11	0.2608986	0.130764100	4.33×10^{-7}	1
36	*NIT1*	1	0.2589696	0.060503570	4.85×10^{-7}	1
37	*GRIA4*	11	0.2580788	0.177060200	5.10×10^{-7}	2
38	*CAMK2G*	10	0.2552114	0.145238500	6.02×10^{-7}	1
39	*DANCR*	4	0.2530703	0.034185400	6.82×10^{-7}	1
40	*PLBD2*	12	0.2530187	0.025798690	6.84×10^{-7}	1

Table S10 Top 40 SS-H12 sweep candidates at RNA- and protein-coding genes shared between the East Asian JPT and West African YRI populations. Candidates presented are those that remained after application of a mappability and alignability filter to data (see *Materials and Methods*). Target genes that pass the significance threshold are colored in gold in the "*P*-value" column. Genes whose sweeps are assigned as hard ($\nu = 1$) are shaded in red in the "Inferred ν" column, while soft sweeps ($\nu \geq 2$) are colored in blue.

	Top gene	Chromosome	Maximum SS−H12	H2tot/H1tot	*P*−value	Inferred ν
1	*RP11−554F20.1*	9	0.3931760	0.106986500	9.35×10^{-10}	1
2	*HEMGN*	9	0.3775289	0.024845670	2.14×10^{-9}	1
3	*ATP6V1A*	3	0.3612693	0.187013600	5.08×10^{-9}	2
4	*PSMD14*	2	0.3478155	0.120552700	1.04×10^{-8}	1
5	*KIAA0825*	5	0.3462541	0.042399750	1.13×10^{-8}	1
6	*ENTHD1*	22	0.3457729	0.024417590	1.15×10^{-8}	1
7	*UCHL5*	1	0.3410178	0.296451800	1.49×10^{-8}	3
8	*EHBP1*	2	0.3296022	0.040707210	2.72×10^{-8}	1
9	*DDHD2*	8	0.3232796	0.047658110	3.81×10^{-8}	1
10	*GRIK5*	19	0.3201569	0.022160500	4.49×10^{-8}	1
11	*CPNE1*	20	0.3095707	0.020447800	7.87×10^{-8}	1
12	*CASC4*	15	0.3082424	0.008452639	8.45×10^{-8}	1
13	*PIGV*	1	0.3080457	0.019652480	8.54×10^{-8}	1
14	*GRIA4*	11	0.2877642	0.076983380	2.50×10^{-7}	1
15	*FBXW4*	10	0.2812126	0.032817680	3.54×10^{-7}	1
16	*USP46*	4	0.2778346	0.050033190	4.23×10^{-7}	1
17	*PPAPDC1B*	8	0.2770218	0.067697790	4.42×10^{-7}	1
18	*CSMD3*	8	0.2767410	0.025265590	4.49×10^{-7}	1
19	*AUTS2*	7	0.2739576	0.048349210	5.20×10^{-7}	1
20	*WDPCP*	2	0.2732119	0.160070400	5.41×10^{-7}	2
21	*NNT*	5	0.2719657	0.011428060	5.78×10^{-7}	1
22	*WDR75*	2	0.2713068	0.477669300	5.98×10^{-7}	3
23	*MAST2*	1	0.2710749	0.113317100	6.06×10^{-7}	1
24	*MPHOSPH9*	12	−0.2671972	0.500226700	7.44×10^{-7}	3
25	*ATF2*	2	0.2661096	0.050953780	7.88×10^{-7}	1
26	*MIR548H3*	6	0.2657886	0.044716950	8.02×10^{-7}	1
27	*DKK2*	4	0.2654977	0.020832640	8.14×10^{-7}	1
28	*RALGAPA2*	20	0.2634601	0.018345170	9.07×10^{-7}	1
29	*PLEKHA8*	7	0.2629720	0.065646650	9.31×10^{-7}	1
30	*ABCA17P*	16	0.2627850	0.029987580	9.40×10^{-7}	1
31	*ERLIN2*	8	0.2612417	0.051206410	1.02×10^{-6}	1
32	*LOC644554*	19	0.2599085	0.046211070	1.09×10^{-6}	1
33	*EXOC6B*	2	−0.2591453	0.400289300	1.14×10^{-6}	3
34	*ARID1A*	1	0.2586148	0.012315850	1.17×10^{-6}	1
35	*AC016582.2*	19	0.2575930	0.184115400	1.24×10^{-6}	2
36	*USP31*	16	0.2542219	0.048774290	1.48×10^{-6}	1
37	*WDR87*	19	0.2539212	0.052847190	1.50×10^{-6}	1
38	*NCK1*	3	0.2533815	0.105668600	1.55×10^{-6}	1
39	*MIR548AE2*	16	0.2530337	0.012070400	1.58×10^{-6}	1
40	*LONP2*	16	0.2530337	0.012070400	1.58×10^{-6}	1

Table S11 Top 40 SS-H12 sweep candidates at RNA- and protein-coding genes shared between the East Asian JPT and South Asian GIH populations. Candidates presented are those that remained after application of a mappability and alignability filter to data (see *Materials and Methods*). Target genes that pass the significance threshold are colored in gold in the "*P*-value" column. Genes whose sweeps are assigned as hard ($\nu = 1$) are shaded in red in the "Inferred ν" column, while soft sweeps ($\nu \geq 2$) are colored in blue.

	Top gene	Chromosome	Maximum SS−H12	H2tot/H1tot	*P*−value	Inferred ν
1	*RUNX1T1*	8	0.4474761	0.013112090	8.89×10^{-9}	1
2	*P4HTM*	3	0.4140126	0.004079071	3.36×10^{-8}	1
3	*TMTC2*	12	0.3420391	0.025676240	5.92×10^{-7}	1
4	*EXOC6B*	2	0.3326926	0.019515560	8.60×10^{-7}	1
5	*RNF121*	11	0.3155150	0.030228890	1.71×10^{-6}	1
6	*BCAS3*	17	0.3120734	0.020570740	1.96×10^{-6}	1
7	*HELZ*	17	0.3098360	0.111157800	2.15×10^{-6}	1
8	*ADAMTS6*	5	0.3076773	0.407162800	2.34×10^{-6}	3
9	*ORC2*	2	0.3055687	0.018545290	2.55×10^{-6}	1
10	*CUX2*	12	0.3012879	0.114718000	3.02×10^{-6}	1
11	*APPBP2*	17	0.2943597	0.018755230	3.99×10^{-6}	1
12	*ZNF546*	19	0.2903935	0.026486970	4.67×10^{-6}	1
13	*RP11−682N22.1*	7	0.2866539	0.025520560	5.43×10^{-6}	1
14	*LINC00478*	21	0.2768036	0.051422320	8.06×10^{-6}	1
15	*DBT*	1	0.2754919	0.019618240	8.50×10^{-6}	1
16	*SLC44A1*	9	0.2751889	0.027447370	8.60×10^{-6}	1
17	*DPH5*	1	0.2734798	0.063964150	9.21×10^{-6}	1
18	*MBOAT2*	2	0.2732935	0.022872390	9.28×10^{-6}	1
19	*DR1*	1	0.2719058	0.117944900	9.81×10^{-6}	1
20	*ZNF780B*	19	0.2710979	0.027775370	1.01×10^{-5}	1
21	*PRPF40B*	12	0.2704860	0.009056569	1.04×10^{-5}	1
22	*LOC100188947*	10	0.2693331	0.091476680	1.09×10^{-5}	1
23	*HECTD2*	10	0.2693331	0.091476680	1.09×10^{-5}	1
24	*USP32*	17	0.2668435	0.030825700	1.20×10^{-5}	1
25	*NF1*	17	0.2650127	0.446732600	1.29×10^{-5}	2
26	*RP11−53O19.1*	5	0.2645393	0.266671000	1.32×10^{-5}	2
27	*HDAC1*	1	0.2631774	0.038364270	1.39×10^{-5}	1
28	*ABCB1*	7	0.2624699	0.032952010	1.43×10^{-5}	1
29	*RUNDC3B*	7	0.2624699	0.032952010	1.43×10^{-5}	1
30	*ADK*	10	0.2592457	0.395106900	1.63×10^{-5}	2
31	*CNNM4*	2	0.2583070	0.084782740	1.69×10^{-5}	1
32	*DDB1*	11	0.2571627	0.012680740	1.77×10^{-5}	1
33	*XXYLT1*	3	0.2563662	0.022777440	1.83×10^{-5}	1
34	*COMMD3−BMI1*	10	0.2549803	0.029266380	1.94×10^{-5}	1
35	*BMI1*	10	0.2549803	0.029266380	1.94×10^{-5}	1
36	*PRKAR2A*	3	0.2543194	0.029957870	1.99×10^{-5}	1
37	*USP25*	21	0.2500539	0.039729580	2.36×10^{-5}	1
38	*ATP6V0D1*	16	0.2497646	0.015632540	2.39×10^{-5}	1
39	*GPC5*	13	0.2484834	0.088347000	2.52×10^{-5}	1
40	*SPATA31D3*	9	0.2473412	0.031572110	2.63×10^{-5}	1

Table S12 Top 40 SS-H12 sweep candidates at RNA- and protein-coding genes shared between the East Asian JPT and Southeast Asian KHV populations. Candidates presented are those that remained after application of a mappability and alignability filter to data (see *Materials and Methods*). Target genes that pass the significance threshold are colored in gold in the "*P*-value" column. Genes whose sweeps are assigned as hard ($\nu = 1$) are shaded in red in the "Inferred ν" column, while soft sweeps ($\nu \geq 2$) are colored in blue.

	Top gene	Chromosome	Maximum SS−H12	H2tot/H1tot	*P*−value	Inferred ν
1	*EXOC6B*	2	0.5264721	0.006772899	1.52×10^{-5}	1
2	*SPAG6*	10	0.4968819	0.006607293	2.78×10^{-5}	1
3	*P4HTM*	3	0.4842239	0.003800968	3.60×10^{-5}	1
4	*RUNX1T1*	8	0.4762151	0.012305660	4.24×10^{-5}	1
5	*C11orf49*	11	0.4727695	0.068502980	4.55×10^{-5}	1
6	*RP11−696N14.1*	4	0.4622633	0.047157540	5.64×10^{-5}	1
7	*EXD2*	14	0.4488191	0.012119380	7.42×10^{-5}	1
8	*BCL2L1*	20	0.4334603	0.011505080	1.02×10^{-4}	1
9	*SPIDR*	8	0.4323823	0.121947000	1.04×10^{-4}	2
10	*TMEM33*	4	0.4163834	0.013441980	1.44×10^{-4}	1
11	*HMCN1*	1	0.4139426	0.433746300	1.52×10^{-4}	2
12	*TRMT11*	6	0.4132626	0.008565410	1.54×10^{-4}	1
13	*CSPP1*	8	0.4131015	0.370451200	1.54×10^{-4}	2
14	*BCL7C*	16	0.4116698	0.017374970	1.59×10^{-4}	1
15	*AMBRA1*	11	0.4078245	0.026064920	1.72×10^{-4}	1
16	*ADH1A*	4	0.4068527	0.054411550	1.75×10^{-4}	1
17	*LINC00536*	8	0.4047586	0.319893200	1.83×10^{-4}	2
18	*TRUB1*	10	0.3960872	0.012888670	2.19×10^{-4}	1
19	*SLC25A20*	3	0.3951800	0.306872500	2.23×10^{-4}	2
20	*NOVA1*	14	0.3937128	0.296372000	2.30×10^{-4}	2
21	*UBE3A*	15	0.3881960	0.421256400	2.57×10^{-4}	2
22	*RAD51B*	14	0.3877928	0.020655190	2.60×10^{-4}	1
23	*C2orf66*	2	0.3847481	0.011183300	2.76×10^{-4}	1
24	*ARIH2*	3	0.3835818	0.011305710	2.83×10^{-4}	1
25	*FBXO4*	5	0.3830810	0.060543860	2.86×10^{-4}	1
26	*PURA*	5	0.3821055	0.043743930	2.92×10^{-4}	1
27	*LOC100188947*	10	0.3819967	0.126665100	2.92×10^{-4}	2
28	*HECTD2*	10	0.3819967	0.126665100	2.92×10^{-4}	2
29	*ZNF282*	7	0.3789665	0.013728050	3.11×10^{-4}	1
30	*SPATS2*	12	0.3779965	0.018103710	3.17×10^{-4}	1
31	*DPH6*	15	0.3765334	0.016983230	3.27×10^{-4}	1
32	*ARIH2OS*	3	0.3750646	0.011348290	3.37×10^{-4}	1
33	*KCNT2*	1	0.3748550	0.093205290	3.39×10^{-4}	1
34	*GPHN*	14	0.3744098	0.478385200	3.42×10^{-4}	2
35	*PHYHIPL*	10	0.3737335	0.020357410	3.46×10^{-4}	1
36	*CCDC18*	1	0.3732415	0.124636300	3.50×10^{-4}	2
37	*ABHD17B*	9	0.3730153	0.059902530	3.52×10^{-4}	1
38	*IFT81*	12	0.3714945	0.220865500	3.63×10^{-4}	2
39	*FHOD1*	16	0.3711776	0.013442940	3.65×10^{-4}	1
40	*SYNJ1*	21	0.3678745	0.211024400	3.91×10^{-4}	2

Table S13 Top 40 SS-G123 sweep candidates at RNA- and protein-coding genes shared between the Central and Western European CEU and GBR populations. Candidates presented are those that remained after application of a mappability and alignability filter to data (see *Materials and Methods*). Genes whose sweeps are assigned as hard ($\nu = 1$) are shaded in red in the "Inferred ν" column, while soft sweeps ($\nu \geq 2$) are colored in blue.

	Top gene	Chromosome	Maximum SS−G123	G2tot/G1tot	Inferred ν
1	*ZRANB3*	2	0.4036658	0.01992548	1
2	*R3HDM1*	2	0.4001688	0.03074343	1
3	*DARS*	2	0.3939288	0.04113419	1
4	*SLC12A1*	15	0.3494603	0.03411498	1
5	*MCM6*	2	0.3425388	0.04473161	1
6	*AC093391.2*	2	0.2944935	0.04039653	1
7	*LCT*	2	0.2864912	0.02114967	1
8	*UBXN4*	2	0.2740023	0.02600907	1
9	*LOC100507600*	2	0.2706452	0.02798382	1
10	*RAB3GAP1*	2	0.2506534	0.06432749	1
11	*KMT2A*	11	0.2041324	0.10449340	1
12	*BCAS3*	17	0.1859900	0.09758002	1
13	*PPM1D*	17	0.1800870	0.07265290	1
14	*UNC5D*	8	0.1780280	0.39270230	3
15	*KAT6B*	10	0.1707262	0.05624037	1
16	*TMEM116*	12	0.1651175	0.18743960	1
17	*PRKDC*	8	0.1628838	0.14634790	1
18	*MYO9A*	15	0.1598302	0.06094675	1
19	*ACMSD*	2	0.1572425	0.15455560	1
20	*CCNT2−AS1*	2	0.1572425	0.15455560	1
21	*ZNF546*	19	0.1563353	0.28800990	2
22	*C4orf22*	4	0.1548723	0.17300060	1
23	*COL5A2*	2	0.1531146	0.07664563	1
24	*KITLG*	12	0.1507429	0.09976581	1
25	*MRPS31*	13	0.1404181	0.66863670	6
26	*LAMA3*	18	0.1397230	0.41137770	3
27	*AGO3*	1	0.1389525	0.18726490	1
28	*RALGAPA1*	14	0.1372367	0.10397130	1
29	*RALGAPA1P*	14	0.1372367	0.10397130	1
30	*SYT1*	12	0.1368878	0.18617020	1
31	*GFRA2*	8	0.1354658	0.51413190	4
32	*CNBD2*	20	0.1345655	0.10348770	1
33	*PIK3R4*	3	0.1315715	0.31331700	2
34	*CDK6*	7	0.1302599	0.19966670	1
35	*DIRC3*	2	0.1301000	0.13940720	1
36	*GNA14*	9	0.1297811	0.11111110	1
37	*EXOC5*	14	0.1292055	0.27603760	1
38	*SPATA5L1*	15	0.1291950	0.50091660	4
39	*AC005592.1*	5	0.1283393	0.05882353	1
40	*TMEM163*	2	0.1271473	0.27047560	1

Table S14 Top 40 SS-G123 sweep candidates at RNA- and protein-coding genes shared between the Western European CEU and South Asian GIH populations. Candidates presented are those that remained after application of a mappability and alignability filter to data (see *Materials and Methods*). Genes whose sweeps are assigned as hard ($\nu = 1$) are shaded in red in the "Inferred ν" column, while soft sweeps ($\nu \geq 2$) are colored in blue.

	Top gene	Chromosome	Maximum SS−G123	G2tot/G1tot	Inferred ν
1	*SLC12A1*	15	0.24849900	0.07039983	1
2	*RUNX1T1*	8	0.16146630	0.14275120	1
3	*ZNF546*	19	0.13139160	0.31590110	2
4	*RNU6−28P*	15	0.12412150	0.49297750	2
5	*PPIP5K1*	15	0.12412150	0.49297750	2
6	*PRMT9*	4	0.12362840	0.12395830	1
7	*BCAS3*	17	0.12155650	0.05834652	1
8	*HDAC1*	1	0.11263350	0.10144550	1
9	*P4HA1*	10	0.10999700	0.16650150	1
10	*PITPNB*	22	0.10563580	0.35822780	2
11	*CUX2*	12	0.10209060	0.06924939	1
12	*NECAB1*	8	0.10197640	0.25569620	1
13	*HS2ST1*	1	0.10041530	0.10199000	1
14	*METTL25*	12	0.09952687	0.08587185	1
15	*CELSR3*	3	0.09761571	0.12500000	1
16	*KCNQ5*	6	0.09516938	0.08284819	1
17	*USP25*	21	0.09485193	0.11653040	1
18	*OSBPL9*	1	0.09477321	0.16461200	1
19	*PPM1D*	17	0.09457751	0.08187773	1
20	*PSMB2*	1	0.09368669	0.10872130	1
21	*KITLG*	12	0.09321913	0.10938490	1
22	*PTPRK*	6	0.09238986	0.15235110	1
23	*PRPF40B*	12	0.08811411	0.10312900	1
24	*EXOC5*	14	0.08680119	0.14383560	1
25	*NF1*	17	0.08654684	0.53987730	2
26	*KIAA0825*	5	0.08651185	0.13956570	1
27	*KLHL28*	14	0.08623216	0.08287895	1
28	*UNC5D*	8	0.08584013	0.23278010	1
29	*C8orf44−SGK3*	8	0.08500952	0.10876730	1
30	*SGK3*	8	0.08500952	0.10876730	1
31	*GNA14*	9	0.08464131	0.20441990	1
32	*POLN*	4	0.08228096	0.25619470	1
33	*FMNL3*	12	0.08227142	0.09967949	1
34	*IFT80*	3	0.08224157	0.65133170	4
35	*TFAP2E*	1	0.08005606	0.45766930	2
36	*KIAA0947*	5	0.08003881	0.33080330	1
37	*LINC00478*	21	0.07852482	0.16499670	1
38	*EXOC6B*	2	0.07730652	0.14328060	1
39	*FAM149B1*	10	0.07630036	0.14383560	1
40	*CCDC178*	18	0.07628428	0.33479110	1

Table S15 Top 40 SS-G123 sweep candidates at RNA- and protein-coding genes shared between the Western European CEU and East Asian JPT populations. Candidates presented are those that remained after application of a mappability and alignability filter to data (see *Materials and Methods*). Genes whose sweeps are assigned as hard ($\nu = 1$) are shaded in red in the "Inferred ν" column, while soft sweeps ($\nu \geq 2$) are colored in blue.

	Top gene	Chromosome	Maximum SS−G123	G2tot/G1tot	Inferred ν
1	*SPIDR*	8	0.19359700	0.31787350	3
2	*RUNX1T1*	8	0.11275520	0.05393330	1
3	*MRAP2*	6	0.11102260	0.25897350	1
4	*BVES−AS1*	6	0.10952930	0.51920530	2
5	*LINC00478*	21	0.10122100	0.27387330	1
6	*USP25*	21	0.09815414	0.14385860	1
7	*BCAS3*	17	0.09127146	0.06342583	1
8	*DNAH6*	2	0.08296677	0.20867530	1
9	*BEND4*	4	0.08124753	0.09624478	1
10	*ZNF546*	19	0.07817327	0.06845577	1
11	*HDAC1*	1	0.07768263	0.06808180	1
12	*DENND1A*	9	0.07496250	0.22050380	1
13	*ZRANB3*	2	−0.07278140	0.49384360	2
14	*C16orf70*	16	0.07075091	0.43935930	1
15	*EXOC6B*	2	0.06885796	0.10195950	1
16	*DIRC3*	2	0.06861035	0.13584510	1
17	*C4orf22*	4	0.06847775	0.22222220	1
18	*NR6A1*	9	0.06812268	0.55860720	2
19	*LRRC29*	16	0.06519534	0.13352580	1
20	*TMEM116*	12	−0.06340056	0.44410410	1
21	*C2CD5*	12	−0.06292884	0.36420360	1
22	*PRKDC*	8	0.06144151	0.09442680	1
23	*PRPF40B*	12	0.05952341	0.09292184	1
24	*CELSR3*	3	0.05950715	0.15054200	1
25	*MTOR*	1	0.05841437	0.34873240	1
26	*ANGPTL7*	1	0.05841437	0.34873240	1
27	*KIAA1324L*	7	0.05770516	0.16563660	1
28	*EPB41L1*	20	0.05760458	0.24740230	1
29	*EPS8*	12	0.05647792	0.23065250	1
30	*LOC100188947*	10	0.05452677	0.26400000	1
31	*HECTD2*	10	0.05452677	0.26400000	1
32	*R3HDM1*	2	−0.05448265	0.31076440	1
33	*ZNF106*	15	0.05420983	0.10975160	1
34	*C8orf44−SGK3*	8	0.05260365	0.54661300	2
35	*SGK3*	8	0.05260365	0.54661300	2
36	*CCBL2*	1	0.05220339	0.37208040	1
37	*LYRM7*	5	0.05213381	0.12161650	1
38	*C5orf42*	5	0.05108960	0.57542220	2
39	*RCBTB2*	13	0.05067259	0.52998070	2
40	*ARL13B*	3	0.05000593	0.54782610	2

Table S16 Top 40 SS-G123 sweep candidates at RNA- and protein-coding genes shared between the Central European CEU and West African YRI populations. Candidates presented are those that remained after application of a mappability and alignability filter to data (see *Materials and Methods*). Genes whose sweeps are assigned as hard ($\nu = 1$) are shaded in red in the "Inferred ν" column, while soft sweeps ($\nu \geq 2$) are colored in blue.

	Top gene	Chromosome	Maximum SS−G123	G2tot/G1tot	Inferred ν
1	*KIAA0825*	5	0.16262190	0.09800692	1
2	*RP11−554F20.1*	9	0.14328640	0.07170707	1
3	*SPRED3*	19	0.13648870	0.04008778	1
4	*CASC4*	15	0.13642990	0.06088150	1
5	*DEDD*	1	0.12323310	0.19270460	1
6	*GSTT1*	22	0.11632220	0.07518328	1
7	*ENTHD1*	22	0.11574900	0.29510660	1
8	*NNT*	5	0.11500270	0.09709843	1
9	*ATP6V1A*	3	0.11487290	0.46656150	1
10	*DANCR*	4	0.10908560	0.16342230	1
11	*MIR548H3*	6	0.10678070	0.11806440	1
12	*GRIA2*	4	0.10578390	0.36923080	1
13	*GRIK5*	19	0.10082460	0.14846600	1
14	*TYW5*	2	0.10050780	0.52092830	1
15	*PIGV*	1	0.09740419	0.10112360	1
16	*RALGAPA2*	20	0.09590598	0.09440637	1
17	*PLEKHA8*	7	0.09390530	0.29760670	1
18	*GLRX2*	1	0.09374561	0.53420670	1
19	*PAWR*	12	−0.09282636	0.41657080	1
20	*PHKB*	16	0.09044005	0.10755990	1
21	*ERLIN2*	8	0.08847504	0.09065880	1
22	*SPG11*	15	0.08398508	0.14916580	1
23	*RRN3P3*	16	−0.08384446	0.67088040	8
24	*DKK2*	4	0.08252351	0.13276620	1
25	*ABHD17B*	9	0.08249391	0.08387291	1
26	*CNNM2*	10	0.08094510	0.15631830	1
27	*TGFBR1*	9	0.07873090	0.42549370	1
28	*CPNE1*	20	0.07384179	0.19304800	1
29	*PRKAR2A*	3	0.07271481	0.59669160	2
30	*NLK*	17	0.07079549	0.24630340	1
31	*CDK6*	7	0.07054583	0.07748561	1
32	*SYT1*	12	0.06986742	0.27157760	1
33	*GABRA4*	4	0.06971220	0.52556670	1
34	*ZNF451*	6	0.06885744	0.19779490	1
35	*ITFG1*	16	0.06882713	0.16926620	1
36	*FRYL*	4	0.06828603	0.56018310	2
37	*EXOC6B*	2	−0.06782534	0.46576540	1
38	*USP46*	4	0.06639854	0.25667310	1
39	*LGSN*	6	0.06638067	0.19928830	1
40	*ATF2*	2	0.06592706	0.26808610	1

Table S17 Top 40 SS-G123 sweep candidates at RNA- and protein-coding genes shared between the East African LWK and West African YRI populations. Candidates presented are those that remained after application of a mappability and alignability filter to data (see *Materials and Methods*). Genes whose sweeps are assigned as hard ($\nu = 1$) are shaded in red in the "Inferred ν" column, while soft sweeps ($\nu \geq 2$) are colored in blue.

	Top gene	Chromosome	Maximum SS−G123	G2tot/G1tot	Inferred ν
1	*GRIK5*	19	0.2415148	0.12482020	1
2	*GSTT1*	22	0.2247992	0.23472030	3
3	*RP11−554F20.1*	9	0.2067291	0.10210610	1
4	*KIAA0825*	5	0.2003773	0.29785700	2
5	*RGS18*	1	0.1739911	0.21109120	2
6	*RRN3P3*	16	0.1675603	0.40424180	2
7	*PPAPDC1B*	8	0.1654046	0.11850620	1
8	*SPRED3*	19	0.1609167	0.05899437	1
9	*NNT*	5	0.1564619	0.09173050	1
10	*ARID1A*	1	0.1540840	0.14330290	1
11	*CASC4*	15	0.1429575	0.05820969	1
12	*EHBP1*	2	0.1429198	0.17335160	1
13	*ATF2*	2	0.1396078	0.54310600	2
14	*DKK2*	4	0.1378883	0.12261260	1
15	*MIR548AE2*	16	0.1372927	0.09054441	1
16	*LONP2*	16	0.1372927	0.09054441	1
17	*DDHD2*	8	0.1343500	0.11662590	1
18	*PHKB*	16	0.1315935	0.39985720	2
19	*FER1L6*	8	0.1274631	0.42668680	2
20	*FER1L6−AS1*	8	0.1274631	0.42668680	2
21	*SPIDR*	8	0.1269844	0.47826090	2
22	*GRIA4*	11	0.1268945	0.16182810	1
23	*DANCR*	4	0.1260421	0.15609220	1
24	*TCF4*	18	0.1243683	0.20357240	1
25	*PIGV*	1	0.1237784	0.09449782	1
26	*RALGAPA2*	20	0.1233941	0.09403724	1
27	*TMC1*	9	0.1218435	0.28051680	1
28	*PSMD14*	2	0.1205903	0.43648470	2
29	*CNNM2*	10	0.1205598	0.13187100	1
30	*FAM172A*	5	0.1204877	0.46349210	2
31	*BRIP1*	17	0.1186024	0.25193080	1
32	*GSTTP2*	22	0.1184177	0.16994020	1
33	*MAGI3*	1	0.1173924	0.17789680	1
34	*METTL25*	12	0.1168971	0.23853840	1
35	*CCDC178*	18	0.1152967	0.27341230	1
36	*DDX19B*	16	0.1146779	0.23421130	1
37	*RBBP4*	1	0.1145007	0.63782700	2
38	*C10orf32−ASMT*	10	0.1138325	0.38839470	2
39	*AS3MT*	10	0.1138325	0.38839470	2
40	*ZNF451*	6	0.1137655	0.21774440	1

Table S18 Top 40 SS-G123 sweep candidates at RNA- and protein-coding genes shared between the South Asian GIH and West African YRI populations. Candidates presented are those that remained after application of a mappability and alignability filter to data (see *Materials and Methods*). Genes whose sweeps are assigned as hard ($\nu = 1$) are shaded in red in the "Inferred ν" column, while soft sweeps ($\nu \geq 2$) are colored in blue.

	Top gene	Chromosome	Maximum SS−G123	G2tot/G1tot	Inferred ν
1	*CASC4*	15	0.16711390	0.03621655	1
2	*NNT*	5	0.14575420	0.04650487	1
3	*KIAA0825*	5	0.14498090	0.07326733	1
4	*CDK6*	7	0.13787180	0.23060480	1
5	*ATP6V1A*	3	0.12981560	0.28721580	1
6	*DDHD2*	8	0.12639090	0.06514875	1
7	*SYT1*	12	0.12432490	0.04995287	1
8	*DEDD*	1	0.12425620	0.15489440	1
9	*RP11−554F20.1*	9	0.12160850	0.05718271	1
10	*PSMD14*	2	0.11708710	0.43952710	1
11	*FBXW4*	10	0.11552340	0.12795880	1
12	*PIGV*	1	0.11324550	0.10666980	1
13	*MIR548AE2*	16	0.10772440	0.11468500	1
14	*LONP2*	16	0.10772440	0.11468500	1
15	*ABHD17B*	9	0.10372980	0.05366309	1
16	*GRIK5*	19	0.10341290	0.11576920	1
17	*PPAPDC1B*	8	0.10317110	0.12980420	1
18	*C10orf76*	10	0.10178020	0.51611550	1
19	*PLEKHA8*	7	0.10177350	0.30315060	1
20	*PHKB*	16	0.09939696	0.15921020	1
21	*RALGAPA2*	20	0.09639928	0.13588490	1
22	*TULP4*	6	0.09480228	0.14873490	1
23	*ERLIN2*	8	0.09254210	0.13007500	1
24	*EXOC6B*	2	−0.09028512	0.55109110	2
25	*ZNF451*	6	0.08854748	0.09354446	1
26	*CADM1*	11	0.08766952	0.35196440	1
27	*COL7A1*	3	0.08603112	0.12098250	1
28	*PAWR*	12	−0.08580547	0.44387570	1
29	*CAMK2G*	10	0.08306775	0.43884560	1
30	*FRYL*	4	0.08153959	0.50101830	1
31	*SIRPB1*	20	0.07908564	0.23271970	1
32	*USP46*	4	0.07871925	0.11263520	1
33	*SLC4A10*	2	0.07705620	0.12719180	1
34	*CPNE1*	20	0.07523397	0.32026980	1
35	*FER1L6*	8	0.07413957	0.50163820	1
36	*FER1L6−AS1*	8	0.07413957	0.50163820	1
37	*UBE4A*	11	0.07396793	0.50684930	1
38	*LOC100131626*	11	0.07396793	0.50684930	1
39	*NLK*	17	0.07380719	0.33165250	1
40	*ENTHD1*	22	0.07378007	0.20033280	1

Table S19 Top 40 SS-G123 sweep candidates at RNA- and protein-coding genes shared between the East Asian JPT and West African YRI populations. Candidates presented are those that remained after application of a mappability and alignability filter to data (see *Materials and Methods*). Genes whose sweeps are assigned as hard ($\nu = 1$) are shaded in red in the "Inferred ν" column, while soft sweeps ($\nu \geq 2$) are colored in blue.

	Top gene	Chromosome	Maximum SS−G123	G2tot/G1tot	Inferred ν
1	*UCHL5*	1	0.16261050	0.54330180	2
2	*CASC4*	15	0.15414540	0.02859798	1
3	*GRIK5*	19	0.15077710	0.08571429	1
4	*ATP6V1A*	3	0.14779860	0.51696610	2
5	*SIRPB1*	20	0.14373280	0.17088900	1
6	*HEMGN*	9	0.14078020	0.07985481	1
7	*KIAA0825*	5	0.13892610	0.14634150	1
8	*EHBP1*	2	0.13344380	0.15266860	1
9	*RP11−554F20.1*	9	0.12449170	0.28106370	1
10	*ENTHD1*	22	0.11764070	0.12615590	1
11	*PSMD14*	2	0.10605230	0.32749560	1
12	*NNT*	5	0.10287120	0.02879851	1
13	*EXOC6B*	2	−0.09657734	0.32384650	1
14	*DDHD2*	8	0.09268298	0.17119050	1
15	*MIR548AE2*	16	0.09252061	0.04543263	1
16	*LONP2*	16	0.09252061	0.04543263	1
17	*PIGV*	1	0.09246271	0.08195141	1
18	*GRIA4*	11	0.09091467	0.24805340	1
19	*RALGAPA2*	20	0.09018390	0.06541614	1
20	*CSMD3*	8	0.08642643	0.10669980	1
21	*AUTS2*	7	0.08609979	0.23589890	1
22	*MPHOSPH9*	12	−0.08463466	0.52033200	1
23	*PPAPDC1B*	8	0.08450565	0.28654350	1
24	*MIR548H3*	6	0.08341730	0.14782610	1
25	*ABCB1*	7	0.08225091	0.50471290	1
26	*RUNDC3B*	7	0.08225091	0.50471290	1
27	*SIPA1L3*	19	0.08082831	0.16331990	1
28	*NLK*	17	0.08023741	0.25966720	1
29	*CPNE1*	20	0.07997871	0.11175370	1
30	*GRIA2*	4	0.07905065	0.40514080	1
31	*CDK6*	7	0.07856601	0.11933860	1
32	*PLEKHA8*	7	0.07799249	0.29088470	1
33	*DKK2*	4	0.07704189	0.07856381	1
34	*SYT1*	12	0.07684115	0.12255670	1
35	*COL7A1*	3	0.07658377	0.07582045	1
36	*GSTT1*	22	0.07574164	0.10880200	1
37	*FBXW4*	10	0.07431220	0.15773660	1
38	*USP46*	4	0.07174521	0.19367210	1
39	*AC016582.2*	19	0.07004390	0.18775370	1
40	*ARID1A*	1	0.06960214	0.02739301	1

Table S20 Top 40 SS-G123 sweep candidates at RNA- and protein-coding genes shared between the East Asian JPT and South Asian GIH populations. Candidates presented are those that remained after application of a mappability and alignability filter to data (see *Materials and Methods*). Genes whose sweeps are assigned as hard ($\nu = 1$) are shaded in red in the "Inferred ν" column, while soft sweeps ($\nu \geq 2$) are colored in blue.

	Top gene	Chromosome	Maximum SS−G123	G2tot/G1tot	Inferred ν
1	*RUNX1T1*	8	0.19081280	0.08034745	1
2	*P4HTM*	3	0.17561530	0.02724586	1
3	*EXOC6B*	2	0.11912730	0.09503897	1
4	*TMTC2*	12	0.11638210	0.18265330	1
5	*SUGCT*	7	0.11594030	0.12736710	1
6	*HELZ*	17	0.11386080	0.35123210	2
7	*DBT*	1	0.11216520	0.06377143	1
8	*BCAS3*	17	0.10947050	0.06812121	1
9	*RP11−53O19.1*	5	0.10879940	0.52299610	2
10	*ZNF546*	19	0.09867813	0.13472000	1
11	*ADAMTS6*	5	0.09839895	0.49891630	2
12	*APPBP2*	17	0.09796838	0.09183407	1
13	*DR1*	1	0.09702526	0.42016090	1
14	*USP25*	21	0.09547922	0.16971110	1
15	*RNF121*	11	0.09440660	0.09574218	1
16	*NEGR1*	1	0.09420501	0.28006000	1
17	*RNU6−28P*	15	0.09050468	0.27059630	1
18	*PPIP5K1*	15	0.09050468	0.27059630	1
19	*ORC2*	2	0.08524372	0.07114440	1
20	*HDAC1*	1	0.08444452	0.12845180	1
21	*USP32*	17	0.08419480	0.14071580	1
22	*CCDC18*	1	0.08341467	0.34291580	1
23	*LYRM7*	5	0.08066234	0.07455296	1
24	*LOC100188947*	10	0.08039944	0.38098430	1
25	*HECTD2*	10	0.08039944	0.38098430	1
26	*SSH2*	17	0.07918183	0.29931230	1
27	*ZNF780B*	19	0.07884324	0.14236710	1
28	*NLK*	17	0.07866030	0.15058970	1
29	*MTF2*	1	0.07827113	0.56458640	2
30	*ATP6V0D1*	16	0.07404407	0.08471815	1
31	*MBOAT2*	2	0.07358927	0.11950500	1
32	*BCL2L1*	20	0.07326540	0.13298940	1
33	*CENPW*	6	0.07324676	0.21777780	1
34	*BEND4*	4	0.07308935	0.08658982	1
35	*LINC00478*	21	0.07294715	0.17406650	1
36	*XXYLT1*	3	0.07133674	0.10906100	1
37	*ABCB1*	7	0.07111757	0.14704880	1
38	*RUNDC3B*	7	0.07111757	0.14704880	1
39	*NGLY1*	3	0.06960764	0.15325250	1
40	*CELSR3*	3	0.06809979	0.09836612	1

Table S21 Top 40 SS-G123 sweep candidates at RNA- and protein-coding genes shared between the East Asian JPT and Southeast Asian KHV populations. Candidates presented are those that remained after application of a mappability and alignability filter to data (see *Materials and Methods*). Genes whose sweeps are assigned as hard ($\nu = 1$) are shaded in red in the "Inferred ν" column, while soft sweeps ($\nu \geq 2$) are colored in blue.

	Top gene	Chromosome	Maximum SS−G123	G2tot/G1tot	Inferred ν
1	*SPIDR*	8	0.2784003	0.38334810	2
2	*RP11−696N14.1*	4	0.2744507	0.20046720	2
3	*EXOC6B*	2	0.2617294	0.03631803	1
4	*RUNX1T1*	8	0.2599384	0.06254055	1
5	*SPAG6*	10	0.2444433	0.03124657	1
6	*EXD2*	14	0.2338336	0.06551773	1
7	*P4HTM*	3	0.2265336	0.02184214	1
8	*AMBRA1*	11	0.2041819	0.07887964	1
9	*BCL7C*	16	0.2019106	0.04684318	1
10	*BCL2L1*	20	0.1971090	0.09232554	1
11	*ADH1A*	4	0.1963534	0.27346120	2
12	*PGAP1*	2	0.1945704	0.09764099	1
13	*C11orf49*	11	0.1898302	0.18259830	2
14	*PRPF40B*	12	0.1861633	0.03307622	1
15	*LOC100188947*	10	0.1858056	0.47456660	2
16	*HECTD2*	10	0.1858056	0.47456660	2
17	*NOVA1*	14	0.1830759	0.49632250	2
18	*ZNF282*	7	0.1813378	0.05366309	1
19	*HMCN1*	1	0.1764870	0.47648710	2
20	*PHYHIPL*	10	0.1743157	0.07840000	1
21	*LINC01024*	5	0.1742617	0.13723020	1
22	*ARIH2*	3	0.1734230	0.06296852	1
23	*PURA*	5	0.1727126	0.13155920	1
24	*ARIH2OS*	3	0.1680339	0.05414495	1
25	*TRUB1*	10	0.1677889	0.06171946	1
26	*CEP112*	17	0.1663139	0.06596257	1
27	*USP38*	4	0.1643823	0.14698160	1
28	*C2orf66*	2	0.1629327	0.04013059	1
29	*LINC01088*	4	0.1622231	0.12088800	1
30	*TRMT11*	6	0.1609308	0.04417217	1
31	*CCDC18*	1	0.1591868	0.39498060	2
32	*LINC00536*	8	0.1575138	0.53060490	3
33	*CSPP1*	8	0.1570753	0.46273400	2
34	*RAD51B*	14	0.1546937	0.07764864	1
35	*SPATS2*	12	0.1543295	0.07337854	1
36	*FBXO4*	5	0.1535929	0.03908674	1
37	*PKIA*	8	0.1529611	0.23342180	2
38	*GPHN*	14	0.1511221	0.41336880	2
39	*ZNF660*	3	0.1509682	0.12457300	1
40	*OXCT1*	5	0.1500597	0.04652922	1

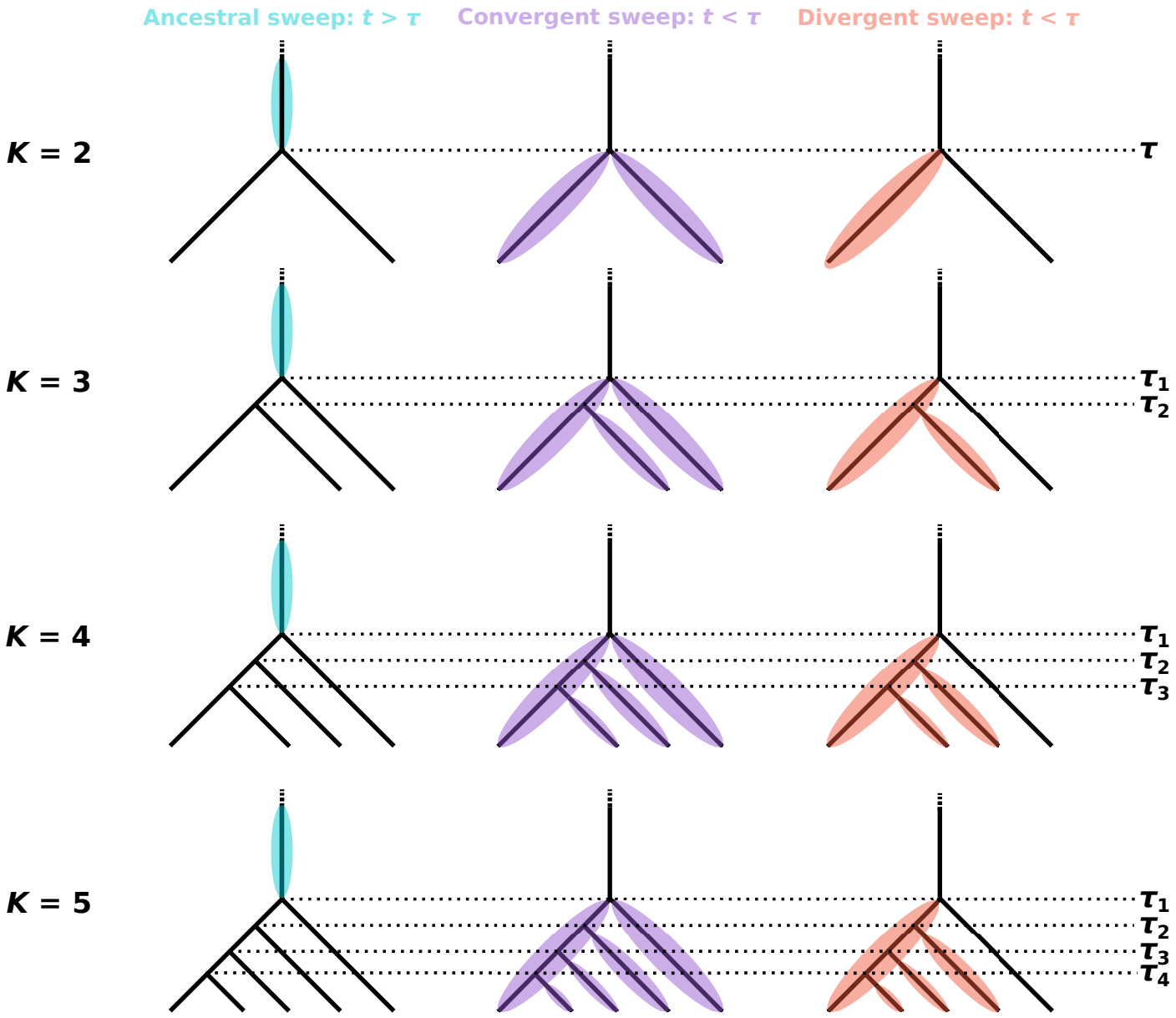

Figure S1 Tree topologies for simplified mammalian model simulation experiments, highlighted to indicate the branches on which ancestral (teal), convergent (purple), and divergent (orange) sweep events, analyzed in Figures S9 and SN1-SN3 were initiated. Ancestral sweeps occurred only in the common ancestor of all sampled modern populations, more ancient than τ or τ_1 (left). Convergent sweeps occur in each existing population independently at the time of selection, explicitly more recent than τ or τ_1 (center). Divergent sweeps also occur more recent than τ or τ_1, but the sweep only arises on the leftmost branch at the time of selection (right; maximum number of affected lineages is highlighted). Times of selection for ancestral sweeps (coalescent units in parentheses) were $t \in \{1100(0.055), 1500(0.075), 2000(0.1), 3000(0.15), 4000(0.2)\}$, while times of selection for convergent and divergent sweeps were $t \in \{200(0.01), 400(0.02), 600(0.03), 800(0.04)\}$. Population splits occurred at regular intervals with $\tau_1 = 1000$ (0.05 coalescent units; equal to τ for $K = 2$ models), $\tau_2 = 750(0.0375)$, $\tau_3 = 500(0.025)$, and $\tau_4 = 250(0.0125)$ generations prior to sampling.

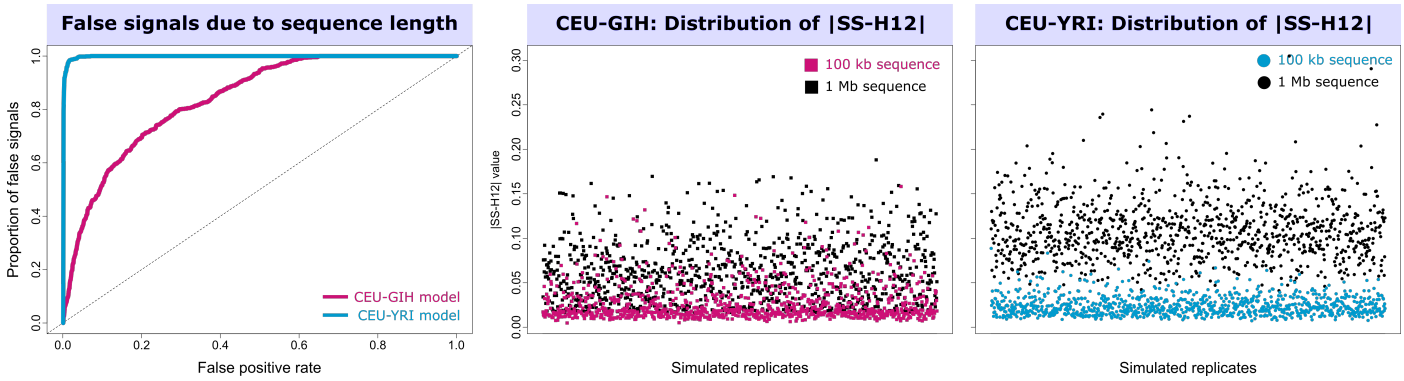

Figure S2 Effect of simulated sequence length on power computations for SS-H12. (Left) Proportion of false signals based on neutral simulations of one Mb sequences as a function of false positive rate based on neutral simulations of 100 kb sequences for CEU-GIH (magenta) and CEU-YRI (blue) demographic histories. (Center) Distribution of |SS-H12| values across 1000 simulated replicates of length 100 kb (magenta) and one Mb (black) for CEU-GIH demographic history. (Right) Distribution of |SS-H12| values across 1000 simulated replicates of length 100 kb (blue) and one Mb (black) for CEU-YRI demographic history.

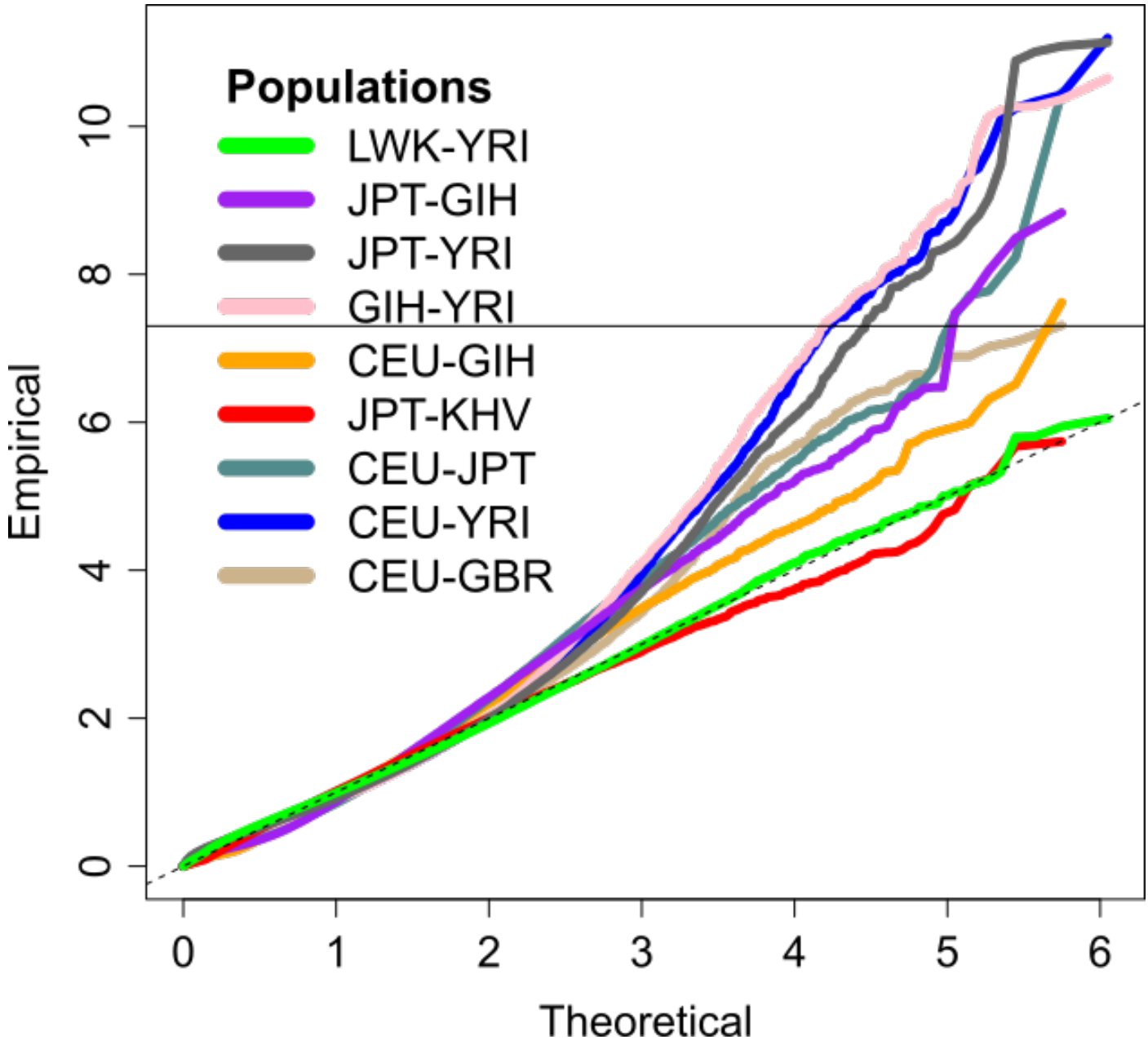

Figure S3 QQ-plot demonstrating the relationship between empirically inferred calibrated p-values and theoretical p-values based on the |SS-H12| score for each genomic analysis window across each population pair. Axes are $-\log_{10}$ transformed. The solid horizontal line in the plot indicates the $p = \alpha/10^6 = 5 \times 10^{-8}$ significance threshold for $\alpha = 0.05$, and the $y = x$ line is included as a dashed line. See *Materials and Methods* for further details.

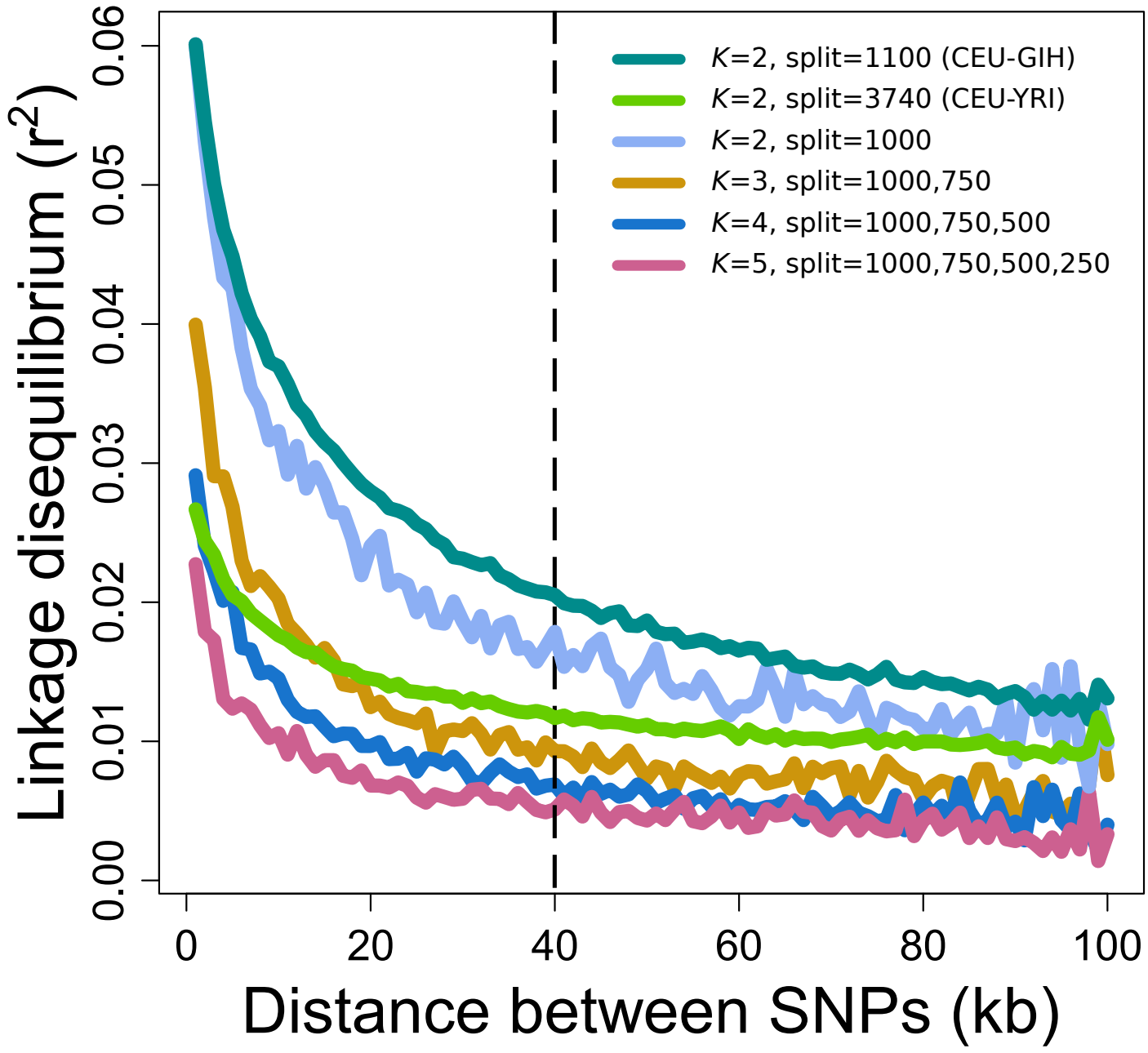

Figure S4 Decay of pairwise LD measured as r^2 over 100 kb for pooled samples simulated under neutrality containing two to five populations. For pairs of populations (cyan, chartreuse, and sky blue), we simulated under the CEU-GIH ($\tau = 1100$; 0.055 coalescent units) or CEU-YRI ($\tau = 3740$; 0.0935) human demographic models, or a simplified constant demographic history model ($\tau = 1000$; 0.05) with $N = 10^4$, where the ancestral population splits once. For trios of populations (goldenrod), two splits underlie the sample phylogeny, occurring $\tau_1 = 1000$ (0.05) and $\tau_2 = 750$ (0.0375) generations before sampling. For quartets of populations (dark blue), there are three splits occurring at $\tau_1 = 1000$, $\tau_2 = 750$, and $\tau_3 = 500$ (0.025) generations before sampling. Finally, quintet phylogenies result from four splits, at $\tau_1 = 1000$ $\tau_2 = 750$, $\tau_3 = 500$, and $\tau_4 = 250$ (0.0125) generations before sampling. All samples are identical to those analyzed in the main text.

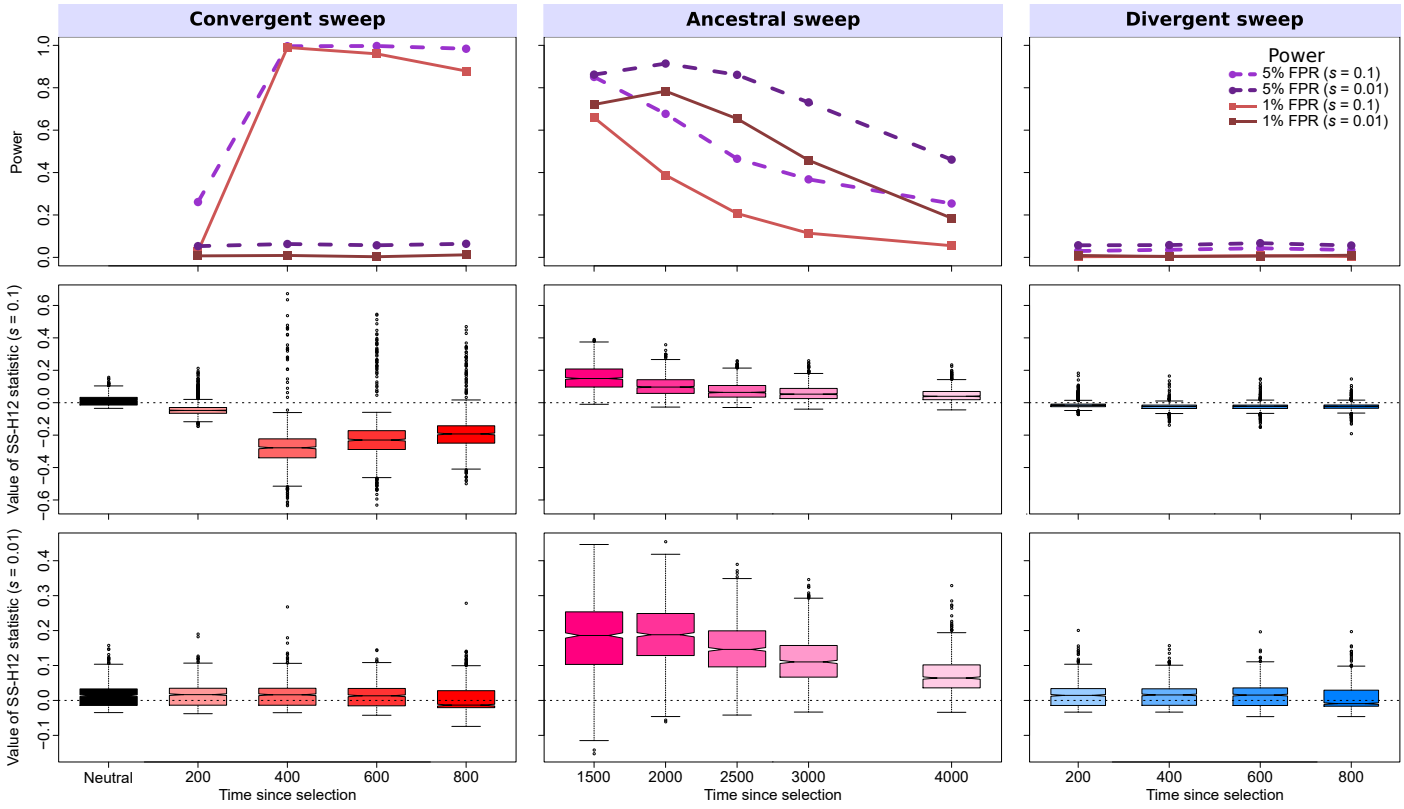

Figure S5 Properties of SS-H12 for simulated strong ($s = 0.1; \sigma = 4N_e s = 4000$) and moderate ($s = 0.01; \sigma = 400$) soft sweep ($\nu = 4$) scenarios under the CEU-GIH model ($\tau = 1100$ generations, or 0.055 coalescent units, before sampling). (Top row) Power at 1% (red lines) and 5% (purple lines) false positive rates (FPRs) to detect recent ancestral, convergent, and divergent soft sweeps from selection on standing genetic variation as a function of time at which selection of the favored haplotypes initiated (t), with FPR based on the distribution of maximum |SS-H12| across simulated neutral replicates. (Middle row) Box plots summarizing the distribution of SS-H12 values from windows of maximum |SS-H12| across strong sweep replicates, corresponding to each time point in the power curves, with dashed lines in each panel representing SS-H12 = 0. (Bottom row) Box plots summarizing the distribution of SS-H12 values across moderate sweep replicates. For convergent and divergent sweeps, $t < \tau$, while for ancestral sweeps, $t > \tau$. All replicate samples for the CEU-GIH model contain 99 simulated CEU individuals and 103 simulated GIH individuals, as in the 1000 Genomes Project dataset (Auton *et al.* 2015), and we performed 1000 replicates for each scenario.

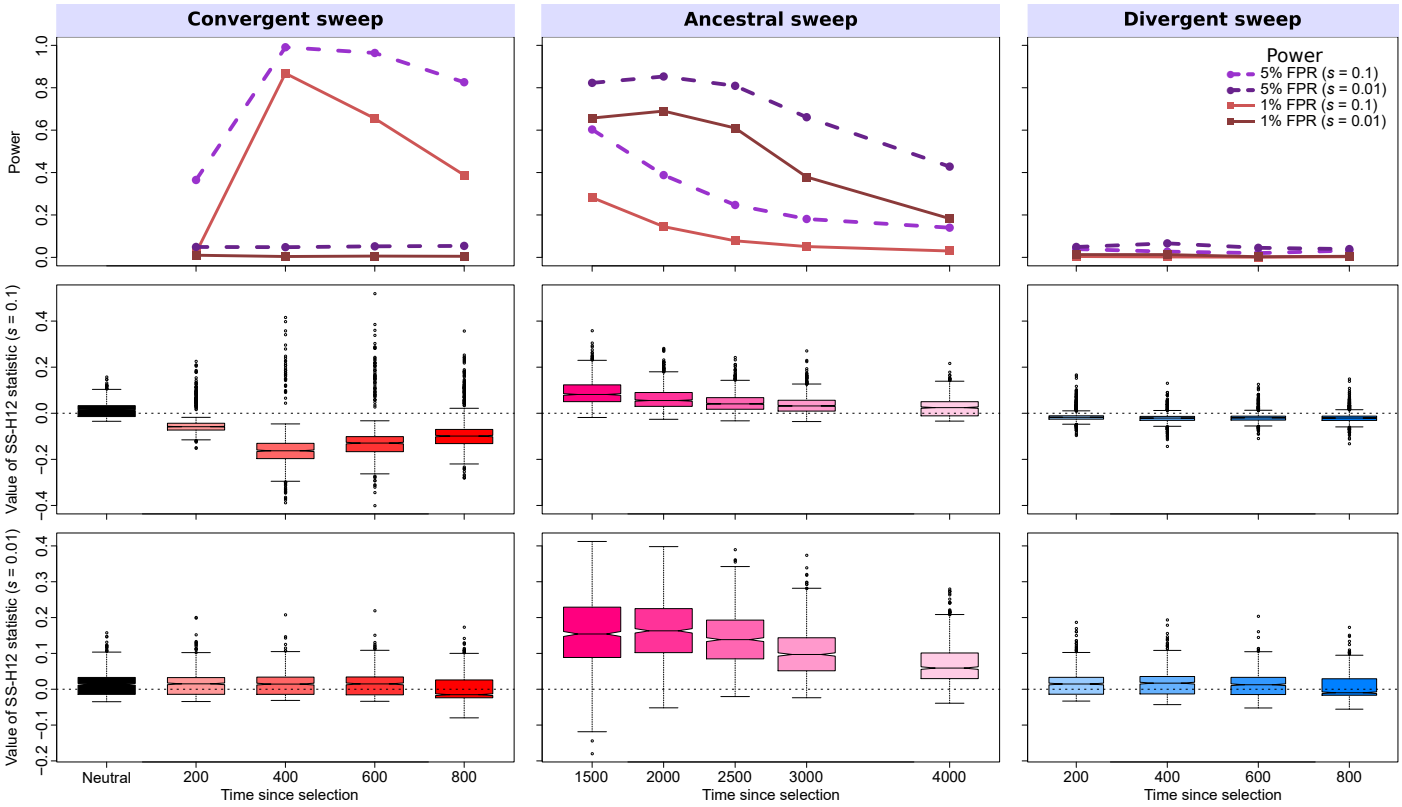

Figure S6 Properties of SS-H12 for simulated strong ($s = 0.1; \sigma = 4N_e s = 4000$) and moderate ($s = 0.01; \sigma = 400$) soft sweep ($\nu = 8$) scenarios under the CEU-GIH model ($\tau = 1100$ generations, or 0.055 coalescent units, before sampling). (Top row) Power at 1% (red lines) and 5% (purple lines) false positive rates (FPRs) to detect recent ancestral, convergent, and divergent soft sweeps from selection on standing genetic variation as a function of time at which selection of the favored haplotypes initiated (t), with FPR based on the distribution of maximum |SS-H12| across simulated neutral replicates. (Middle row) Box plots summarizing the distribution of SS-H12 values from windows of maximum |SS-H12| across strong sweep replicates, corresponding to each time point in the power curves, with dashed lines in each panel representing SS-H12 = 0. (Bottom row) Box plots summarizing the distribution of SS-H12 values across moderate sweep replicates. For convergent and divergent sweeps, $t < \tau$, while for ancestral sweeps, $t > \tau$. All replicate samples for the CEU-GIH model contain 99 simulated CEU individuals and 103 simulated GIH individuals, as in the 1000 Genomes Project dataset (Auton *et al.* 2015), and we performed 1000 replicates for each scenario.

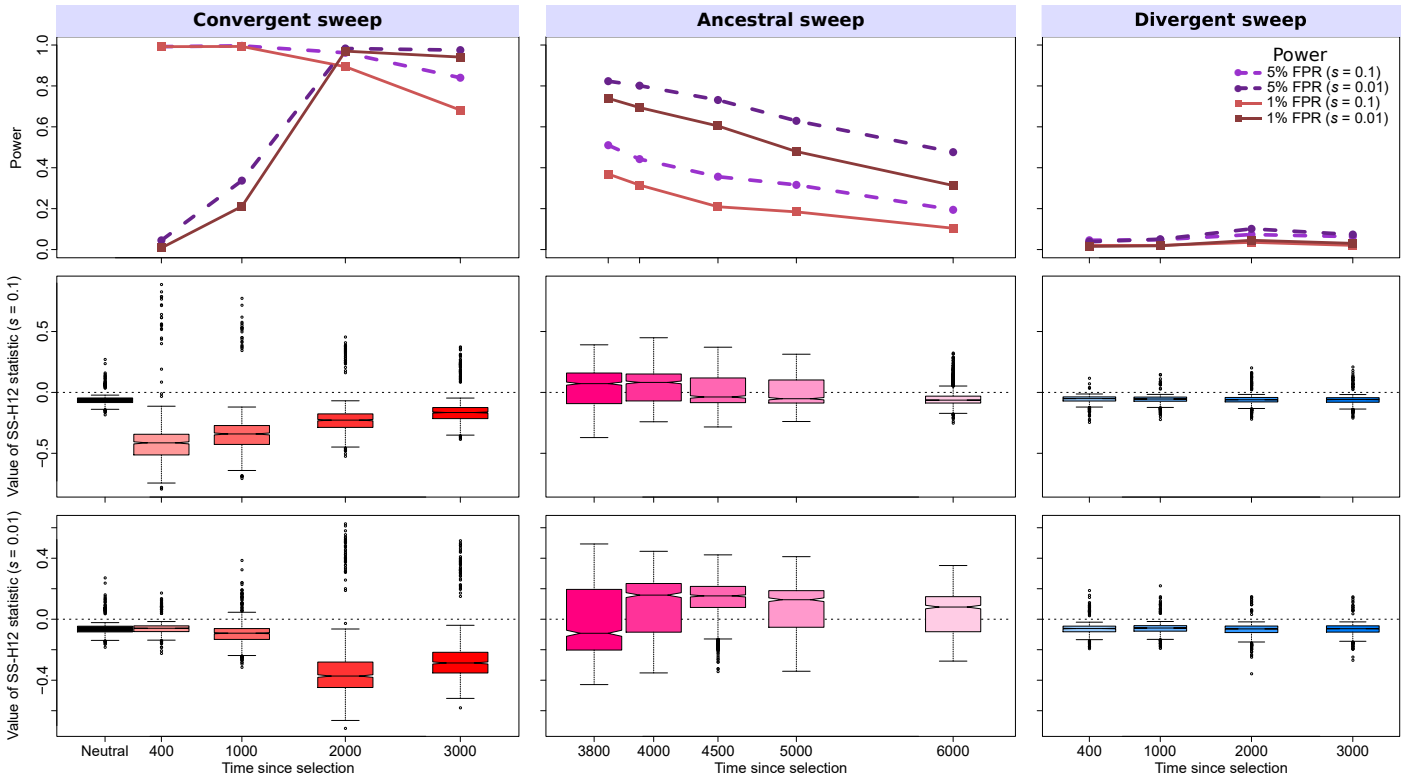

Figure S7 Properties of SS-H12 for simulated strong ($s = 0.1; \sigma = 4N_e s = 8000$) and moderate ($s = 0.01; \sigma = 800$) soft sweep ($\nu = 4$) scenarios under the CEU-YRI model ($\tau = 3740$ generations, or 0.0935 coalescent units, before sampling). (Top row) Power at 1% (red lines) and 5% (purple lines) false positive rates (FPRs) to detect recent ancestral, convergent, and divergent soft sweeps from selection on standing genetic variation as a function of time at which selection of the favored haplotypes initiated (t), with FPR based on the distribution of maximum |SS-H12| across simulated neutral replicates. (Middle row) Box plots summarizing the distribution of SS-H12 values from windows of maximum |SS-H12| across strong sweep replicates, corresponding to each time point in the power curves, with dashed lines in each panel representing SS-H12 = 0. (Bottom row) Box plots summarizing the distribution of SS-H12 values across moderate sweep replicates. For convergent and divergent sweeps, $t < \tau$, while for ancestral sweeps, $t > \tau$. All replicate samples for the CEU-YRI model contain 99 simulated CEU individuals and 108 simulated YRI individuals, as in the 1000 Genomes Project dataset (Auton *et al.* 2015), and we performed 1000 replicates for each scenario.

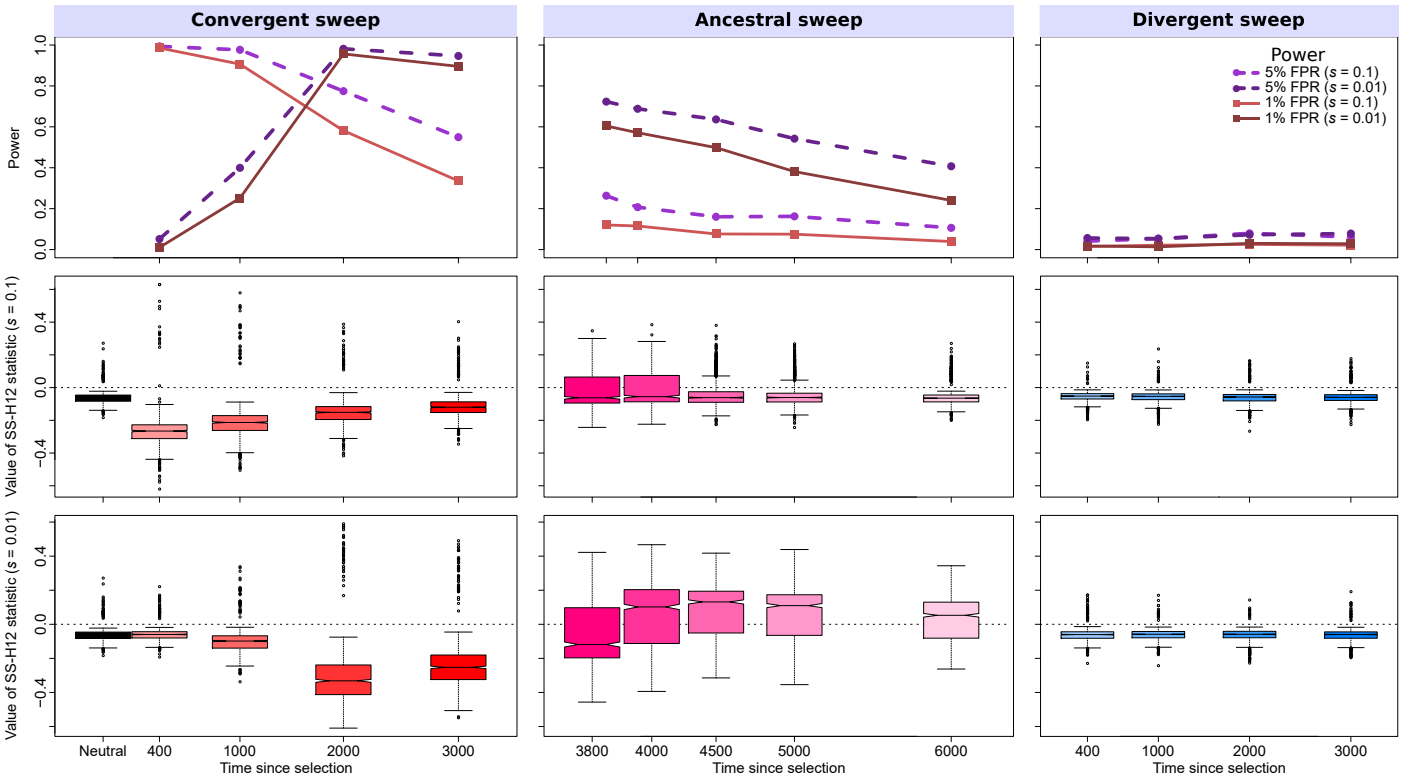

Figure S8 Properties of SS-H12 for simulated strong ($s = 0.1; \sigma = 4N_e s = 8000$) and moderate ($s = 0.01; \sigma = 800$) soft sweep ($\nu = 8$) scenarios under the CEU-YRI model ($\tau = 3740$ generations, or 0.0935 coalescent units, before sampling). (Top row) Power at 1% (red lines) and 5% (purple lines) false positive rates (FPRs) to detect recent ancestral, convergent, and divergent soft sweeps from selection on standing genetic variation as a function of time at which selection of the favored haplotypes initiated (t), with FPR based on the distribution of maximum |SS-H12| across simulated neutral replicates. (Middle row) Box plots summarizing the distribution of SS-H12 values from windows of maximum |SS-H12| across strong sweep replicates, corresponding to each time point in the power curves, with dashed lines in each panel representing SS-H12 = 0. (Bottom row) Box plots summarizing the distribution of SS-H12 values across moderate sweep replicates. For convergent and divergent sweeps, $t < \tau$, while for ancestral sweeps, $t > \tau$. All replicate samples for the CEU-YRI model contain 99 simulated CEU individuals and 108 simulated YRI individuals, as in the 1000 Genomes Project dataset (Auton *et al.* 2015), and we performed 1000 replicates for each scenario.

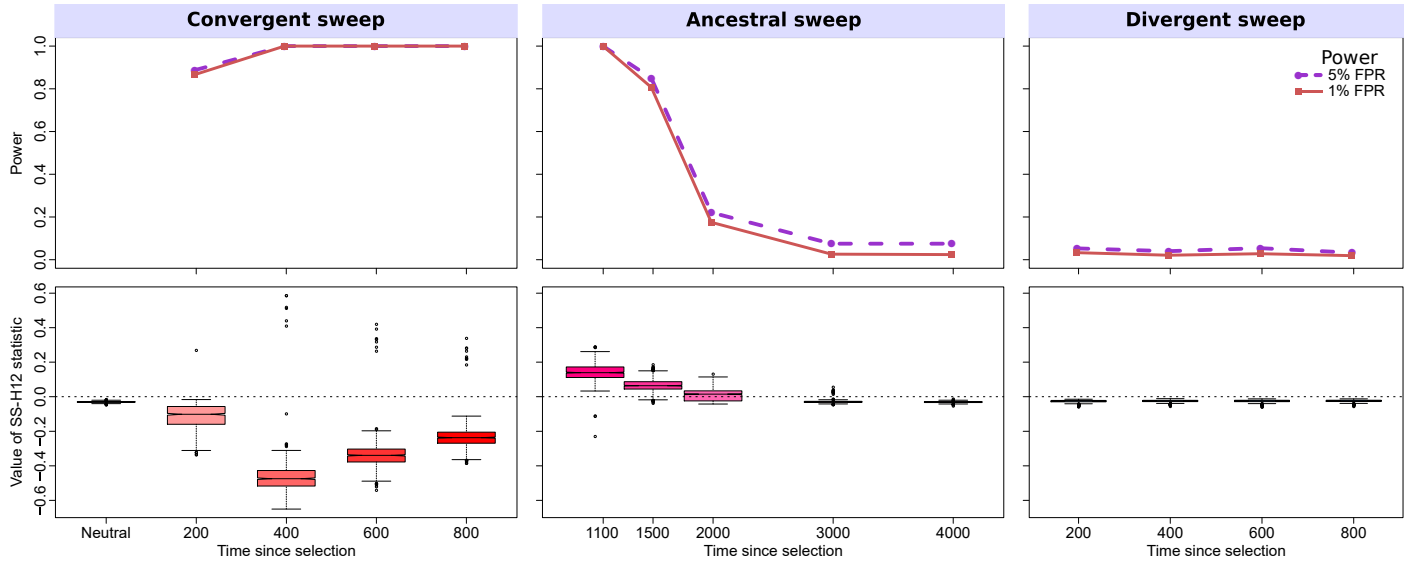

Figure S9 Properties of SS-H12 for simulated hard sweep scenarios for samples drawn from $K = 2$ equally-sized populations in which $\tau = 1000$ generations (0.05 coalescent units) before sampling, for a constant demographic history in which $N = 10^4$ for the duration of the simulation. (Top) Power at 1 and 5% false positive rates (FPRs) to detect recent ancestral, convergent, and divergent hard sweeps (see Figure 1) as a function of time at which selection initiated, with false positive rate based on the distribution of maximum |SS-H12| across simulated neutral replicates. (Middle row) Box plots summarizing the distribution of SS-H12 values from windows of maximum |SS-H12| for each replicate, corresponding to each point in the power curve, with dashed lines in each panel representing SS-H12 $= 0$. Convergent and divergent sweeps occur more recently than this time (200-800 generations, or 0.01-0.04 coalescent units, before sampling), while ancestral sweeps occur more anciently than this time (1100-4000 generations, or 0.055-0.2 coalescent units, before sampling). All sweeps are strong ($s = 0.1$; $\sigma = 4N_e s = 4000$) for a sample of $n = 100$ diploid individuals per population, with 1000 replicates performed for each scenario.

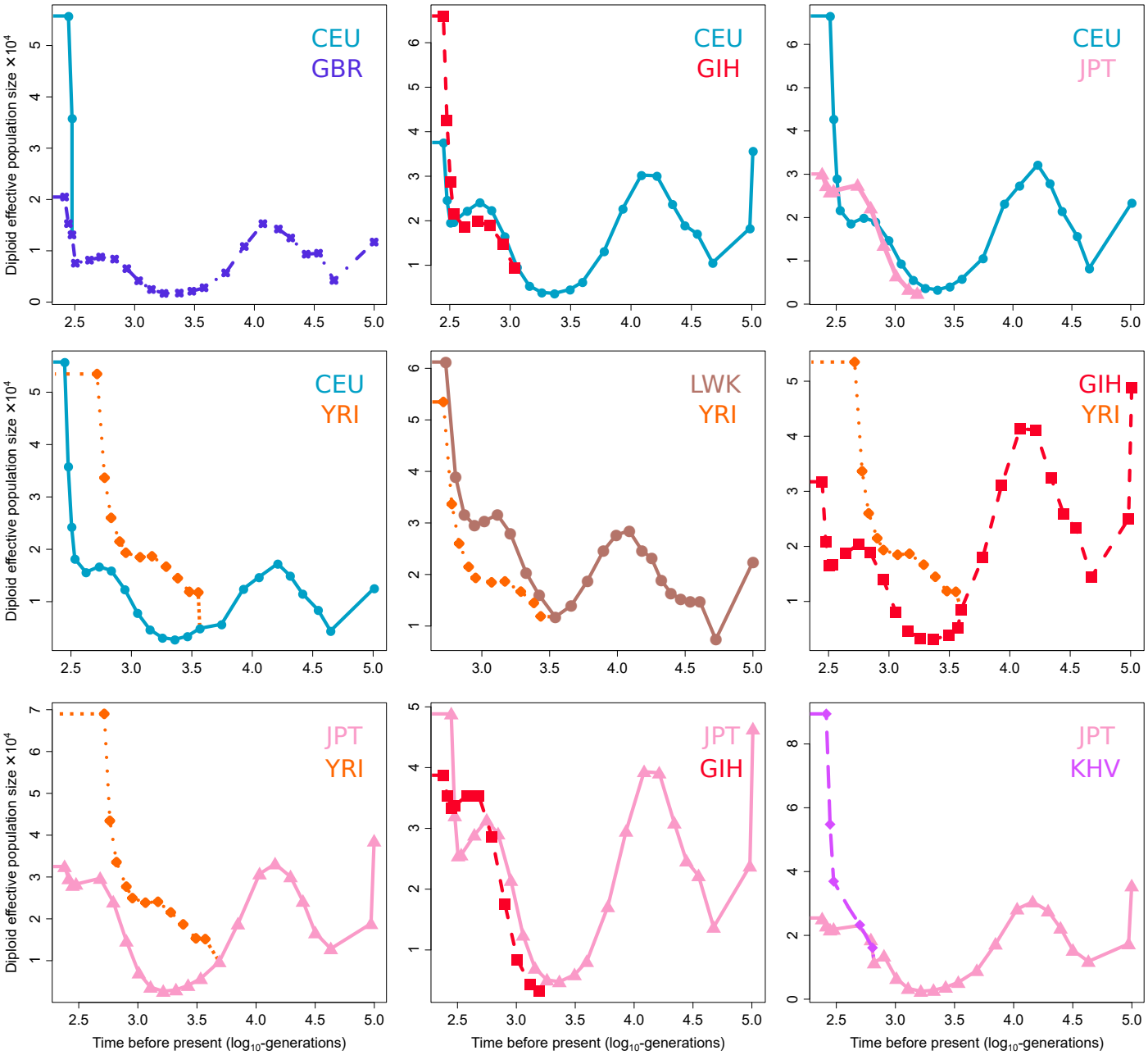

Figure S10 $K = 2$ population clean-split models inferred with `smc++` for all empirical population pair comparisons, comprising CEU-GBR, CEU-GIH, CEU-JPT, CEU-YRI, LWK-YRI, GIH-YRI, JPT-YRI, JPT-GIH, and JPT-KHV. Each curve traces the history of the primary study population in the inference, with the secondary population modeled as instantaneously splitting from it at time τ (considered to be the first observed point of the secondary population). The horizontal axis is rendered on a log-scale, and population size is modeled as constant between the last inferred point on the curve and the present.

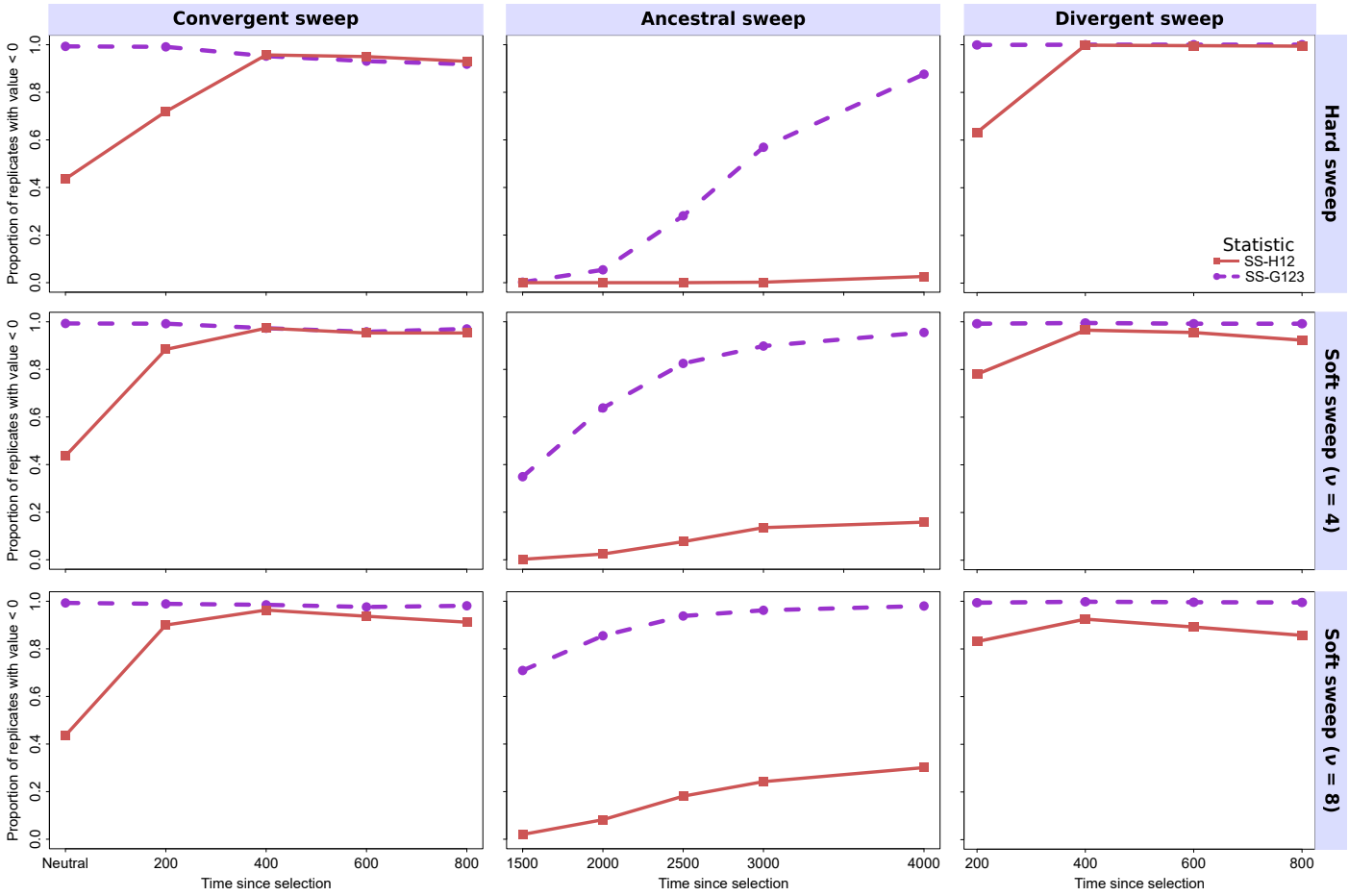

Figure S11 Proportion of negative SS-H12 (red) and SS-G123 (purple) scores across 1000 strong ($s = 0.1; \sigma = 4N_e s = 4000$) hard ($\nu = 1$) and soft ($\nu \in \{4, 8\}$) sweep replicates, and neutrality (first point on convergent sweep curve). Replicates were generated under the European-south Asian CEU-GIH demographic model and are identical to those in Figures 2 and S34.

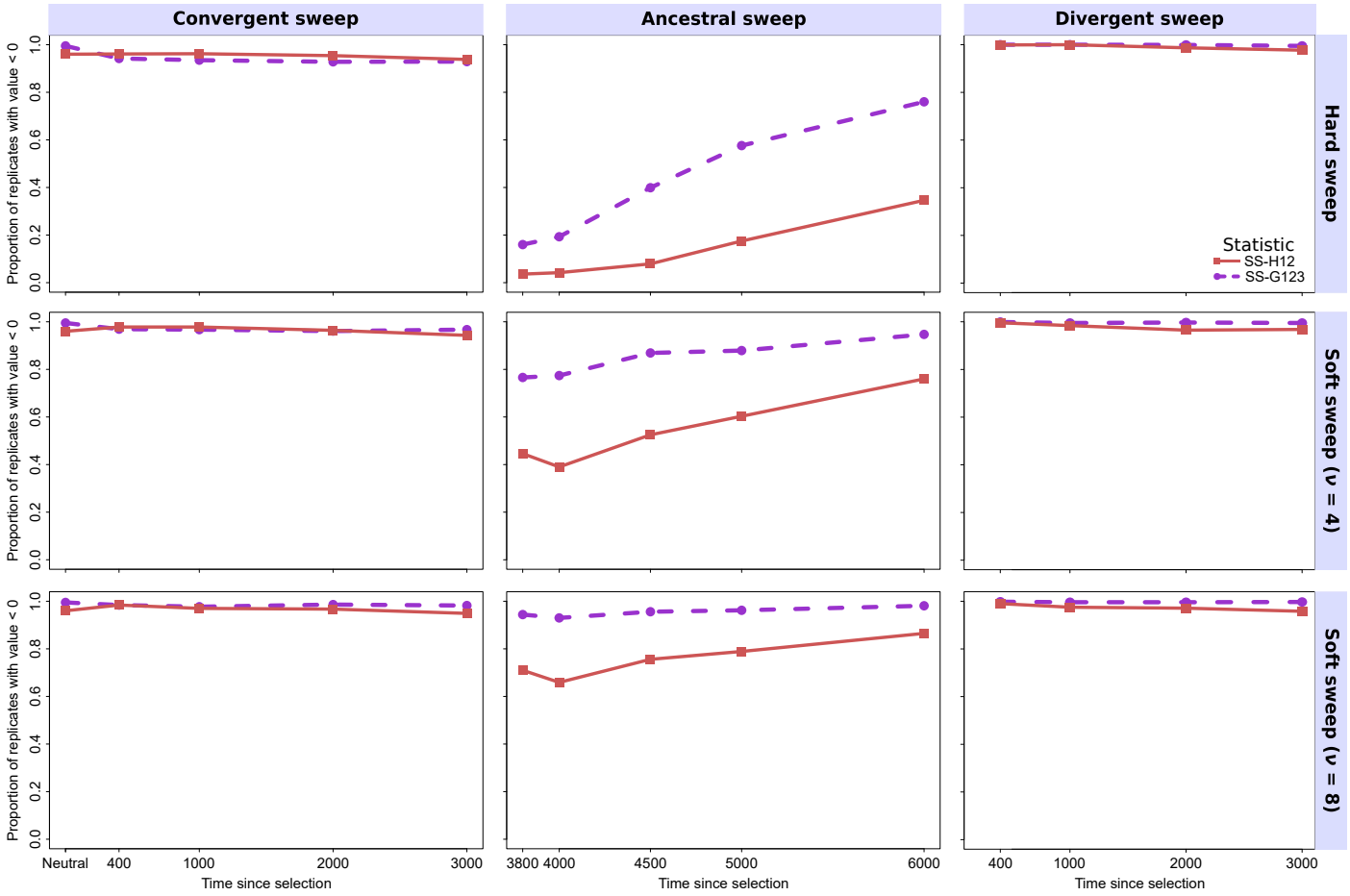

Figure S12 Proportion of negative SS-H12 (red) and SS-G123 (purple) scores across 1000 strong ($s = 0.1; \sigma = 4N_e s = 8000$) hard ($\nu = 1$) and soft ($\nu \in \{4, 8\}$) sweep replicates, and neutrality (first point on convergent sweep curve). Replicates were generated under the European-sub-Saharan African CEU-YRI demographic model and are identical to those in Figures 3 and S39.

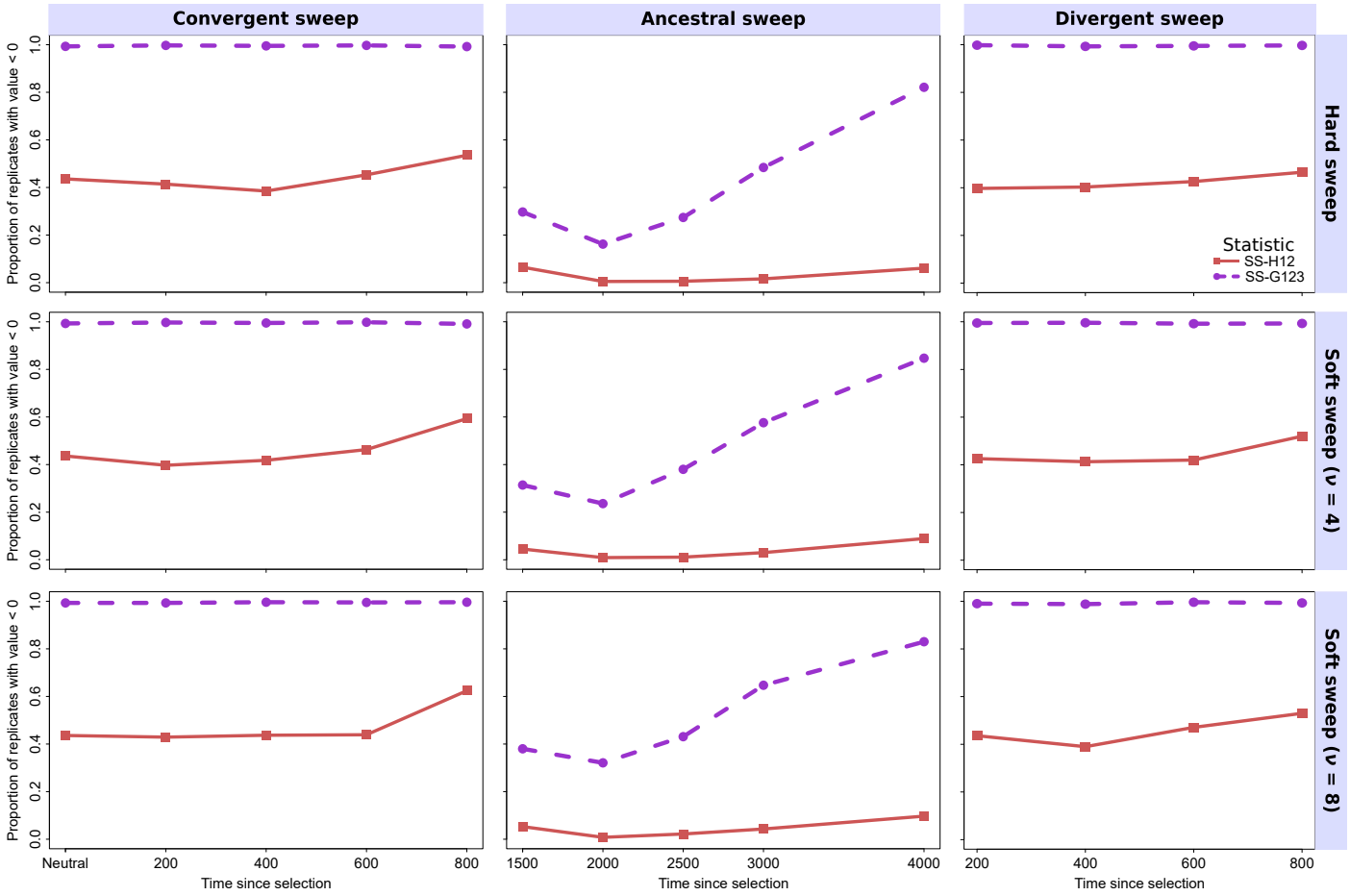

Figure S13 Proportion of negative SS-H12 (red) and SS-G123 (purple) scores across 1000 moderate ($s = 0.01$; $\sigma = 4N_e s = 400$) hard ($\nu = 1$) and soft ($\nu \in \{4, 8\}$) sweep replicates, and neutrality (first point on convergent sweep curve). Replicates were generated under the European-south Asian CEU-GIH demographic model and are identical to those in Figures 2 and S34.

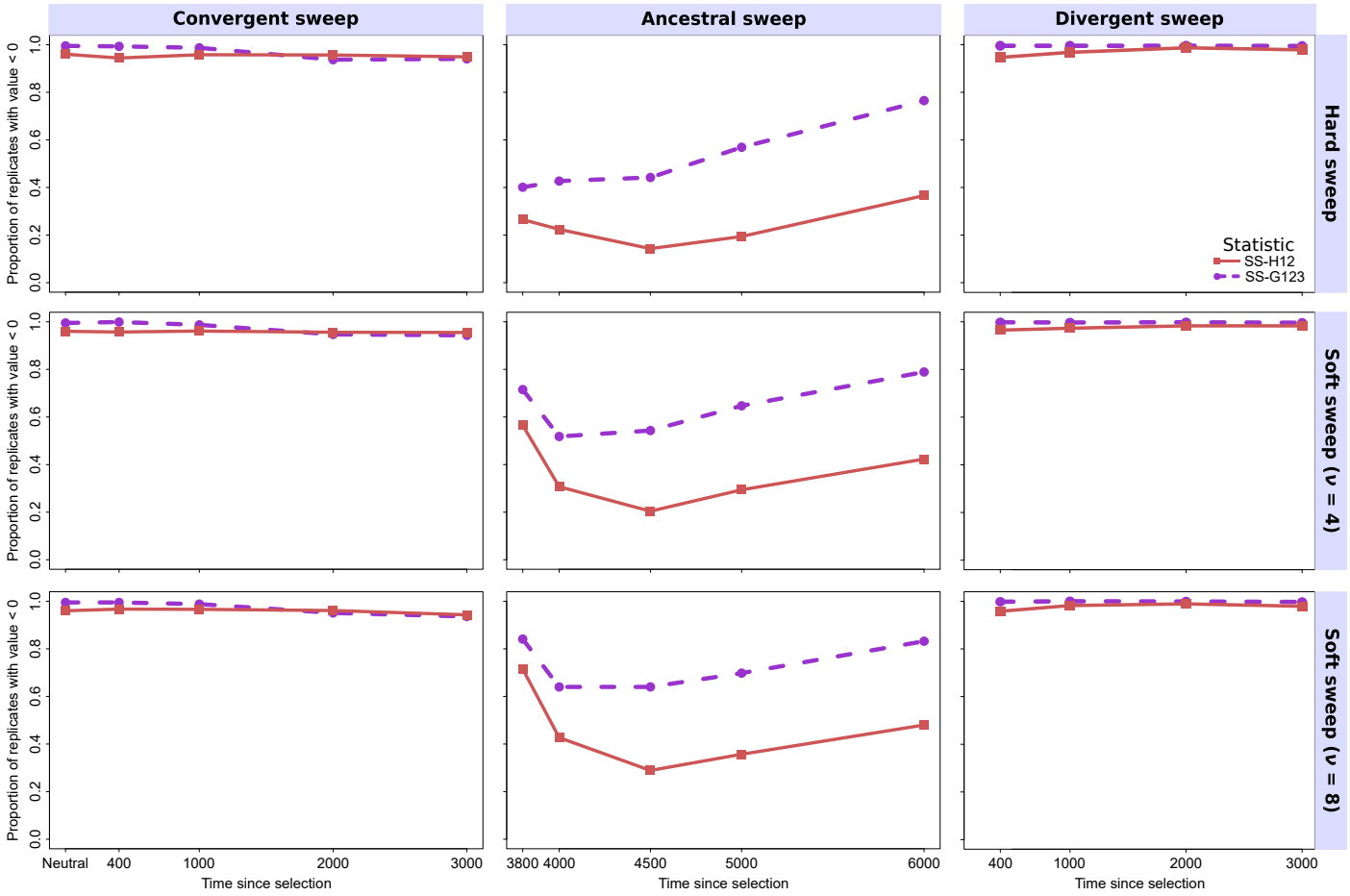

Figure S14 Proportion of negative SS-H12 (red) and SS-G123 (purple) scores across 1000 moderate ($s = 0.01$; $\sigma = 4N_e s = 800$) hard ($\nu = 1$) and soft ($\nu \in \{4, 8\}$) sweep replicates, and neutrality (first point on convergent sweep curve). Replicates were generated under the European-sub-Saharan African CEU-YRI demographic model and are identical to those in Figures 3 and S39.

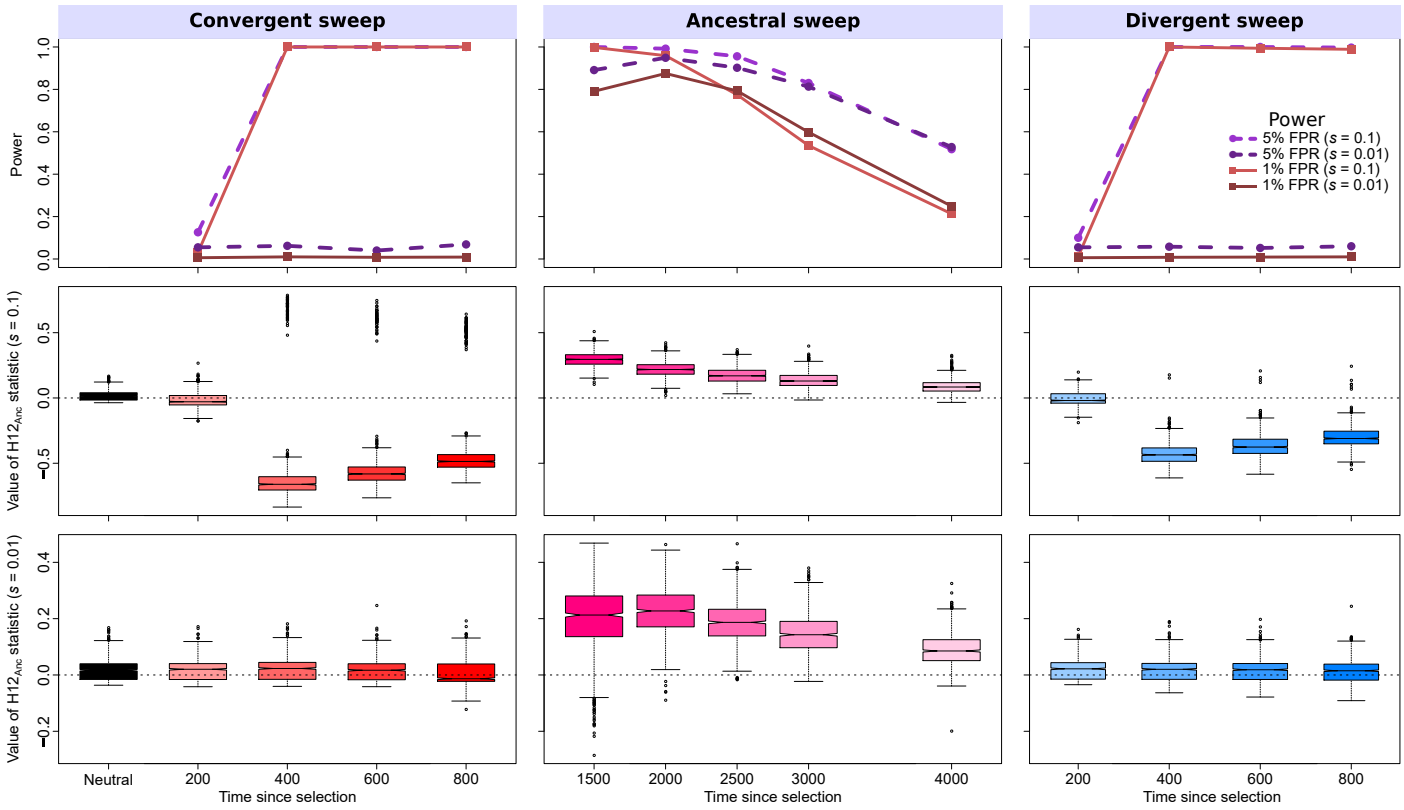

Figure S15 Properties of uncorrected $H12_{Anc}$ for simulated strong ($s = 0.1; \sigma = 4N_e s = 4000$) and moderate ($s = 0.01; \sigma = 400$) hard sweep scenarios under the CEU-GIH model ($\tau = 1100$ generations, or 0.055 coalescent units, before sampling). Data analyzed are identical to those in Figure 2. (Top row) Power at 1% (red) and 5% (purple) false positive rates (FPRs) to detect recent ancestral, convergent, and divergent hard sweeps, with FPR based on the distribution of maximum $|H12_{Anc}|$ across simulated neutral replicates. (Middle row) Box plots summarizing the distribution of $H12_{Anc}$ values from windows of maximum $|H12_{Anc}|$ across strong sweep replicates, with dashed lines in each panel representing $H12_{Anc} = 0$. (Bottom row) Box plots summarizing the distribution of $H12_{Anc}$ values across moderate sweep replicates.

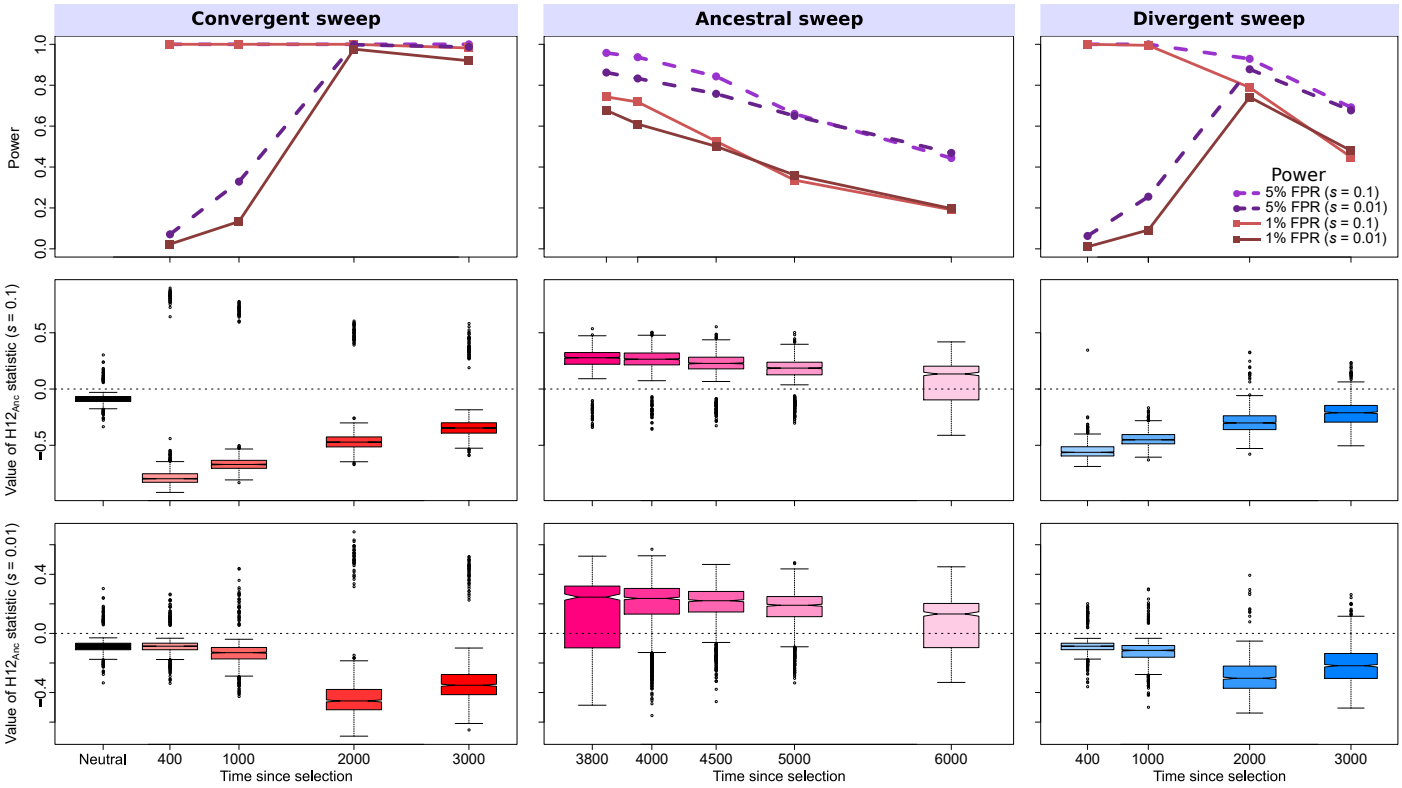

Figure S16 Properties of uncorrected $H12_{Anc}$ for simulated strong ($s = 0.1; \sigma = 4N_e s = 8000$) and moderate ($s = 0.01; \sigma = 800$) hard sweep scenarios under the CEU-YRI model ($\tau = 3740$ generations, or 0.0935 coalescent units, before sampling). Data analyzed are identical to those in Figure 3. (Top row) Power at 1% (red) and 5% (purple) false positive rates (FPRs) to detect recent ancestral, convergent, and divergent hard sweeps, with FPR based on the distribution of maximum $|H12_{Anc}|$ across simulated neutral replicates. (Middle row) Box plots summarizing the distribution of $H12_{Anc}$ values from windows of maximum $|H12_{Anc}|$ across strong sweep replicates, with dashed lines in each panel representing $H12_{Anc} = 0$. (Bottom row) Box plots summarizing the distribution of $H12_{Anc}$ values across moderate sweep replicates.

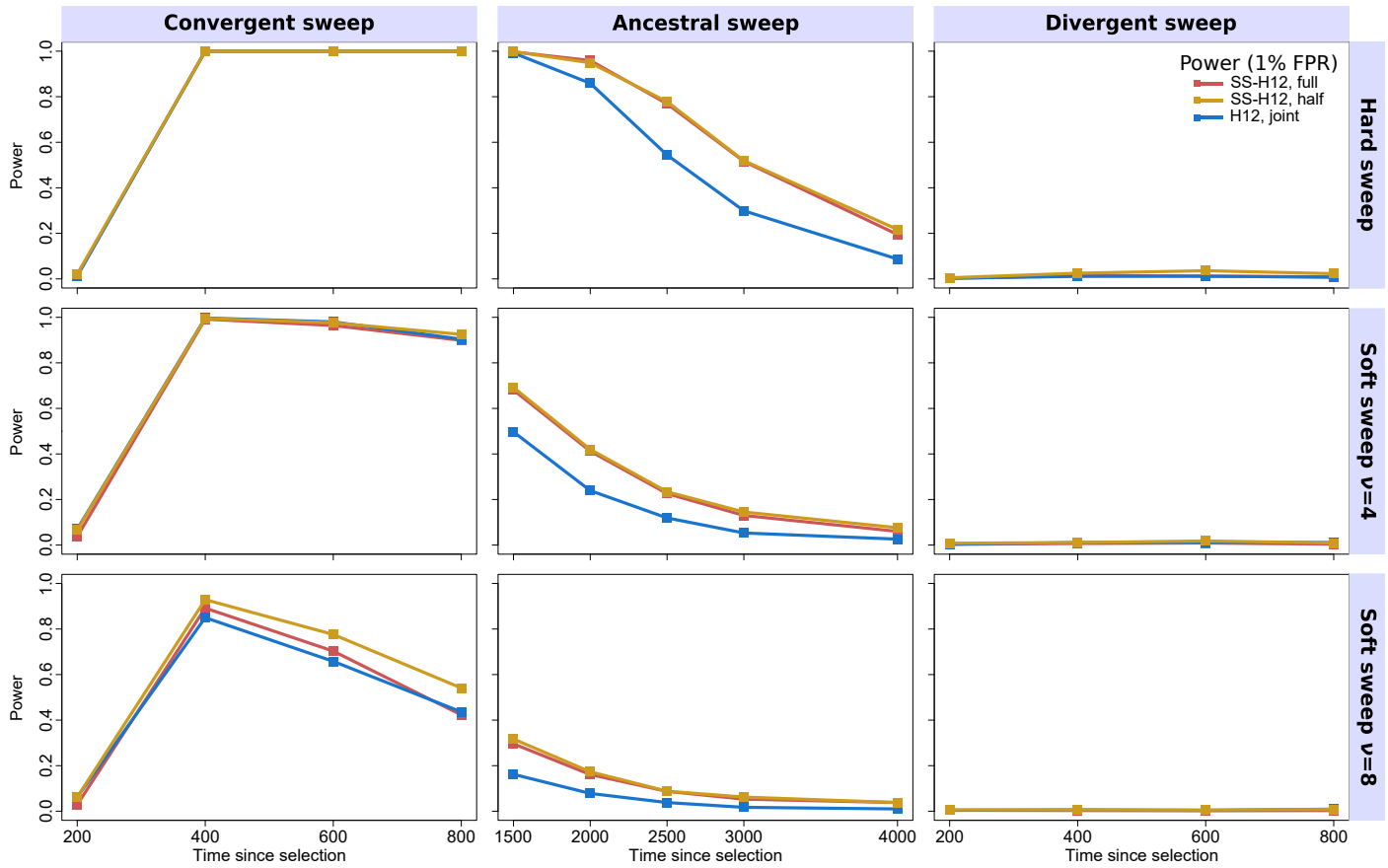

Figure S17 Powers of SS-H12 and H12 at a 1% false positive rate (FPR) to detect recent ancestral, convergent, and divergent simulated strong ($s = 0.1$; $\sigma = 4N_e s = 4000$) selective sweeps under the CEU-GIH model ($\tau = 1100$ generations, or 0.055 coalescent units, before sampling) for hard (top) and soft ($\nu = 4$, middle; $\nu = 8$, bottom) sweeps as a function of time at which positive selection of the favored allele initiated (t), with FPR based on the distribution of maximum |SS-H12| or H12 across simulated neutral replicates. "SS-H12, full" refers to analyses in which we generated full-size pooled samples consisting of 99 simulated CEU individuals and 103 simulated GIH individuals, whereas "SS-H12, half" used only half of the alleles in each sample. "H12, joint" analyses used the full sample size for both populations. For convergent and divergent sweeps, $t < \tau$, while for ancestral sweeps, $t > \tau$. We performed 1000 replicates for each scenario.

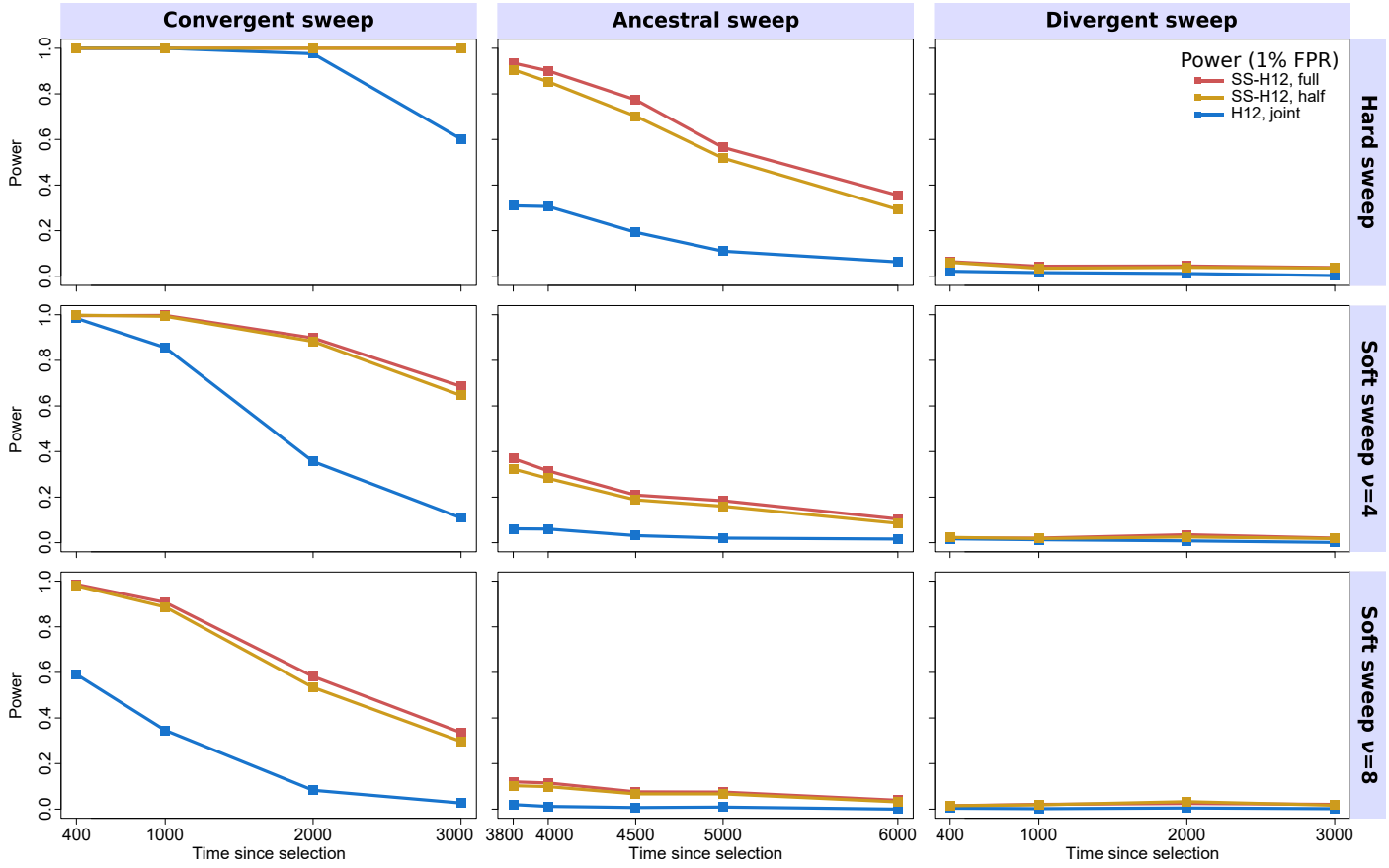

Figure S18 Powers of SS-H12 and H12 at a 1% false positive rate (FPR) to detect recent ancestral, convergent, and divergent simulated strong ($s = 0.1$; $\sigma = 4N_e s = 8000$) selective sweeps under the CEU-YRI model ($\tau = 3740$ generations, or 0.0935 coalescent units, before sampling) for hard (top) and soft ($\nu = 4$, middle; $\nu = 8$, bottom) sweeps as a function of time at which positive selection of the favored allele initiated (t), with FPR based on the distribution of maximum |SS-H12| or H12 across simulated neutral replicates. "SS-H12, full" refers to analyses in which we generated full-size pooled samples consisting of 99 simulated CEU individuals and 108 simulated YRI individuals, while "SS-H12, half" used only half of the alleles in each sample. "H12, joint" analyses used the full sample size for both populations. For convergent and divergent sweeps, $t < \tau$, while for ancestral sweeps, $t > \tau$. We performed 1000 replicates for each scenario.

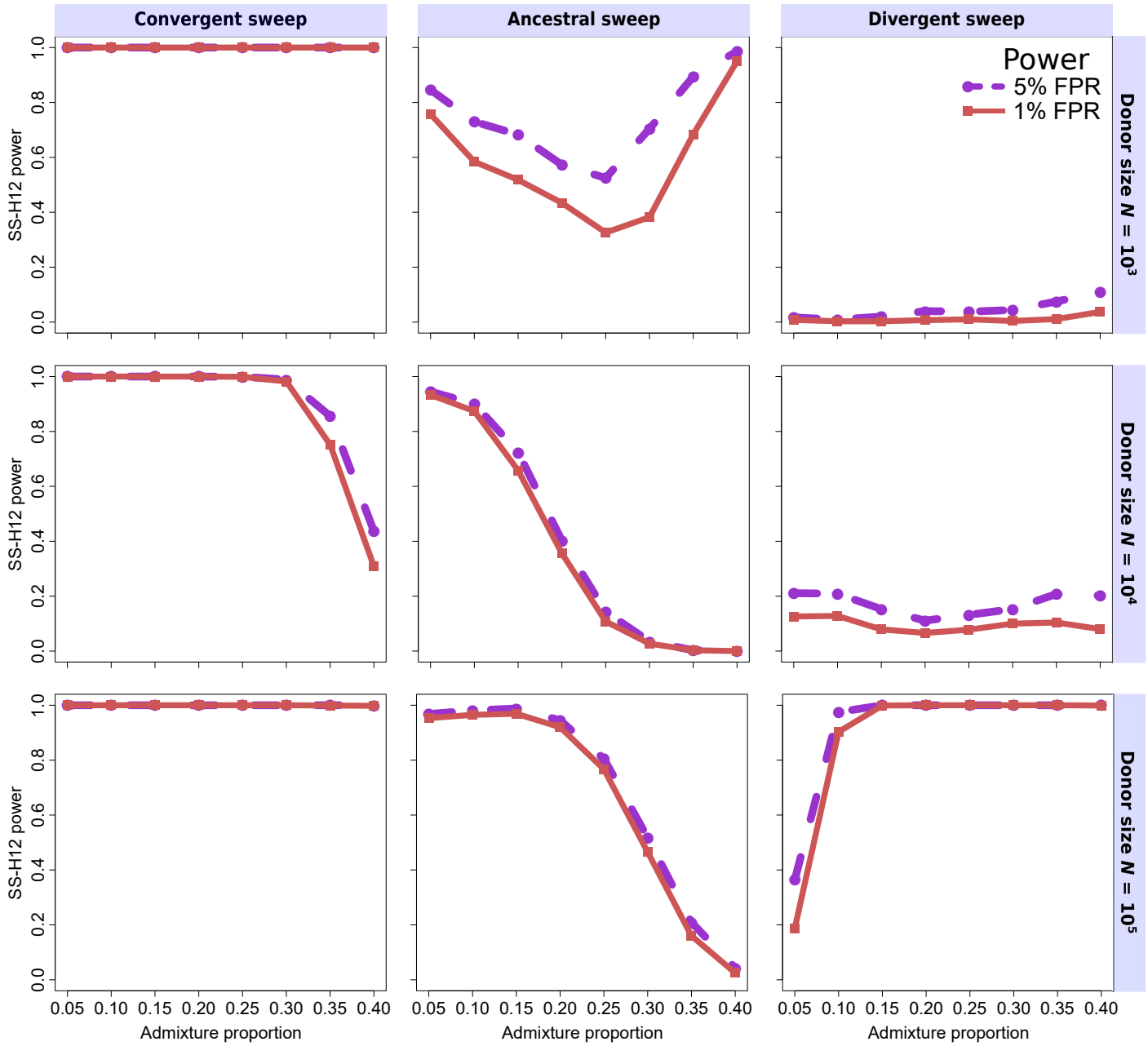

Figure S19 Power at 1 and 5% false positive rates (FPRs) to detect recent strong ($s = 0.1$; $\sigma = 4N_e s = 4000$) ancestral, convergent, and divergent hard sweeps (see Figure 1) as a function of admixture proportion, with false positive rate based on the distribution of maximum |SS-H12| across simulated neutral replicates under a given admixture scenario. Data here are simulated as in Figure 4, with scenarios of admixture proportion 0.2, 0.3, and 0.4 identical to Figure 4.

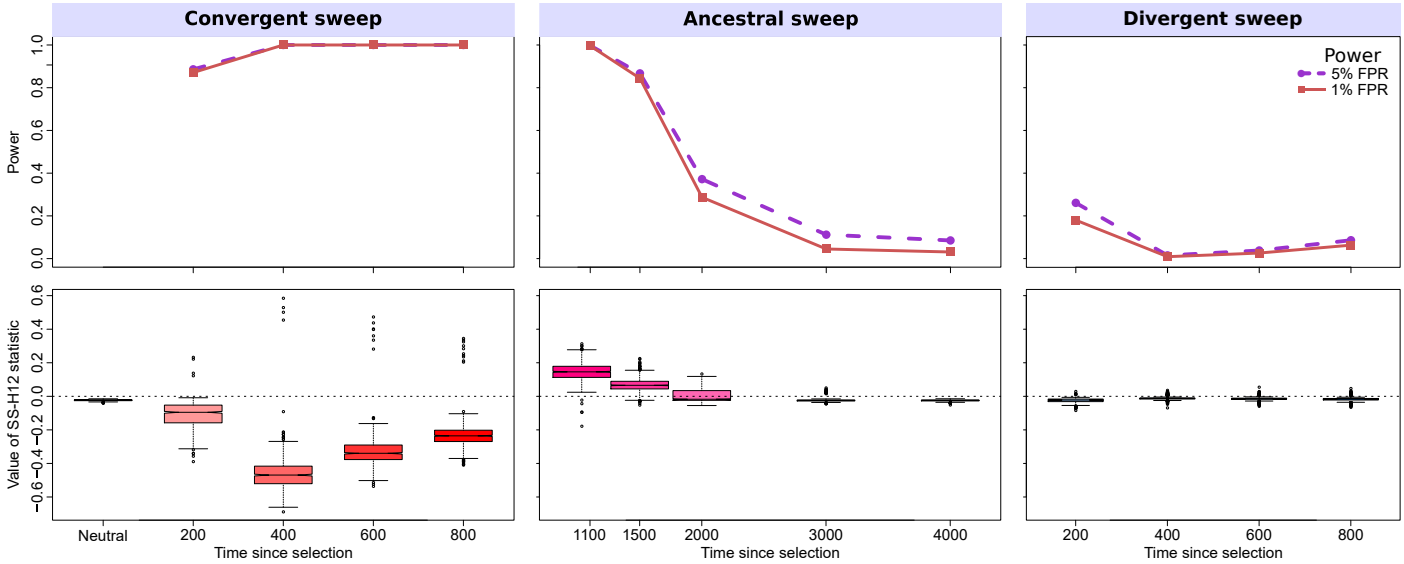

Figure S20 Properties of SS-H12 for simulated strong ($s = 0.1; \sigma = 4N_e s = 4000$) hard sweep scenarios under the simplified mammalian model ($K = 2$, $\tau = 1000$ generations, or 0.05 coalescent units, before sampling) for a sample consisting of individuals unevenly drawn from each subpopulation ($n_1 = 180$ diploids, $n_2 = 20$). (Top row) Power at 1% (red) and 5% (purple) false positive rates (FPRs) to detect recent ancestral, convergent, and divergent hard sweeps, with FPR based on the distribution of maximum |SS-H12| across simulated neutral replicates. (Bottom row) Box plots summarizing the distribution of SS-H12 values from windows of maximum |SS-H12| across strong sweep replicates, corresponding to each time point in the power curves, with dashed lines in each panel representing SS-H12 = 0. Other than choice of sample size, protocol was identical to that of experiments in Figure S9.

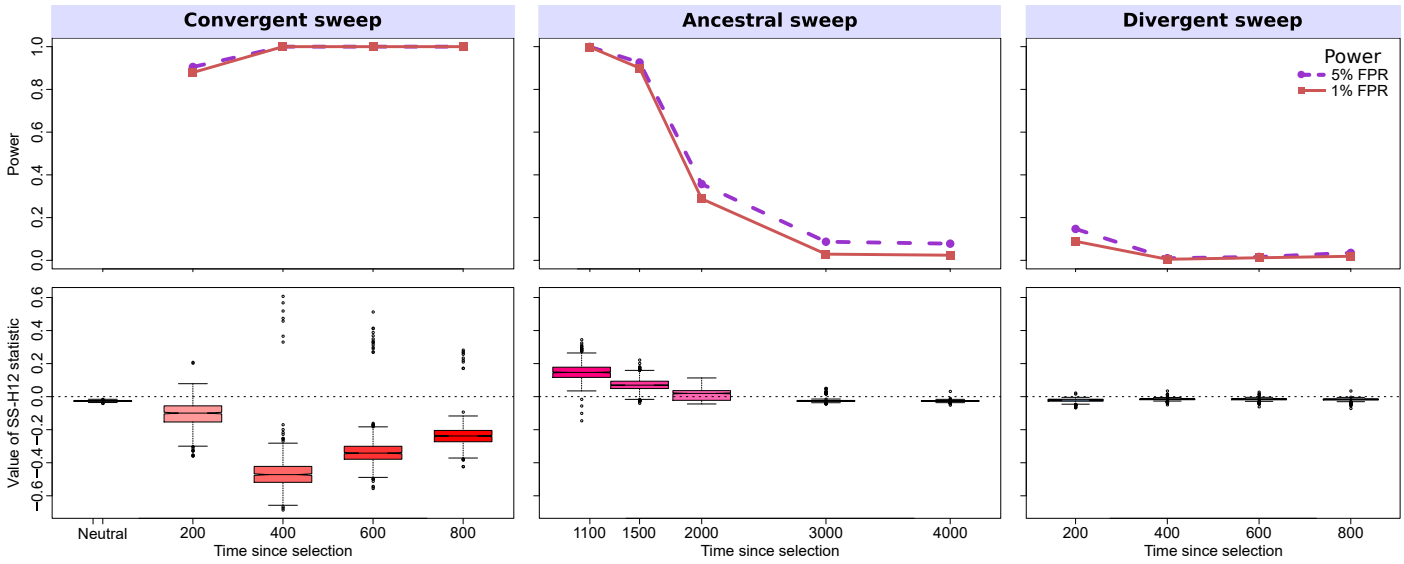

Figure S21 Properties of SS-H12 for simulated strong ($s = 0.1; \sigma = 4N_e s = 4000$) hard sweep scenarios under the simplified mammalian model ($K = 2$, $\tau = 1000$ generations, or 0.05 coalescent units, before sampling) for a sample consisting of individuals unevenly drawn from each subpopulation ($n_1 = 160$ diploids, $n_2 = 40$). (Top row) Power at 1% (red) and 5% (purple) false positive rates (FPRs) to detect recent ancestral, convergent, and divergent hard sweeps, with FPR based on the distribution of maximum |SS-H12| across simulated neutral replicates. (Bottom row) Box plots summarizing the distribution of SS-H12 values from windows of maximum |SS-H12| across strong sweep replicates, corresponding to each time point in the power curves, with dashed lines in each panel representing SS-H12 = 0. Other than choice of sample size, protocol was identical to that of experiments in Figure S9.

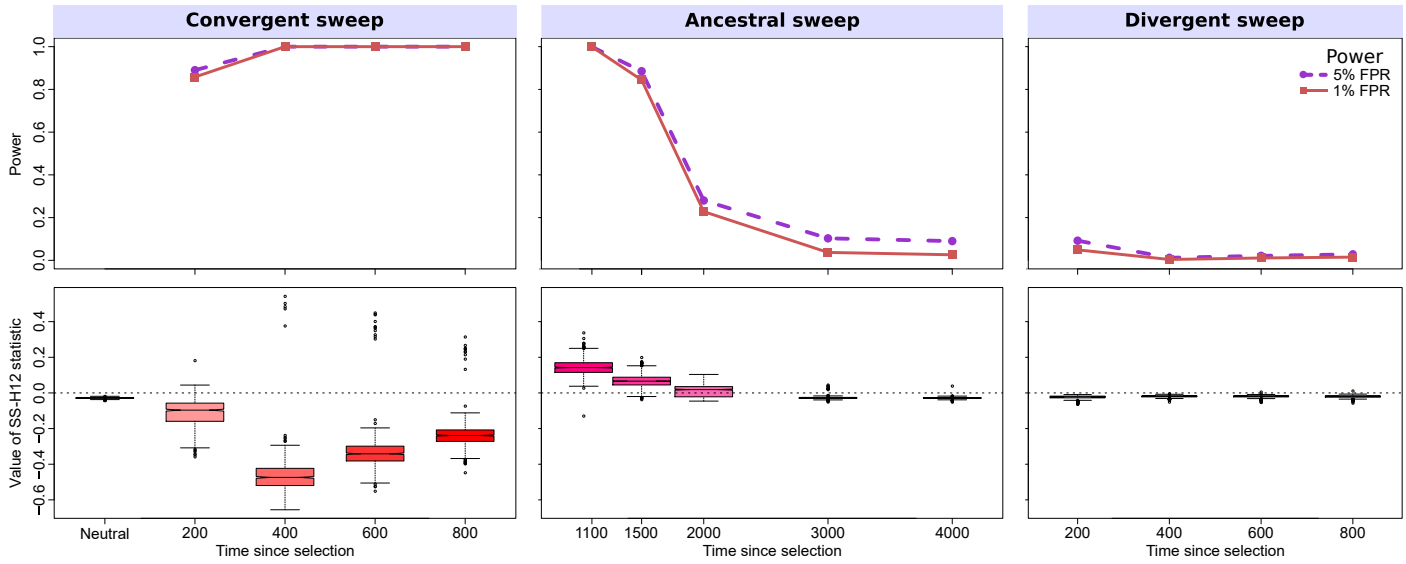

Figure S22 Properties of SS-H12 for simulated strong ($s = 0.1; \sigma = 4N_e s = 4000$) hard sweep scenarios under the simplified mammalian model ($K = 2$, $\tau = 1000$ generations, or 0.05 coalescent units, before sampling) for a sample consisting of individuals unevenly drawn from each subpopulation ($n_1 = 140$ diploids, $n_2 = 60$). (Top row) Power at 1% (red) and 5% (purple) false positive rates (FPRs) to detect recent ancestral, convergent, and divergent hard sweeps, with FPR based on the distribution of maximum |SS-H12| across simulated neutral replicates. (Bottom row) Box plots summarizing the distribution of SS-H12 values from windows of maximum |SS-H12| across strong sweep replicates, corresponding to each time point in the power curves, with dashed lines in each panel representing SS-H12 = 0. Other than choice of sample size, protocol was identical to that of experiments in Figure S9.

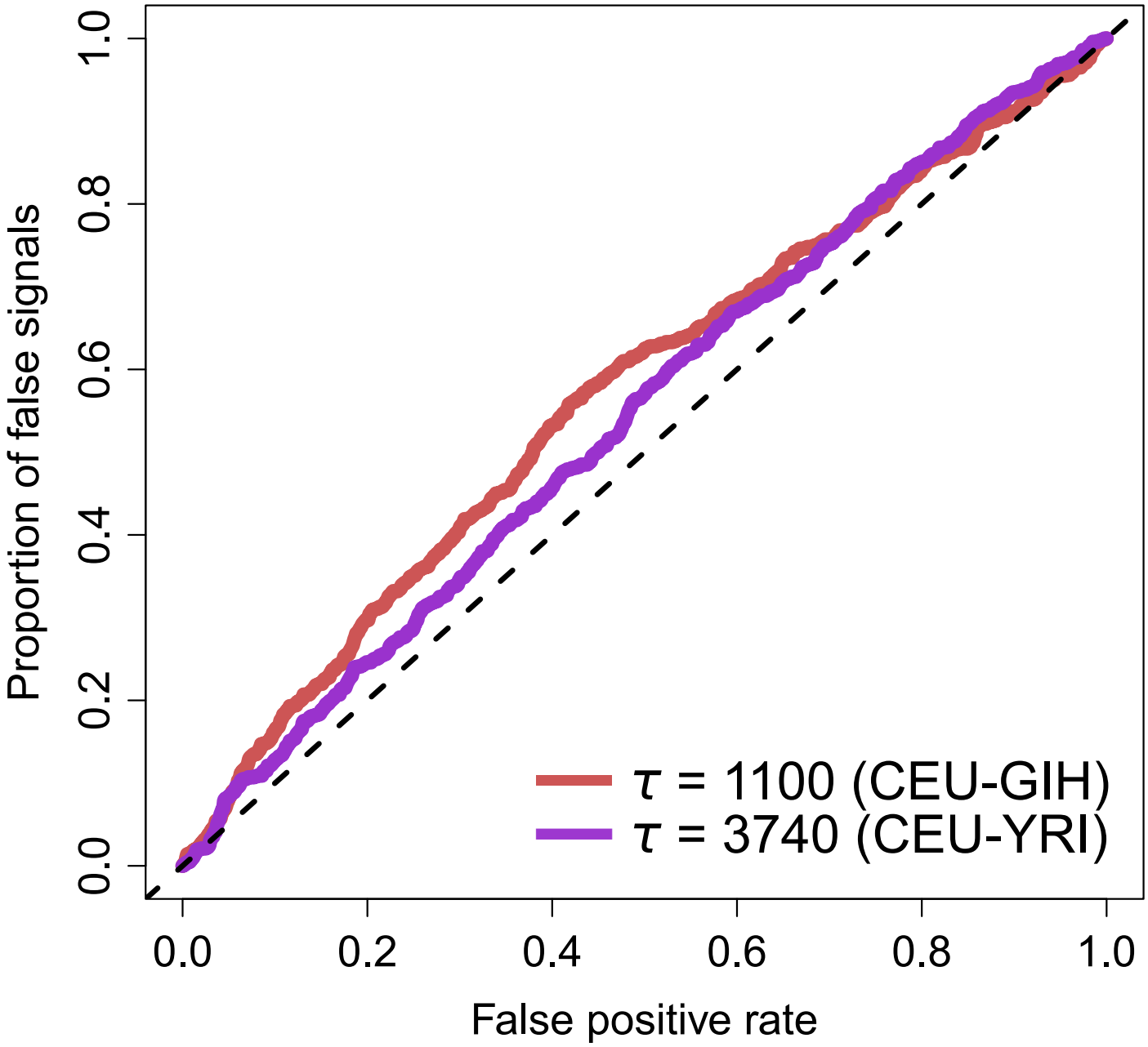

Figure S23 Proportion of false signals generated by background selection as a function of false positive rate based on neutrality for SS-H12 under CEU-GIH (red) or CEU-YRI (purple) demographic models. Neutral replicates used here are identical to those used across Figures 2, 3, and S5-S8. Background selection simulations, totaling 1000 replicates, were generated according to the procedure described in the *Materials and Methods*.

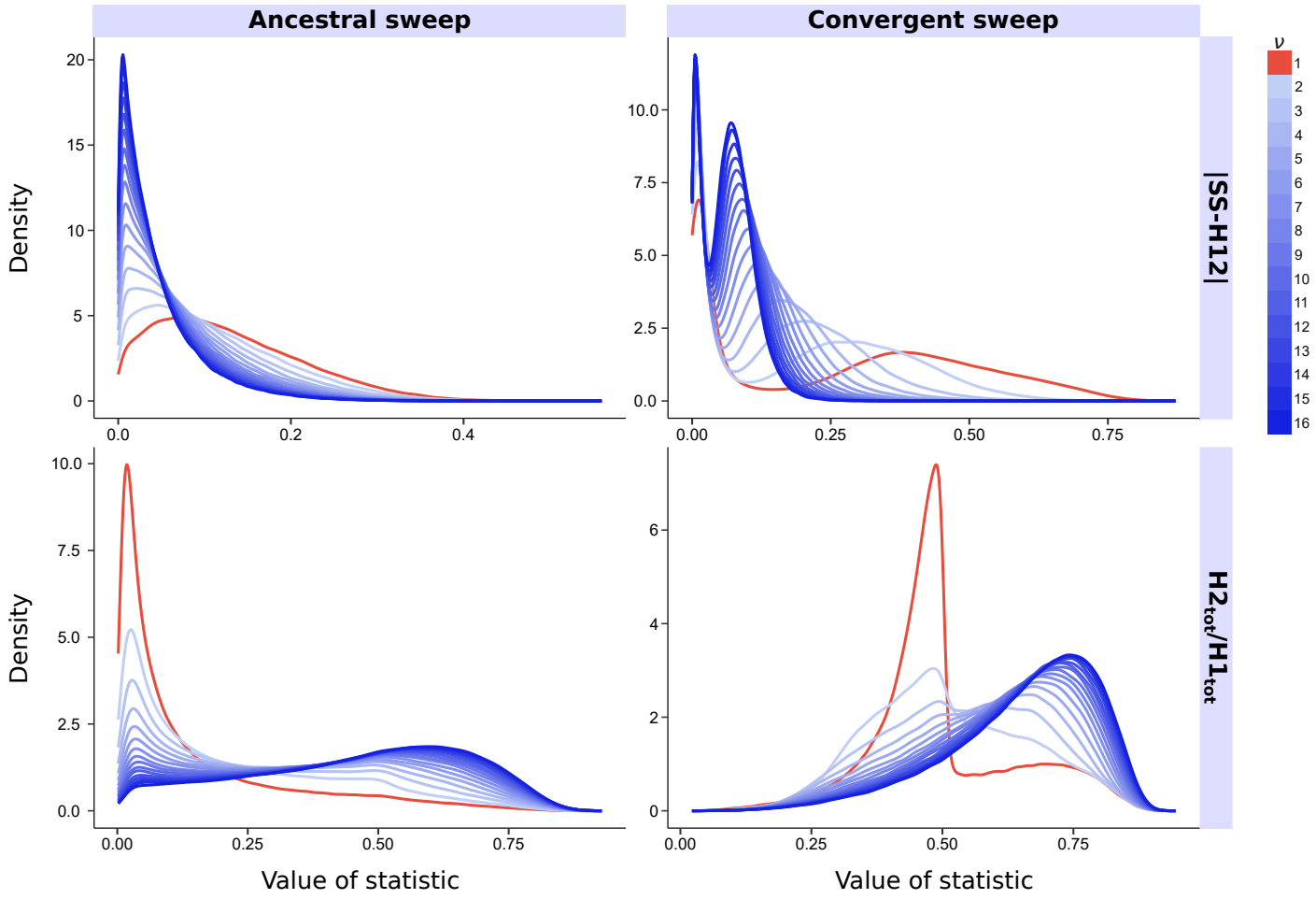

Figure S24 Probability density functions of |SS-H12| (top) and $H2_{Tot}/H1_{Tot}$ (bottom) for ancestral (left) and convergent (right) sweeps drawn from 5×10^6 replicates and $\nu \in \{1, 2, \ldots, 16\}$, for the CEU-GIH model. Data analyzed are identical to those in Figure 5.

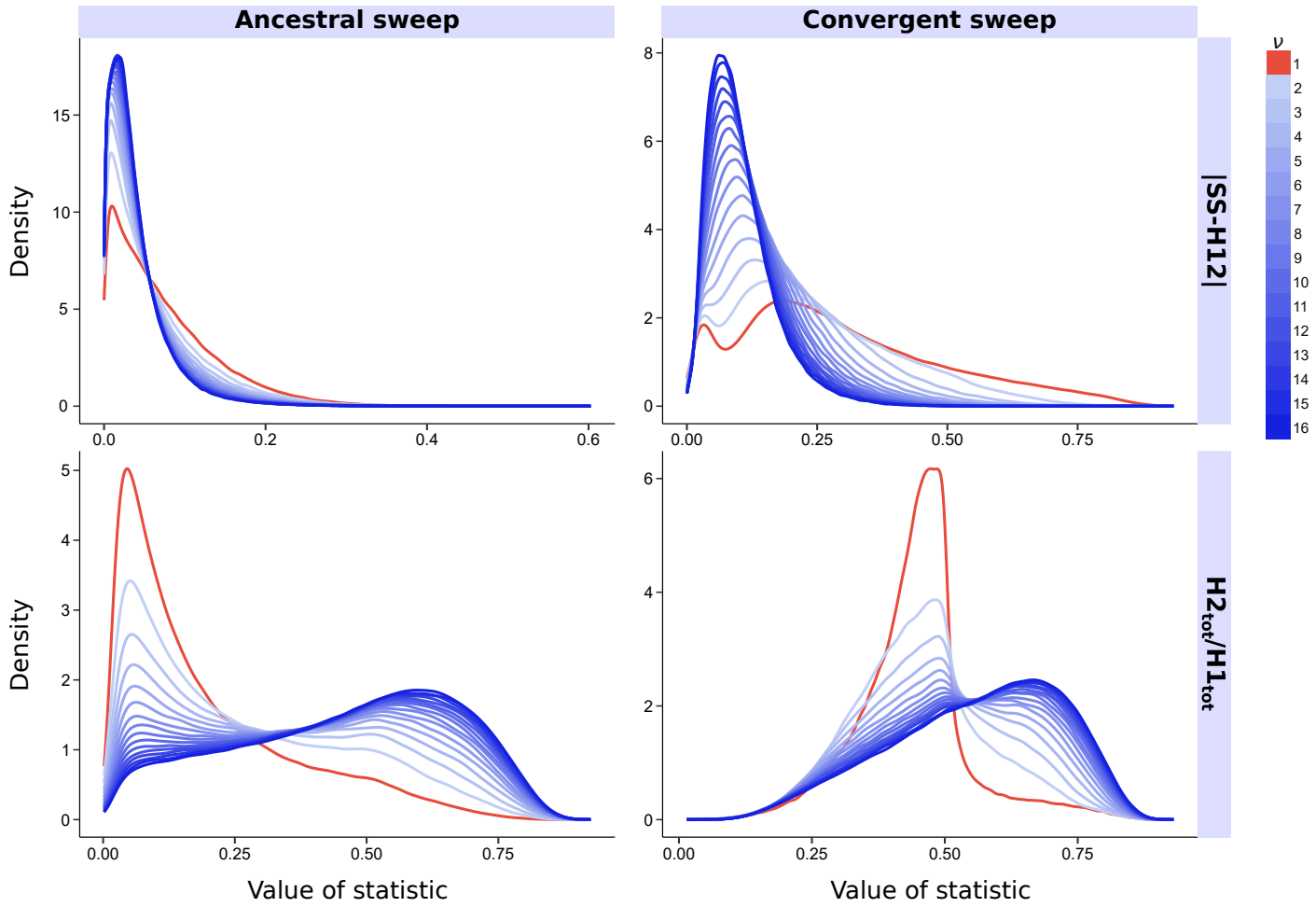

Figure S25 Probability density functions of |SS-H12| (top) and $H2_{Tot}/H1_{Tot}$ (bottom) for ancestral (left) and convergent (right) sweeps drawn from 5×10^6 replicates and $\nu \in \{1, 2, \ldots, 16\}$, for the CEU-YRI model. Data analyzed are identical to those in Figure 5.

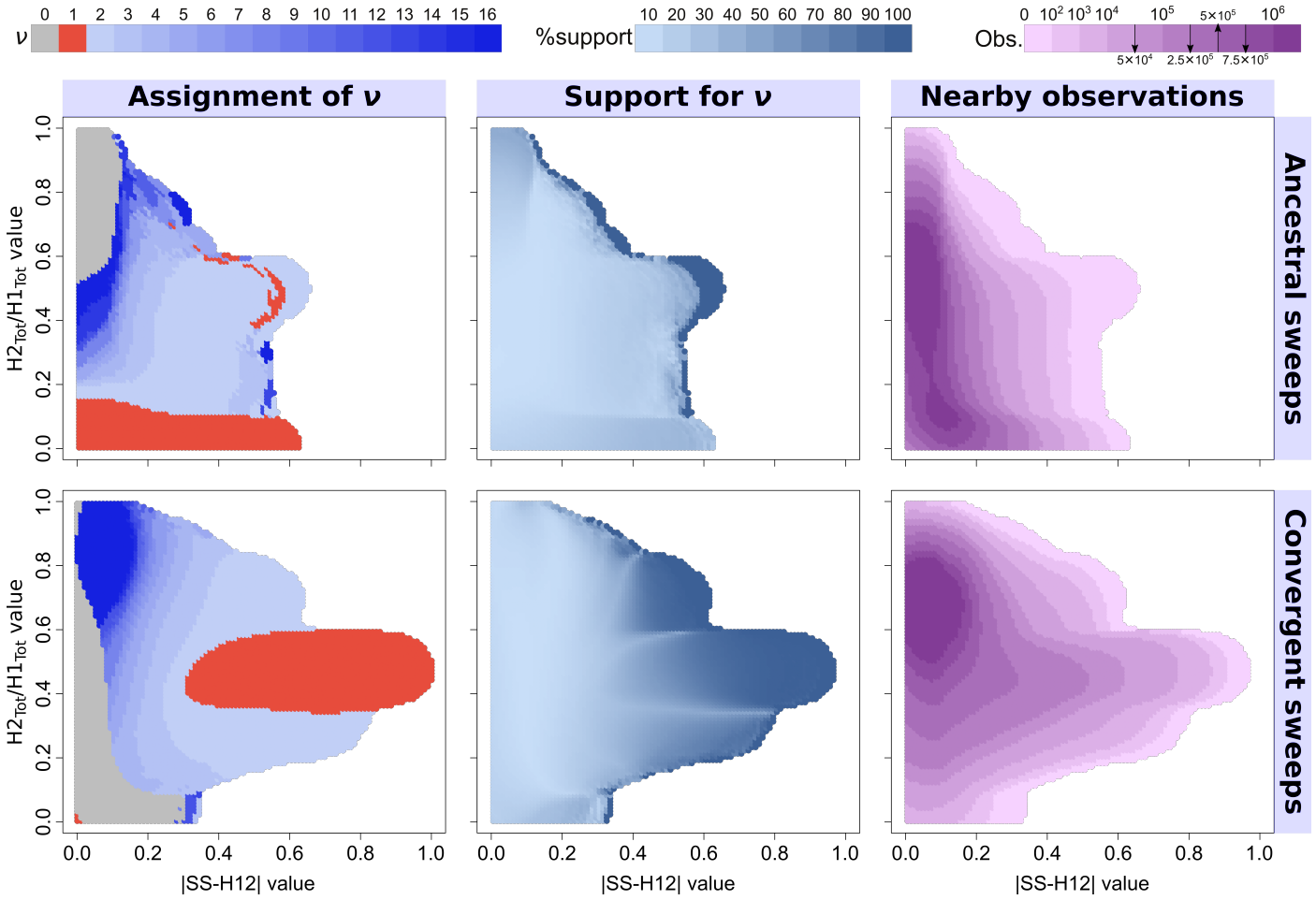

Figure S26 Expansion of Figure 5 for CEU-GIH population model. (Left) Results from Figure 5 for ancestral (top) and convergent (bottom) sweeps. (Center) Indicator of support level for each assigned ν across the paired $(|\text{SS-H12}|, \text{H2}_{\text{Tot}}/\text{H1}_{\text{Tot}})$ classification grids. (Right) Number of observations upon which assignment of ν was based.

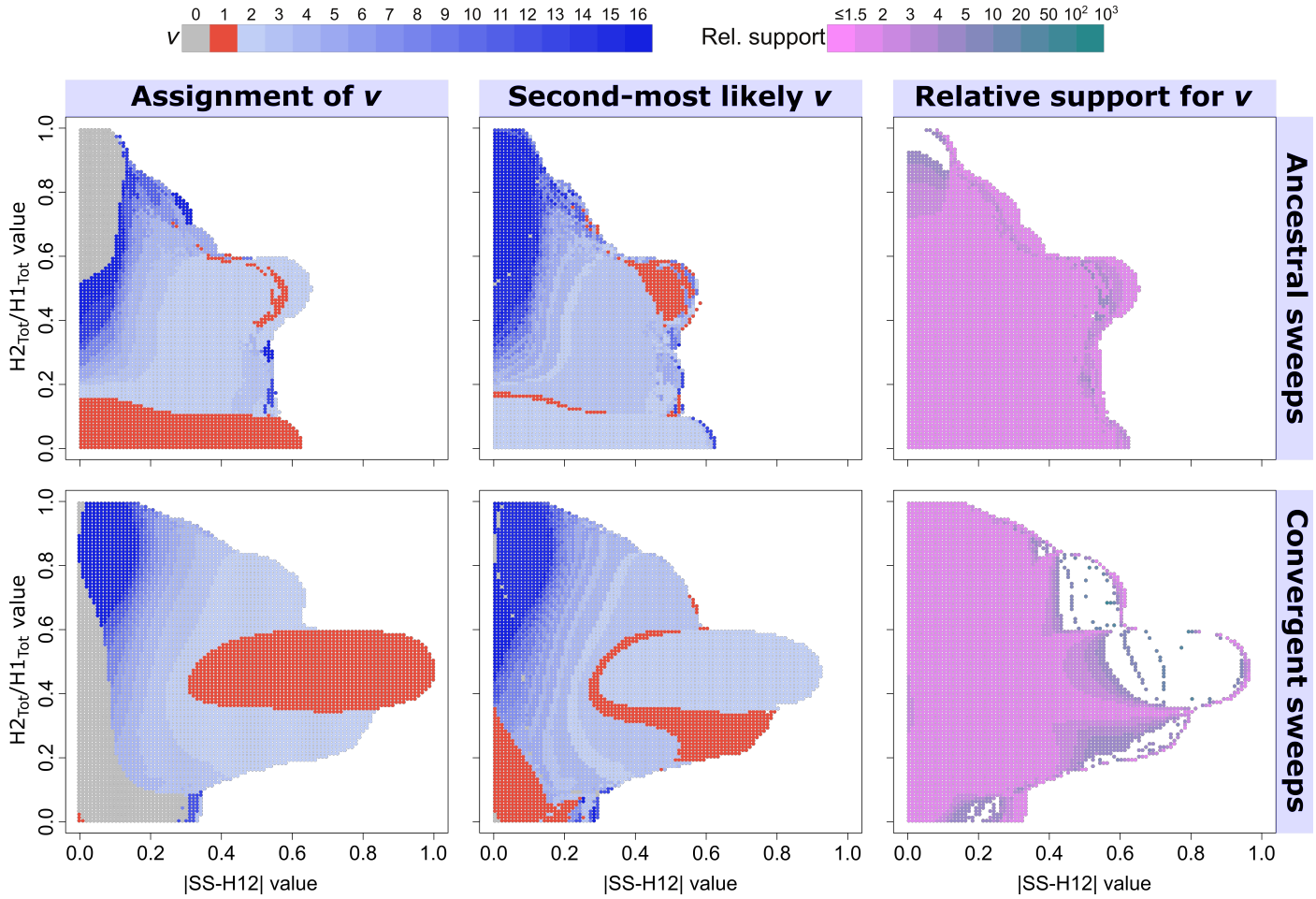

Figure S27 Complement to Figure S26 (CEU-GIH history). (Left) Results from Figure 5 for ancestral (top) and convergent (bottom) sweeps. (Center) Coloration of points indicating the second-most likely ν for paired $(|\text{SS-H12}|, \text{H2}_{\text{Tot}}/\text{H1}_{\text{Tot}})$ values. (Right) Relative support for most likely assigned ν, computed as support for the most likely ν divided by support for the second-most likely ν. Note that gaps in the grid of plotted points in the Center and Right columns represent coordinates for which only one class of nearby observation was recorded, and so no second-most likely classification exists.

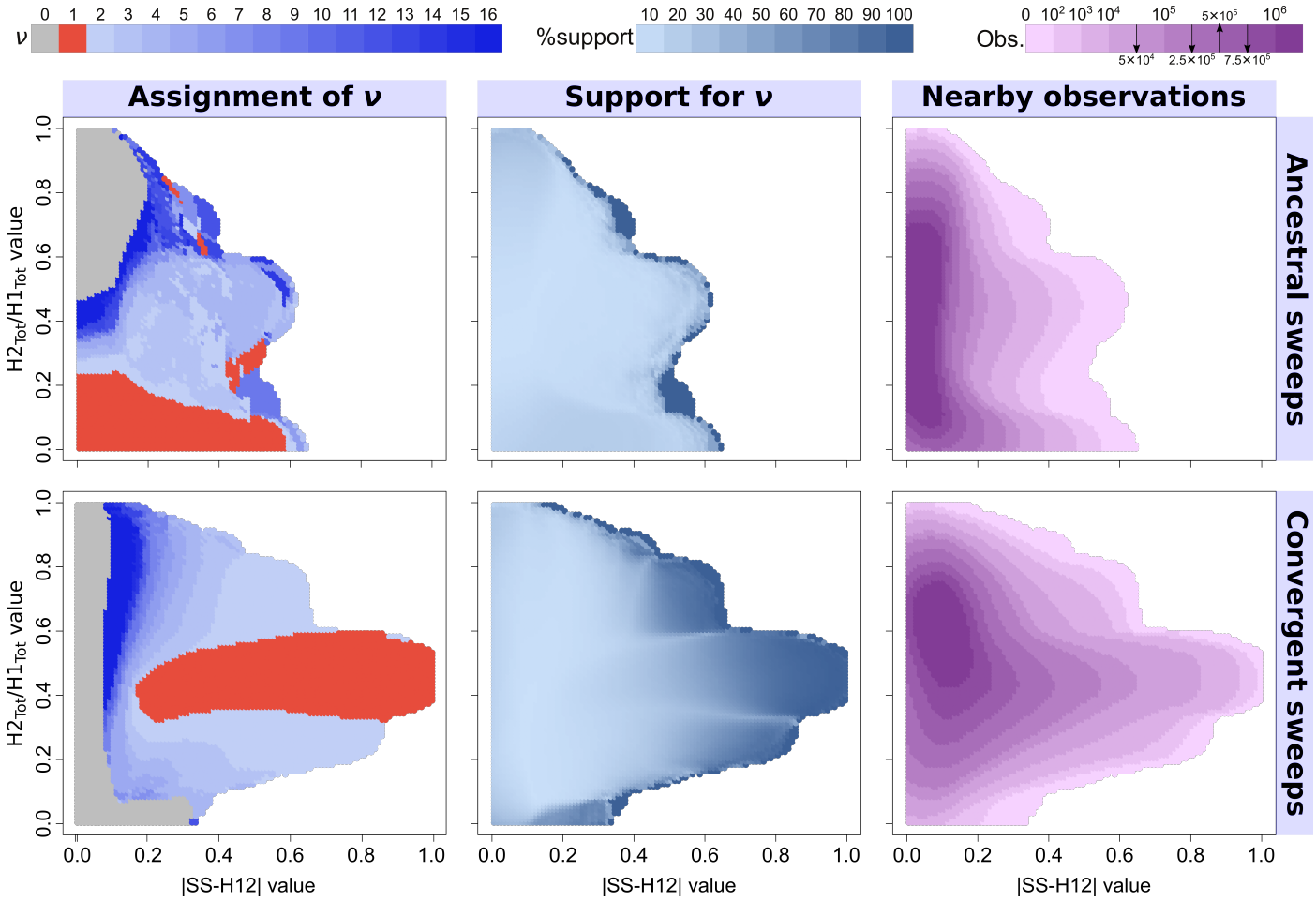

Figure S28 Expansion of Figure 5 for CEU-YRI population model. (Left) Results from Figure 5 for ancestral (top) and convergent (bottom) sweeps. (Center) Indicator of support level for each assigned ν across the paired $(|\text{SS-H12}|, \text{H2}_{\text{Tot}}/\text{H1}_{\text{Tot}})$ classification grids. (Right) Number of observations upon which assignment of ν was based.

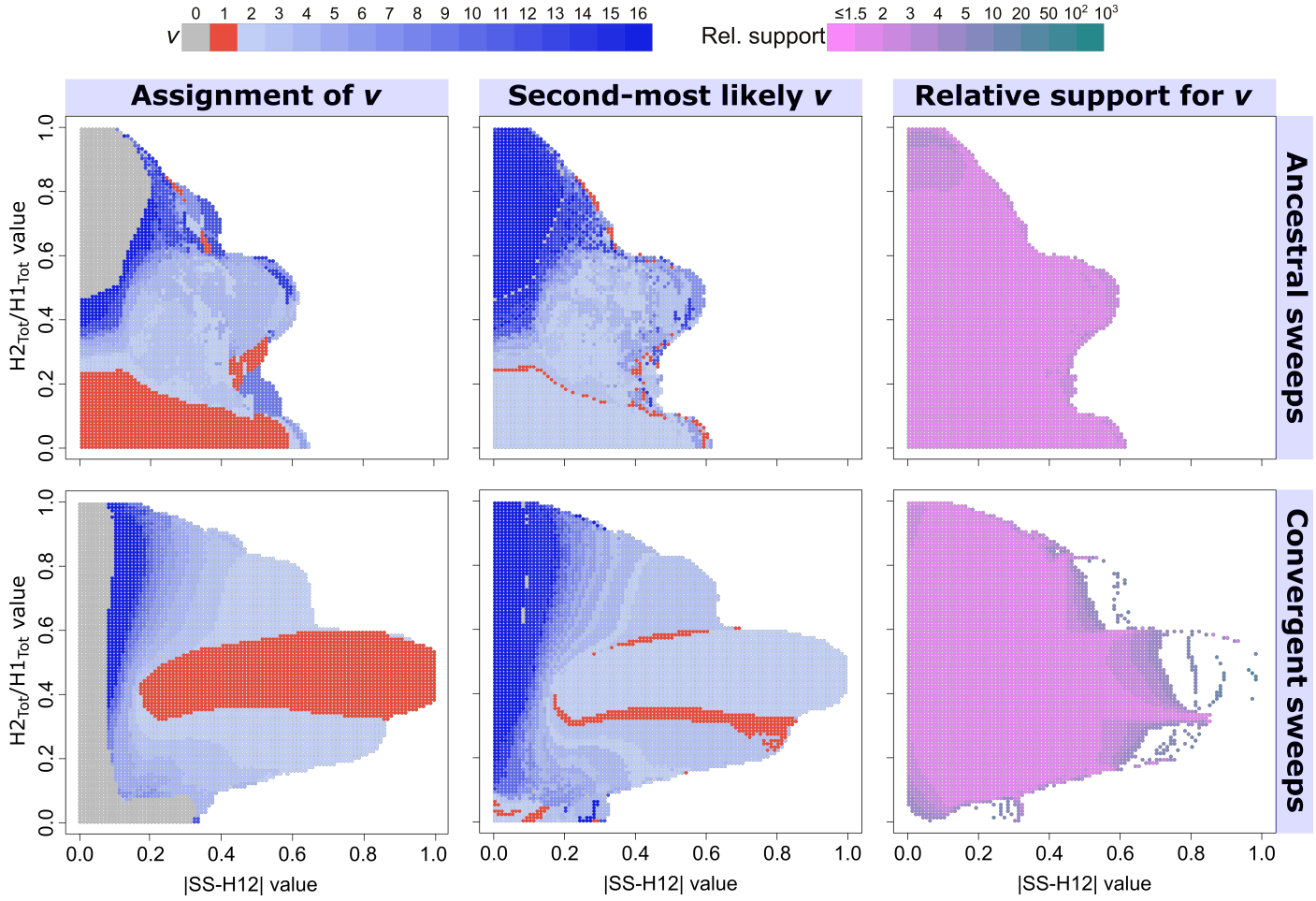

Figure S29 Complement to Figure S28 (CEU-YRI history). (Left) Results from Figure 5 for ancestral (top) and convergent (bottom) sweeps. (Center) Coloration of points indicating the second-most likely ν for paired $(|\text{SS-H12}|, \text{H2}_{\text{Tot}}/\text{H1}_{\text{Tot}})$ values. (Right) Relative support for most likely assigned ν, computed as support for the most likely ν divided by support for the second-most likely ν. Note that gaps in the grid of plotted points in the Center and Right columns represent coordinates for which only one class of nearby observation was recorded, and so no second-most likely classification exists.

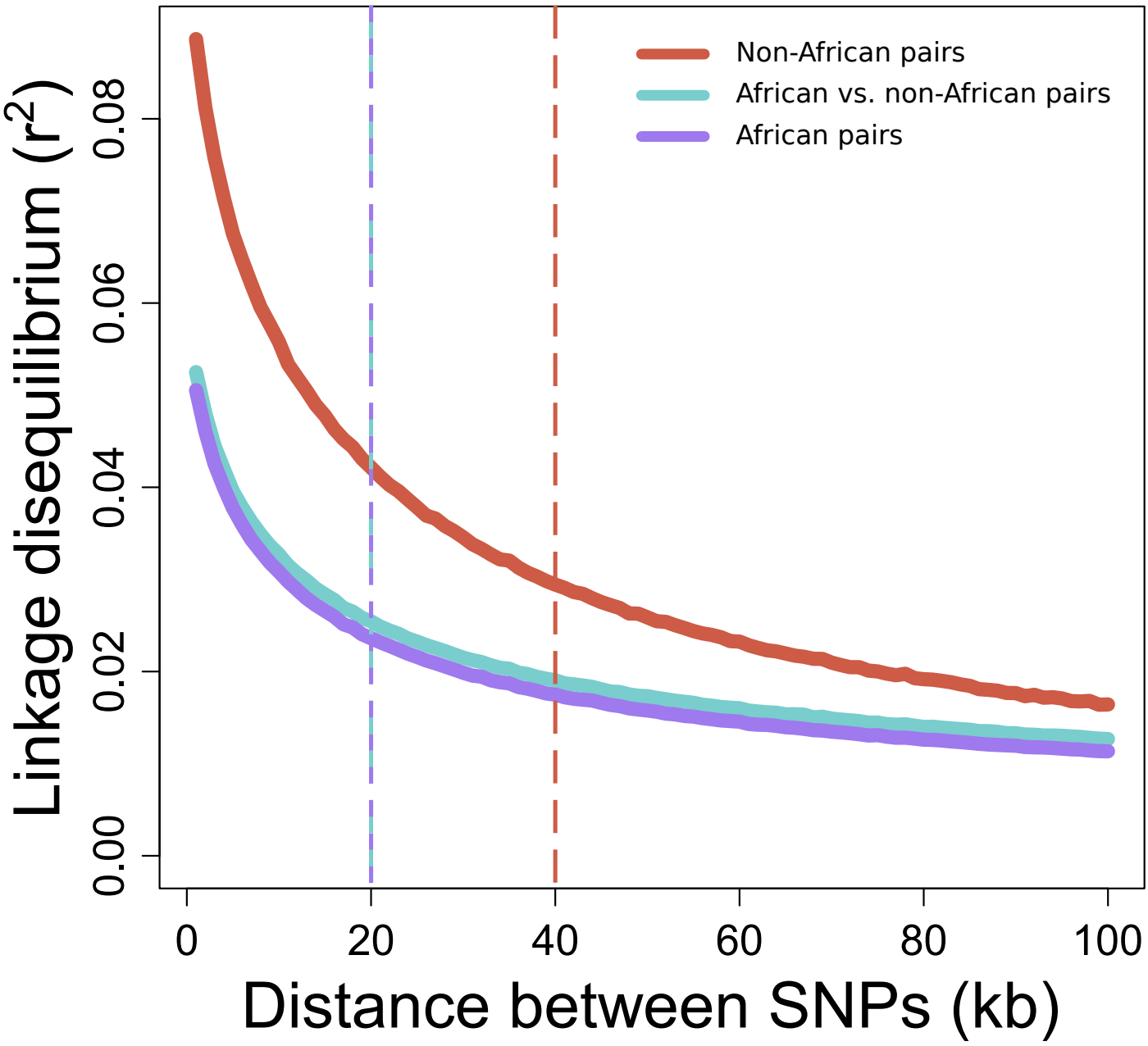

Figure S30 Mean decay of pairwise linkage disequilibrium (LD) measured by r^2 over one to 100 kb intervals downstream of each SNP for pooled population pair samples from the 1000 Genomes Project dataset (Auton *et al.* 2015). We used the pooled CEU-JPT sample as representative of LD between non-African population pairs (red), the pooled CEU-YRI population as representative of LD between African and non-African population pairs (cyan), and the pooled LWK-YRI population as representative of the LD between African population pairs (purple). All samples are identical to those analyzed in the *Results* section.

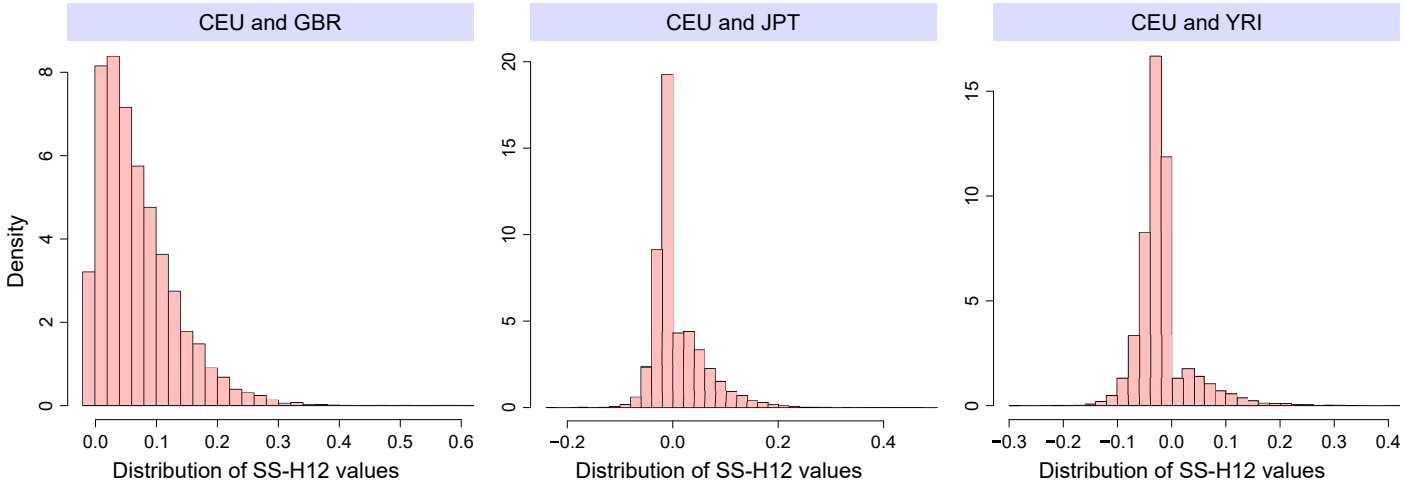

Figure S31 Empirical distributions of SS-H12 values assigned to each protein- and mRNA-coding gene based on the analysis of individuals from the 1000 Genomes Project Consortium (Auton *et al.* 2015) for three population comparisons with CEU. (Left) Distribution of SS-H12 values between the closely-related CEU and GBR populations of European descent. (Middle) Distribution of SS-H12 values between CEU and the East Asian JPT populations, representing a pair that diverged since the out-of-Africa event. (Right) Distribution of SS-H12 values between CEU and the sub-Saharan African YRI populations, representing a distantly-related population pair. SS-H12 is assigned to each gene from the window of maximum |SS-H12| falling between the transcription start and stop of the gene.

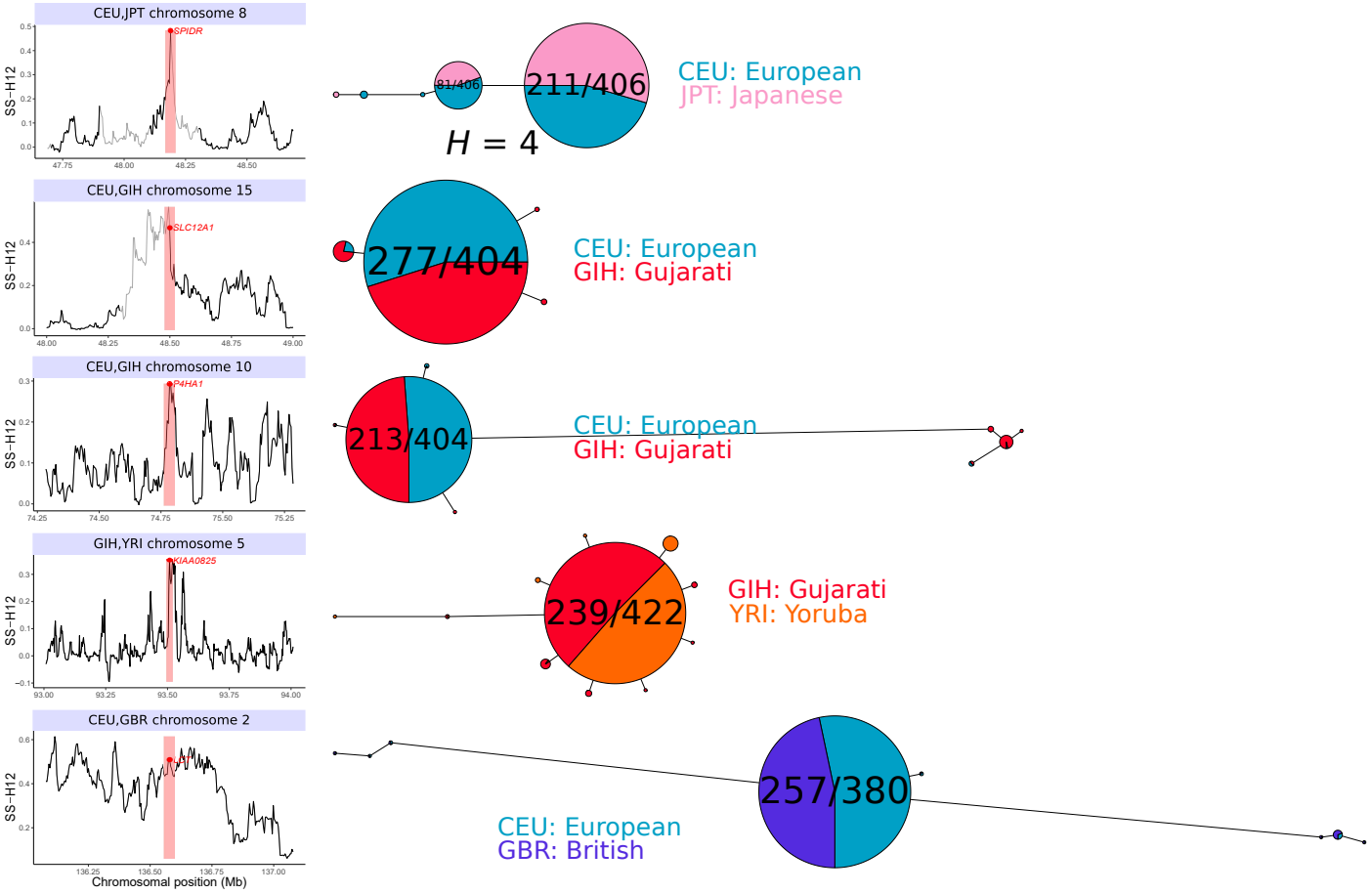

Figure S32 Highlighted outlying ancestral sweep candidates across RNA- and protein-coding genes in global human populations. The signal peak, including chromosomal position, magnitude, and highlighted window of maximum SS-H12 (left column), as well as the haplotype network for the window (Paradis 2010) are displayed for each candidate. The European CEU and East Asian JPT share a soft sweep ($\nu = 2$) at *SPIDR* in which the sweeping haplotypes differ at $H = 4$ sites (top row). The South Asian GIH population shares hard sweeps ($\nu = 1$) with CEU at *SLC12A1* (second row) and *P4HA1* (third row). The GIH and sub-Saharan African YRI populations share a hard sweep at *KIAA0825* (fourth row). Embedded within a cluster of putatively-selected genes is a hard sweep at *LCT* shared between the European CEU and GBR populations (bottom row). Haplotype networks are truncated to retain only haplotypes with an observed count ≥ 6. The number of haplotypes belonging to the sweeping class(es) is indicated as a fraction.

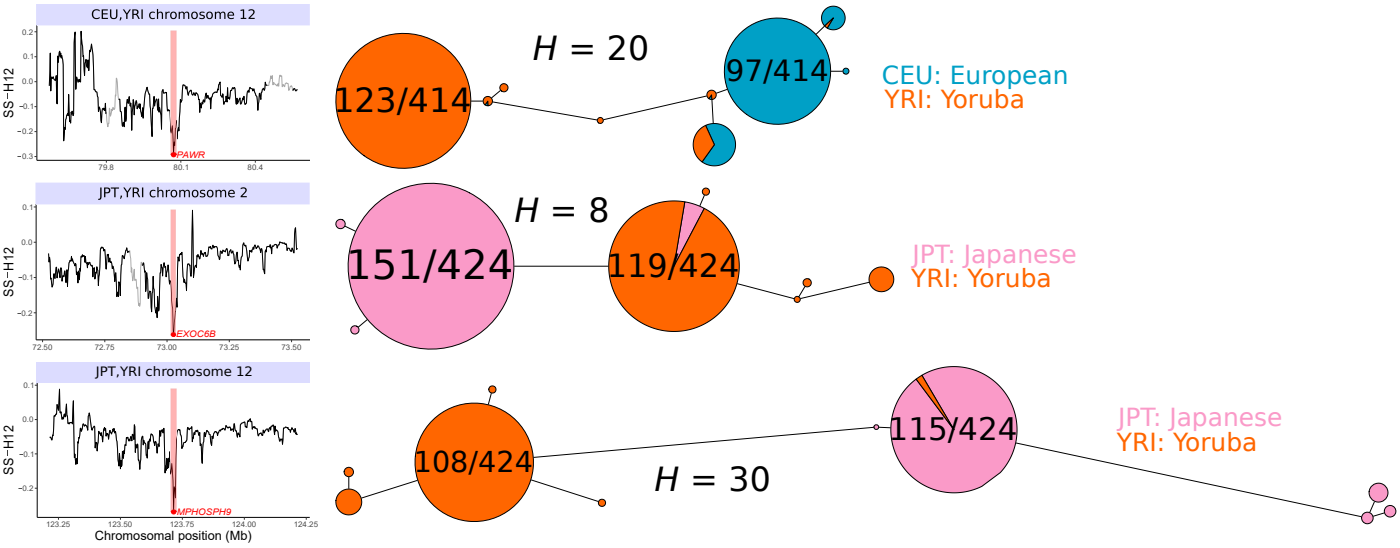

Figure S33 Highlighted outlying convergent sweep candidates across RNA- and protein-coding genes in global human populations. The signal peak, including chromosomal position, magnitude, and highlighted window of maximum SS-H12 (left column), as well as the haplotype network for the window (Paradis 2010) are displayed for each candidate. The European CEU and sub-Saharan African YRI populations each bear a unique high-frequency haplotype at *PAWR* (top row). Putative convergent sweeps between the YRI and East Asian JPT populations are observed at *EXOC6B* (middle row) and *MPHOSPH9* (bottom row). Each candidate was classified as hard ($\nu = 1$). Haplotype networks are truncated to retain only haplotypes with an observed count ≥ 6. The number of haplotypes belonging to the sweeping classes is indicated as a fraction. The Hamming distance (H) between putatively selected haplotypes is indicated for each candidate.

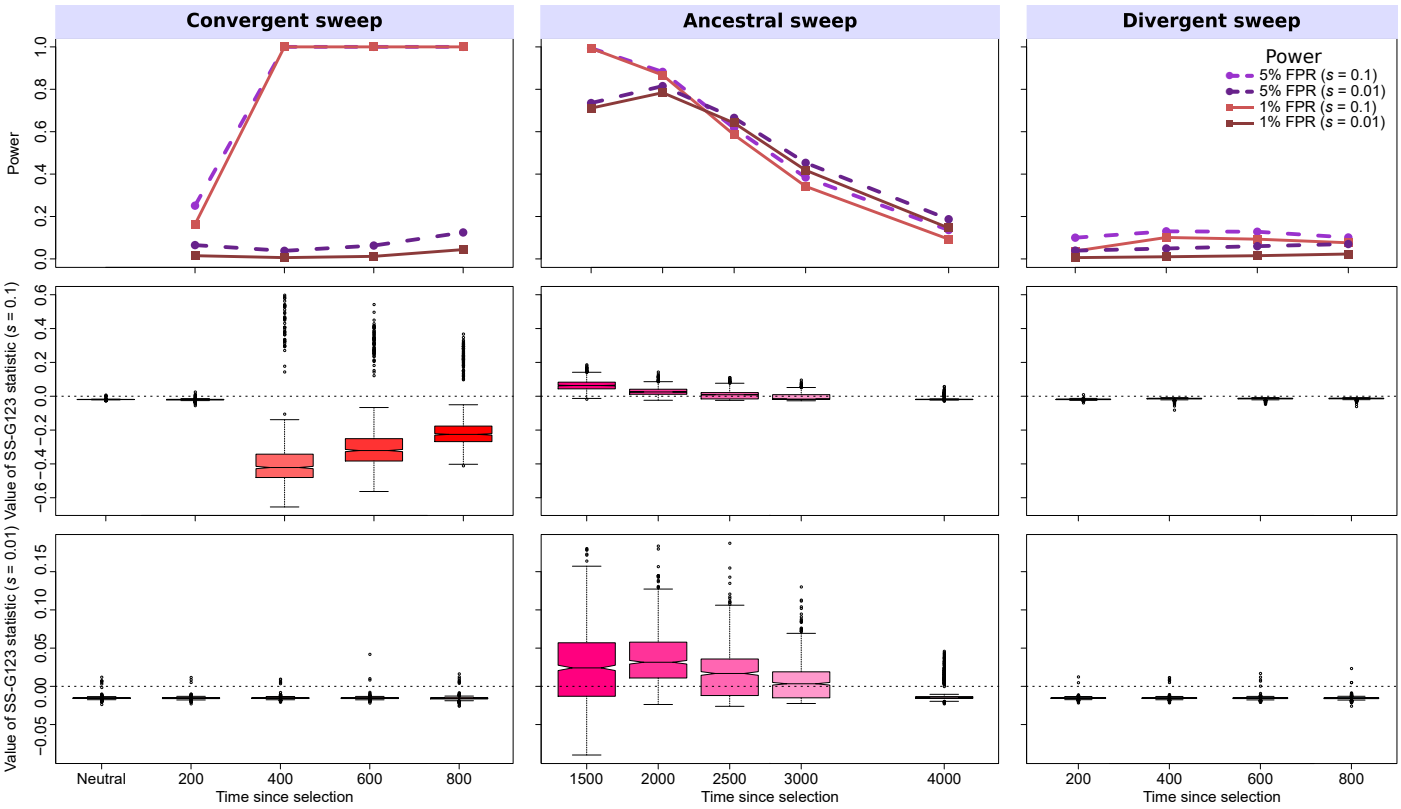

Figure S34 Properties of SS-G123 for simulated strong ($s = 0.1$; $\sigma = 4N_e s = 4000$) and moderate ($s = 0.01$; $\sigma = 400$) hard sweep scenarios under the CEU-GIH model ($\tau = 1100$ generations, or 0.055 coalescent units, before sampling). (Top row) Power at 1% (red lines) and 5% (purple lines) false positive rates (FPRs) to detect recent ancestral, convergent, and divergent hard sweeps (see Figure 1) as a function of time at which positive selection of the favored allele initiated (t), with FPR based on the distribution of maximum |SS-G123| across simulated neutral replicates. (Middle row) Box plots summarizing the distribution of SS-G123 values from windows of maximum |SS-G123| across strong sweep replicates, corresponding to each time point in the power curves, with dashed lines in each panel representing SS-G123 $= 0$. (Bottom row) Box plots summarizing the distribution of SS-G123 values across moderate sweep replicates. For convergent and divergent sweeps, $t < \tau$, while for ancestral sweeps, $t > \tau$. Simulated replicates are identical to those in Figure 2, but with each individual's two haplotypes merged into their multilocus genotypes.

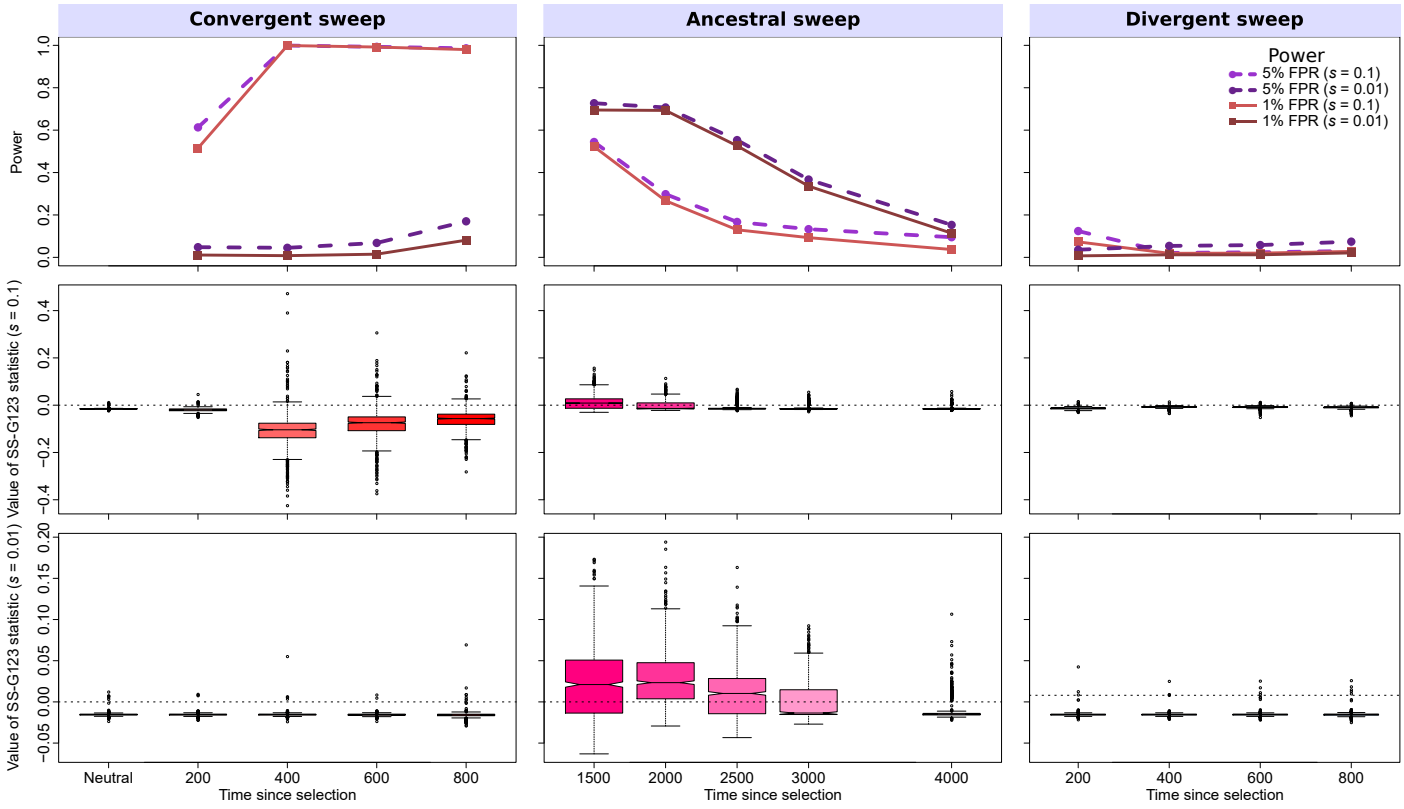

Figure S35 Properties of SS-G123 for simulated strong ($s = 0.1$; $\sigma = 4N_e s = 4000$) and moderate ($s = 0.01$; $\sigma = 400$) soft sweep ($\nu = 4$) scenarios under the CEU-GIH model ($\tau = 1100$ generations, or 0.055 coalescent units, before sampling). (Top row) Power at 1% (red lines) and 5% (purple lines) false positive rates (FPRs) to detect recent ancestral, convergent, and divergent soft sweeps from selection on standing genetic variation as a function of time at which selection of the favored haplotypes initiated (t), with FPR based on the distribution of maximum |SS-G123| across simulated neutral replicates. (Middle row) Box plots summarizing the distribution of SS-G123 values from windows of maximum |SS-G123| across strong sweep replicates, corresponding to each time point in the power curves, with dashed lines in each panel representing SS-G123 $= 0$. (Bottom row) Box plots summarizing the distribution of SS-G123 values across moderate sweep replicates. For convergent and divergent sweeps, $t < \tau$, while for ancestral sweeps, $t > \tau$. Simulated replicates are identical to those in Figure S5, but with each individual's two haplotypes merged into their multilocus genotypes.

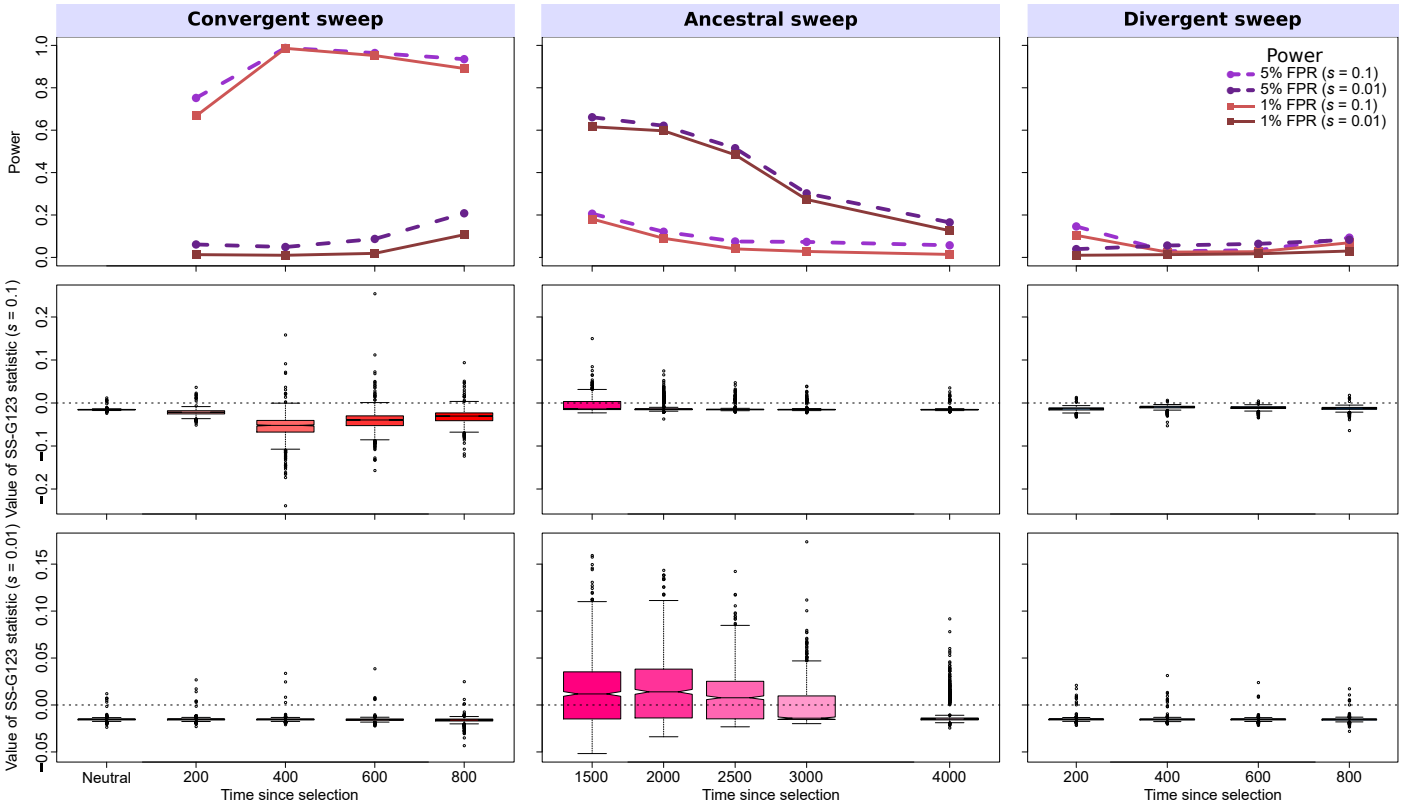

Figure S36 Properties of SS-G123 for simulated strong ($s = 0.1$; $\sigma = 4N_e s = 4000$) and moderate ($s = 0.01$; $\sigma = 400$) soft sweep ($\nu = 8$) scenarios under the CEU-GIH model ($\tau = 1100$ generations, or 0.055 coalescent units, before sampling). (Top row) Power at 1% (red lines) and 5% (purple lines) false positive rates (FPRs) to detect recent ancestral, convergent, and divergent soft sweeps from selection on standing genetic variation as a function of time at which selection of the favored haplotypes initiated (t), with FPR based on the distribution of maximum |SS-G123| across simulated neutral replicates. (Middle row) Box plots summarizing the distribution of SS-G123 values from windows of maximum |SS-G123| across strong sweep replicates, corresponding to each time point in the power curves, with dashed lines in each panel representing SS-G123 $= 0$. (Bottom row) Box plots summarizing the distribution of SS-G123 values across moderate sweep replicates. For convergent and divergent sweeps, $t < \tau$, while for ancestral sweeps, $t > \tau$. Simulated replicates are identical to those in Figure S6, but with each individual's two haplotypes merged into their multilocus genotypes.

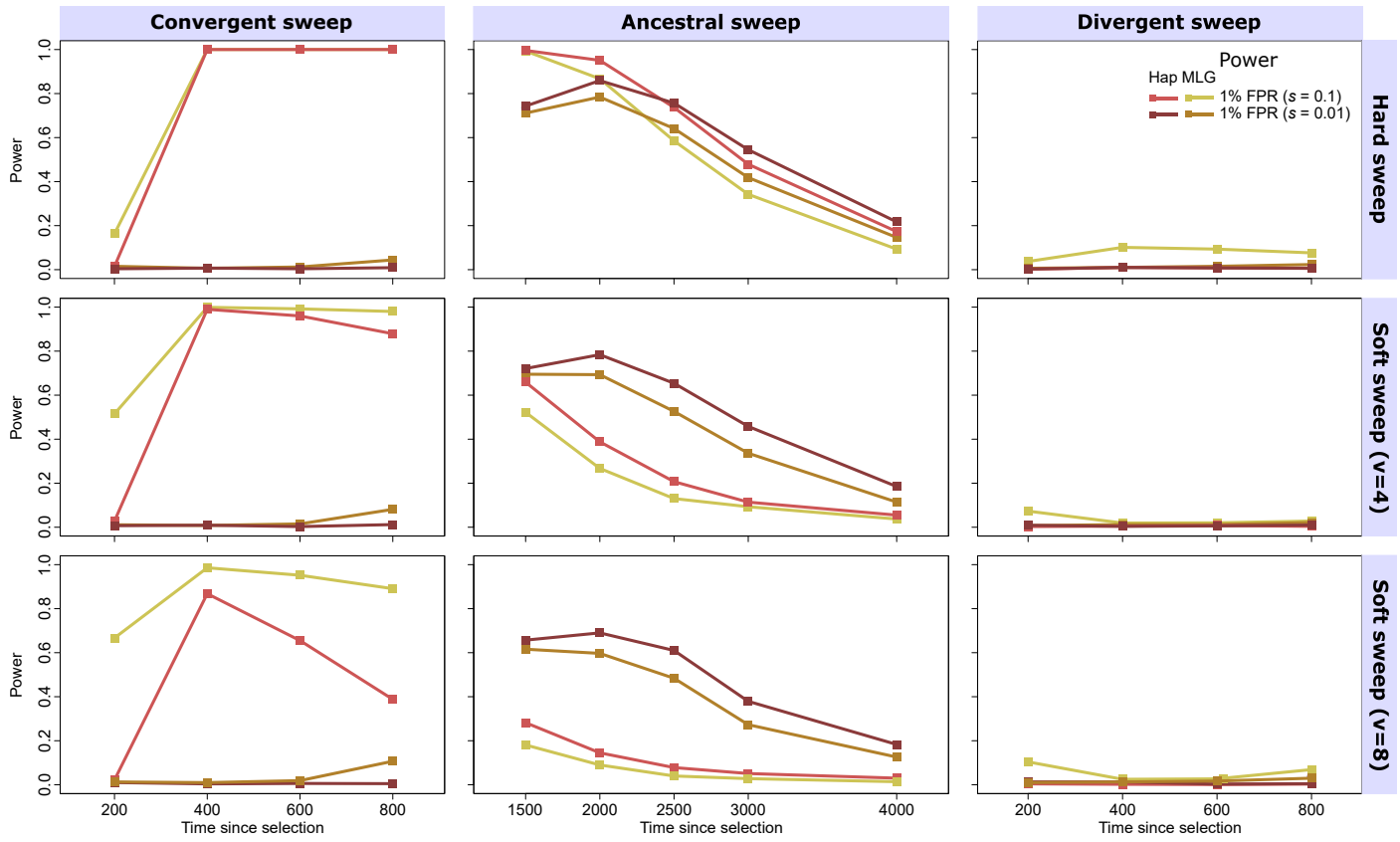

Figure S37 Direct comparison of power at a 1% false positive rate (FPR) for SS-H12 and SS-G123 for simulated sweeps on the CEU-GIH demographic history. Power curves for hard (top), soft ($\nu = 4$ [middle] and $\nu = 8$ [bottom]) sweeps are identical to those in Figures 2, S5, and S6 (SS-H12) and S34, S35, and S36 (SS-G123).

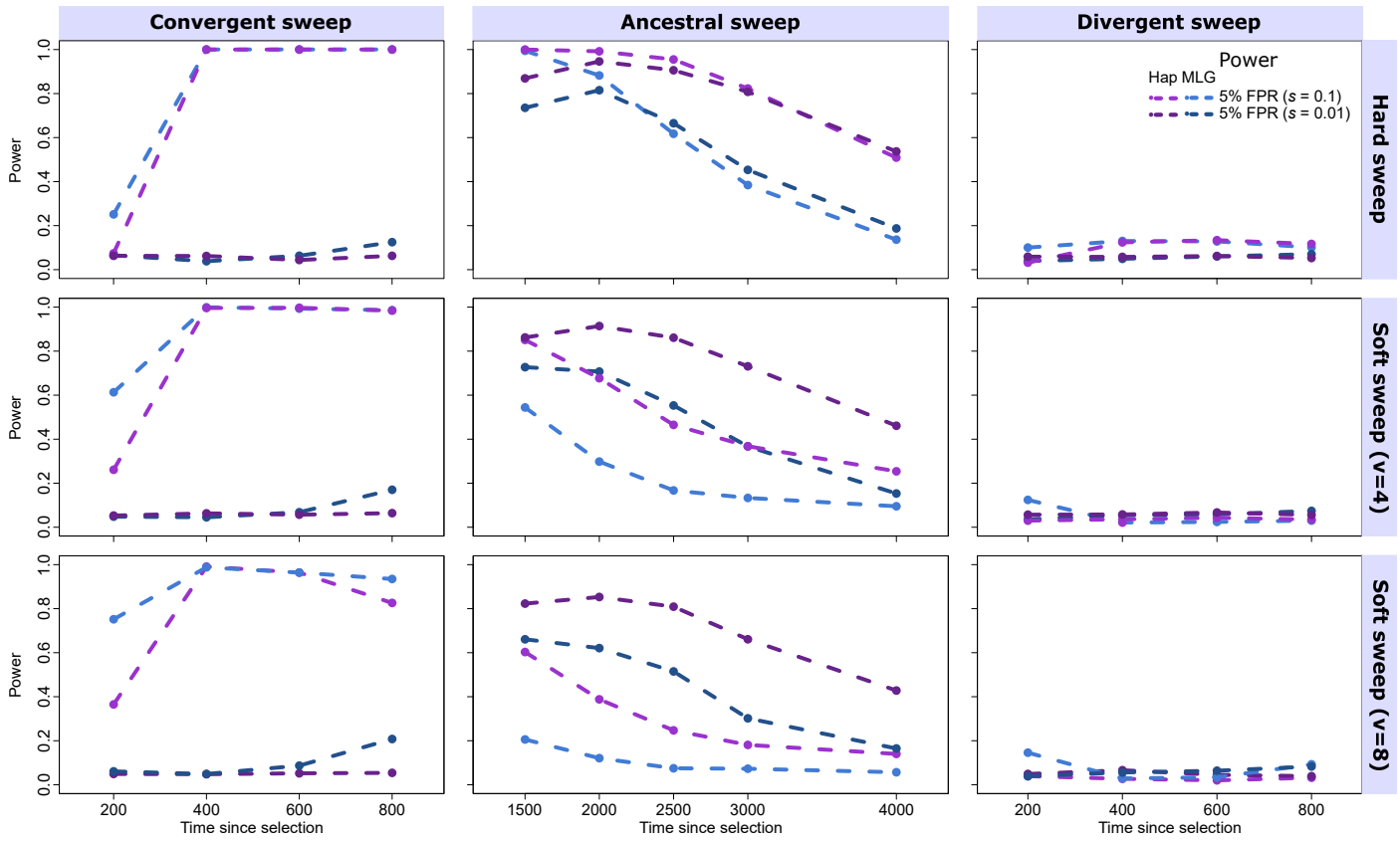

Figure S38 Direct comparison of power at a 5% false positive rate (FPR) for SS-H12 and SS-G123 for simulated sweeps on the CEU-GIH demographic history. Power curves for hard (top), soft ($\nu = 4$ [middle] and $\nu = 8$ [bottom]) sweeps are identical to those in Figures 2, S5, and S6 (SS-H12) and S34, S35, and S36 (SS-G123).

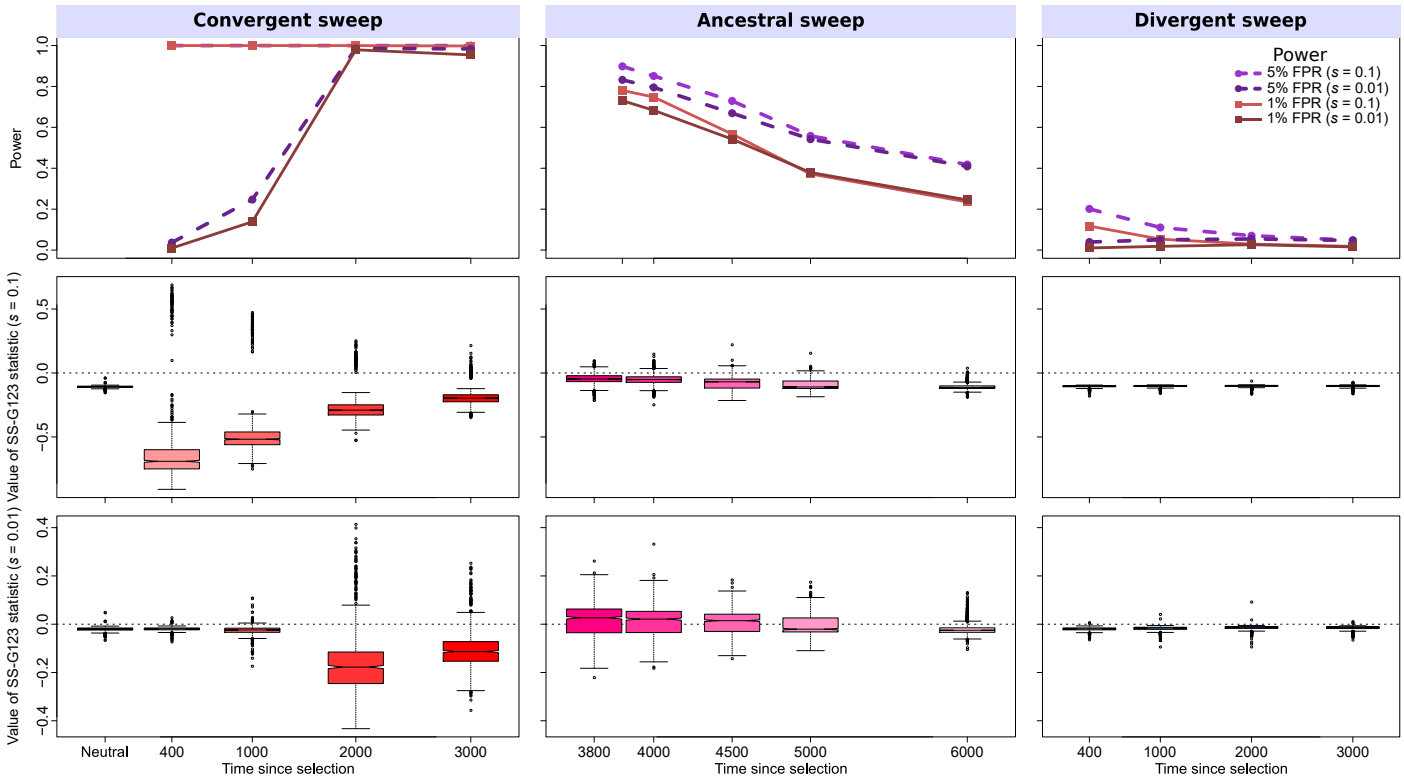

Figure S39 Properties of SS-G123 for simulated strong ($s = 0.1$; $\sigma = 4N_e s = 8000$) and moderate ($s = 0.01$; $\sigma = 800$) hard sweep scenarios under the CEU-YRI model ($\tau = 3740$ generations, or 0.0935 coalescent units, before sampling). (Top row) Power at 1% (red lines) and 5% (purple lines) false positive rates (FPRs) to detect recent ancestral, convergent, and divergent hard sweeps (see Figure 1) as a function of time at which positive selection of the favored allele initiated (t), with FPR based on the distribution of maximum |SS-G123| across simulated neutral replicates. (Middle row) Box plots summarizing the distribution of SS-G123 values from windows of maximum |SS-G123| across strong sweep replicates, corresponding to each time point in the power curves, with dashed lines in each panel representing SS-G123 $= 0$. (Bottom row) Box plots summarizing the distribution of SS-G123 values across moderate sweep replicates. For convergent and divergent sweeps, $t < \tau$, while for ancestral sweeps, $t > \tau$. Simulated replicates are identical to those in Figure 3, but with each individual's two haplotypes merged into their multilocus genotypes.

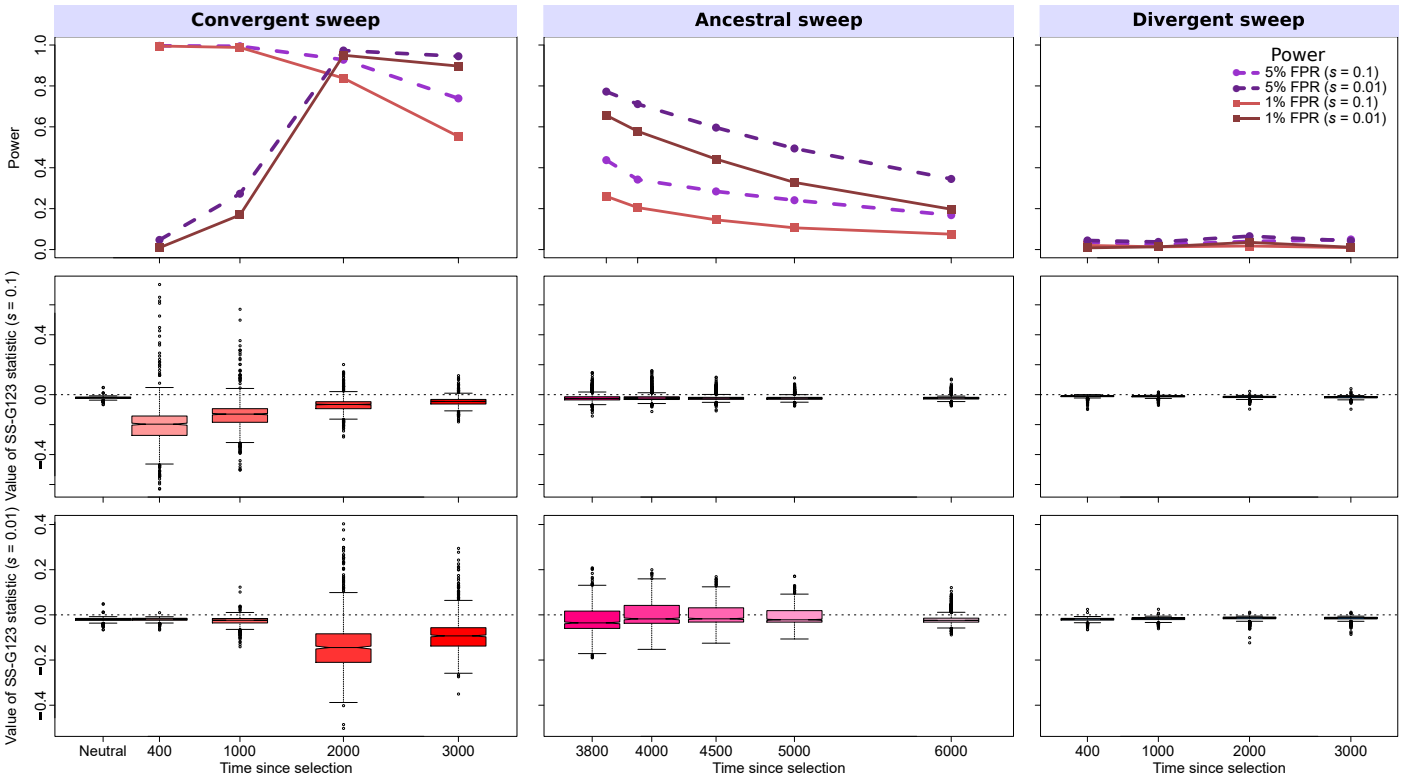

Figure S40 Properties of SS-G123 for simulated strong ($s = 0.1; \sigma = 4N_e s = 8000$) and moderate ($s = 0.01; \sigma = 800$) soft sweep ($\nu = 4$) scenarios under the CEU-YRI model ($\tau = 3740$ generations, or 0.0935 coalescent units, before sampling). (Top row) Power at 1% (red lines) and 5% (purple lines) false positive rates (FPRs) to detect recent ancestral, convergent, and divergent soft sweeps from selection on standing genetic variation as a function of time at which selection of the favored haplotypes initiated (t), with FPR based on the distribution of maximum |SS-G123| across simulated neutral replicates. (Middle row) Box plots summarizing the distribution of SS-G123 values from windows of maximum |SS-G123| across strong sweep replicates, corresponding to each time point in the power curves, with dashed lines in each panel representing SS-G123 $= 0$. (Bottom row) Box plots summarizing the distribution of SS-G123 values across moderate sweep replicates. For convergent and divergent sweeps, $t < \tau$, while for ancestral sweeps, $t > \tau$. Simulated replicates are identical to those in Figure S7, but with each individual's two haplotypes merged into their multilocus genotypes.

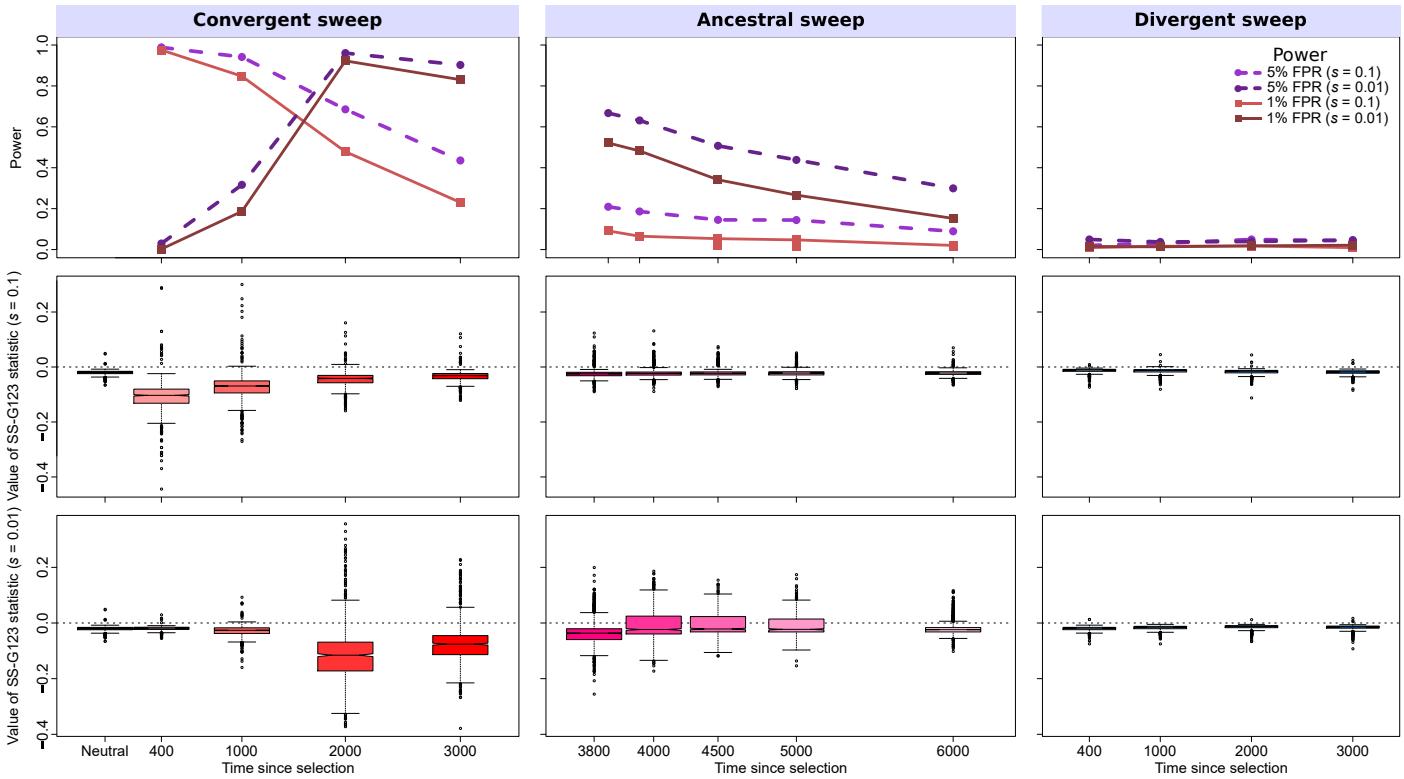

Figure S41 Properties of SS-G123 for simulated strong ($s = 0.1$; $\sigma = 4N_e s = 8000$) and moderate ($s = 0.01$; $\sigma = 800$) soft sweep ($\nu = 8$) scenarios under the CEU-YRI model ($\tau = 3740$ generations, or 0.0935 coalescent units, before sampling). (Top row) Power at 1% (red lines) and 5% (purple lines) false positive rates (FPRs) to detect recent ancestral, convergent, and divergent soft sweeps from selection on standing genetic variation as a function of time at which selection of the favored haplotypes initiated (t), with FPR based on the distribution of maximum |SS-G123| across simulated neutral replicates. (Middle row) Box plots summarizing the distribution of SS-G123 values from windows of maximum |SS-G123| across strong sweep replicates, corresponding to each time point in the power curves, with dashed lines in each panel representing SS-G123 $= 0$. (Bottom row) Box plots summarizing the distribution of SS-G123 values across moderate sweep replicates. For convergent and divergent sweeps, $t < \tau$, while for ancestral sweeps, $t > \tau$. Simulated replicates are identical to those in Figure S8, but with each individual's two haplotypes merged into their multilocus genotypes.

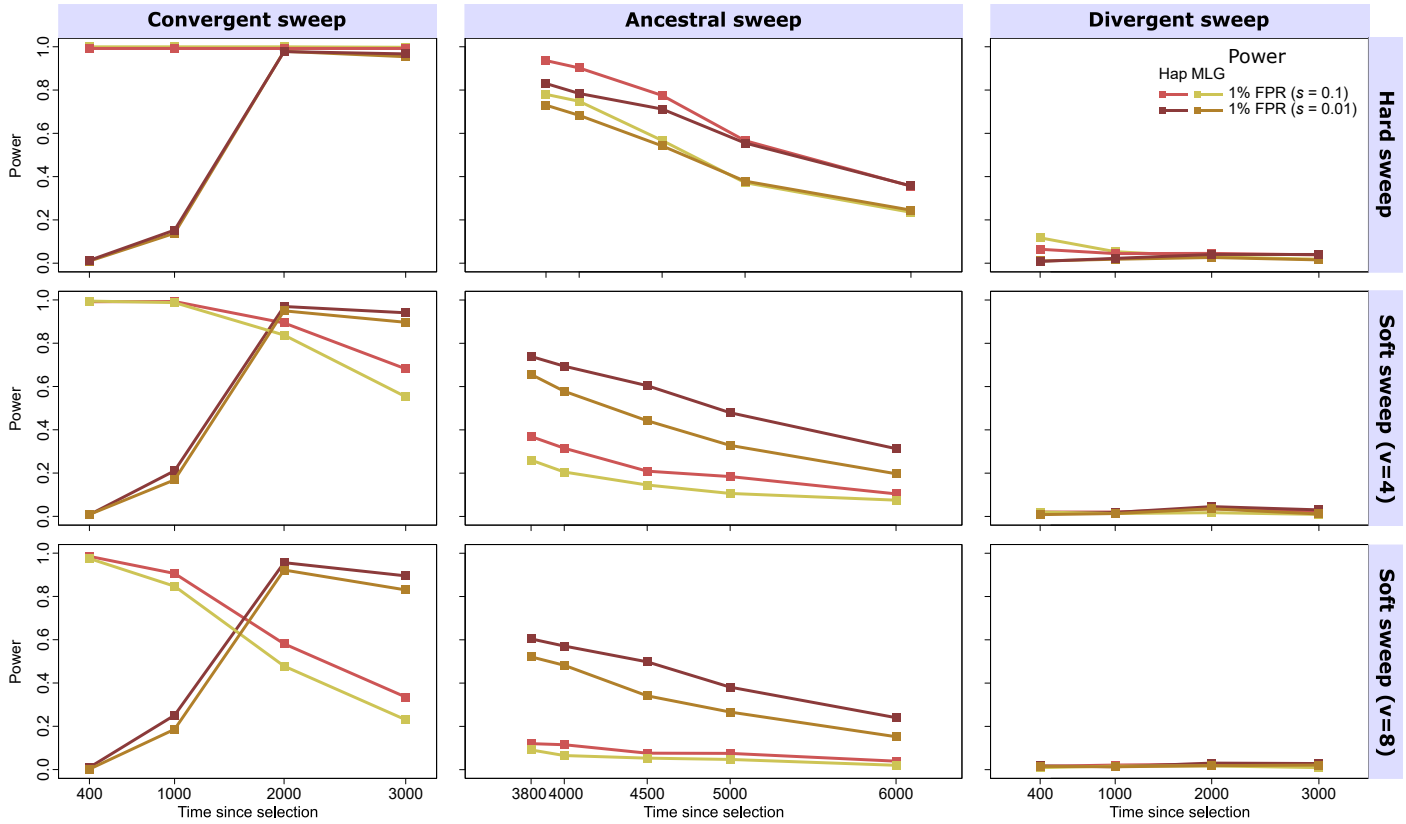

Figure S42 Direct comparison of power at a 1% false positive rate (FPR) for SS-H12 and SS-G123 for simulated sweeps on the CEU-YRI demographic history. Power curves for hard (top), soft ($\nu = 4$ [middle] and $\nu = 8$ [bottom]) sweeps are identical to those in Figures 3, S7, and S8 (SS-H12) and S39, S40, and S41 (SS-G123).

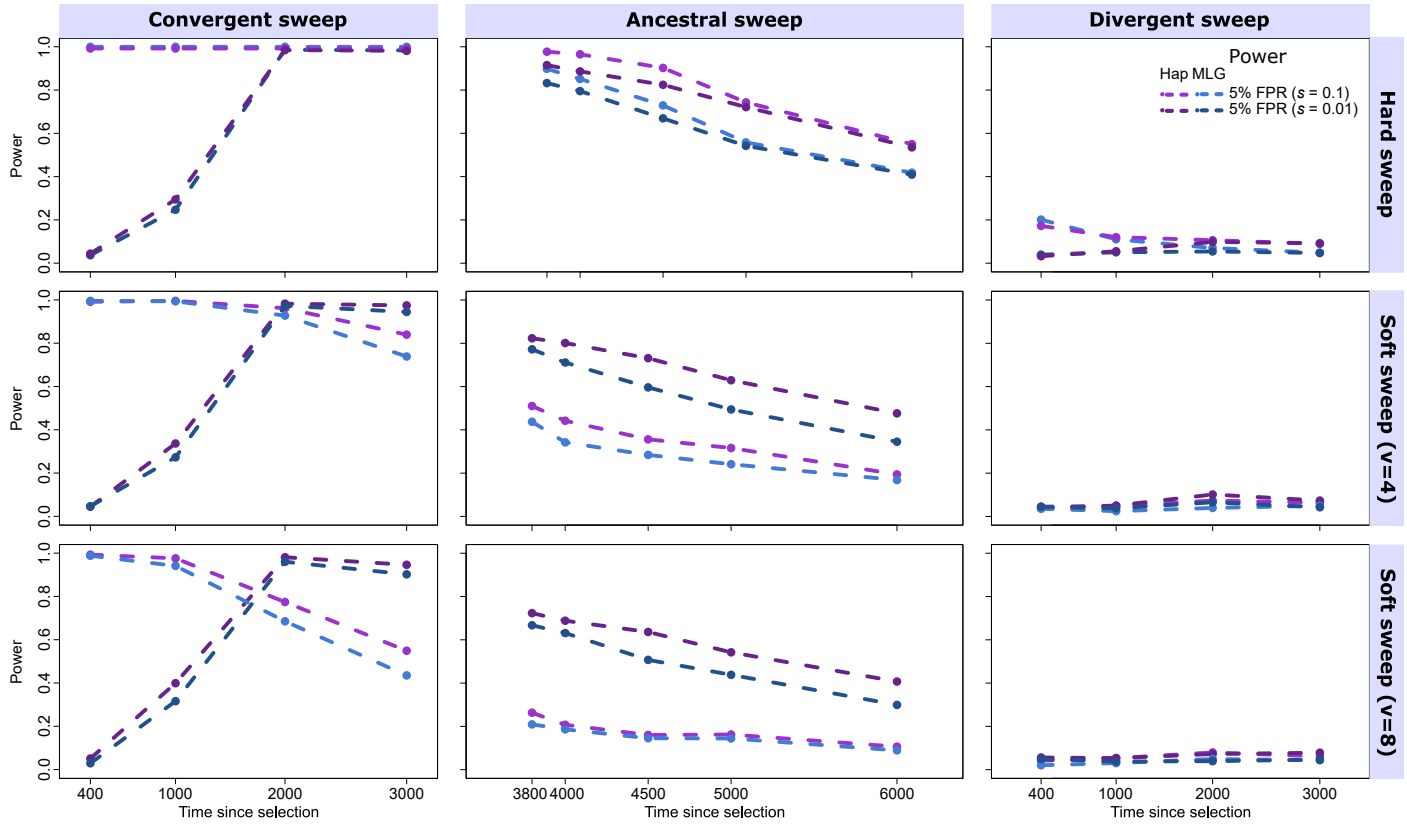

Figure S43 Direct comparison of power at a 5% false positive rate (FPR) for SS-H12 and SS-G123 for simulated sweeps on the CEU-YRI demographic history. Power curves for hard (top), soft ($\nu = 4$ [middle] and $\nu = 8$ [bottom]) sweeps are identical to those in Figures 3, S7, and S8 (SS-H12) and S39, S40, and S41 (SS-G123).

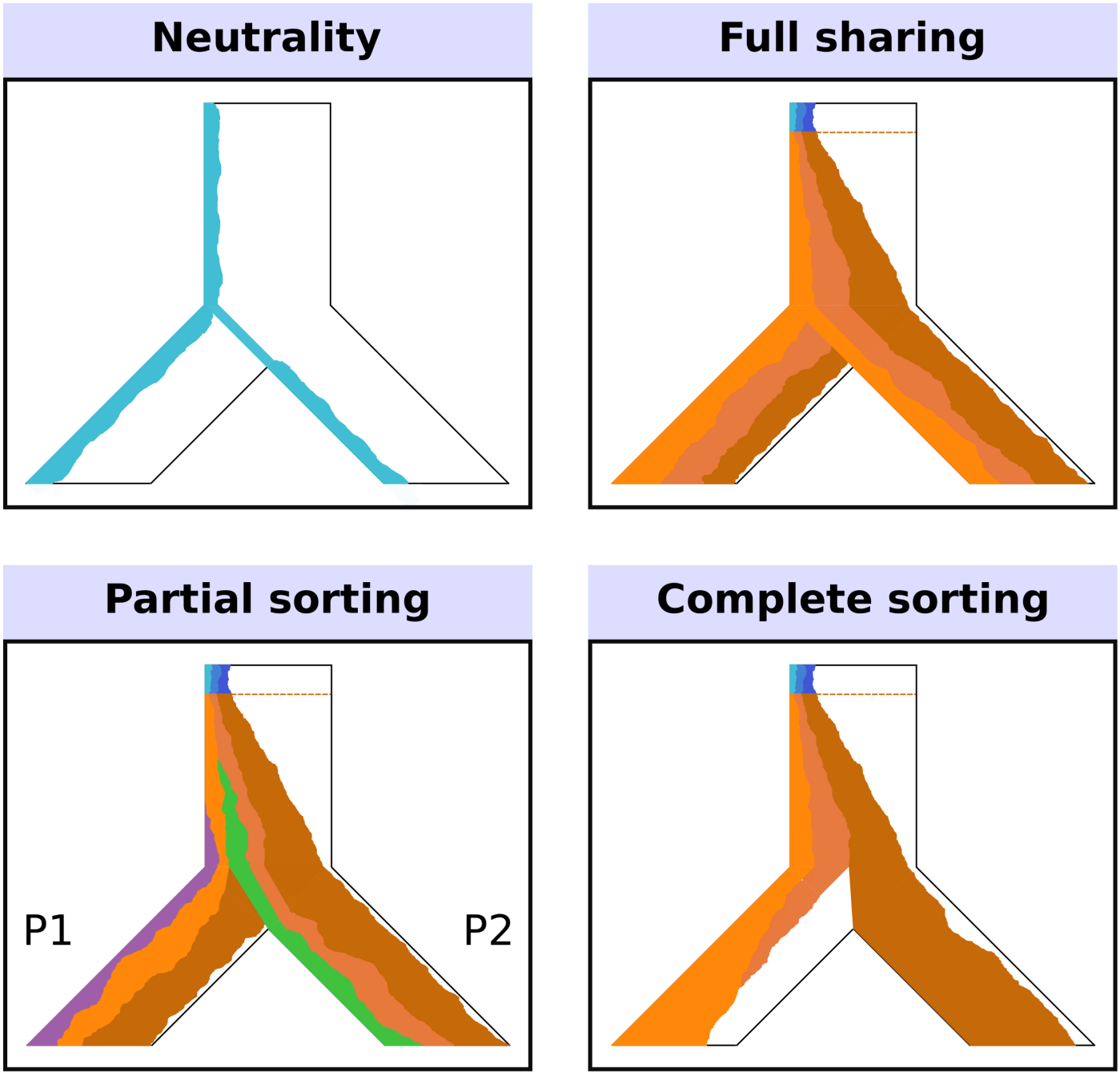

Figure S44 Model of a two-population phylogeny for which SS-H12 detects recent shared sweeps. Here, an ancestral population splits in the past into two modern populations, which are sampled. Each panel displays the frequency trajectory of haplotypes across the populations under neutrality (top-left, identical to Figure 1), or during an ancestral soft sweep (all others). Most ancestral soft sweeps feature full sharing of sweeping haplotypes (shades of orange) between sampled populations if they have established in the ancestral population (top-right). We may observe a partial sorting of the soft sweep if the descendant populations unevenly receive sweeping haplotypes (orange, purple, green) during the divergence process (bottom-left, P1 and P2 defined as in the *Discussion*). Complete sorting of an ancestral soft sweep should be rare, but results in modern populations sharing no sweeping haplotypes (bottom-right).

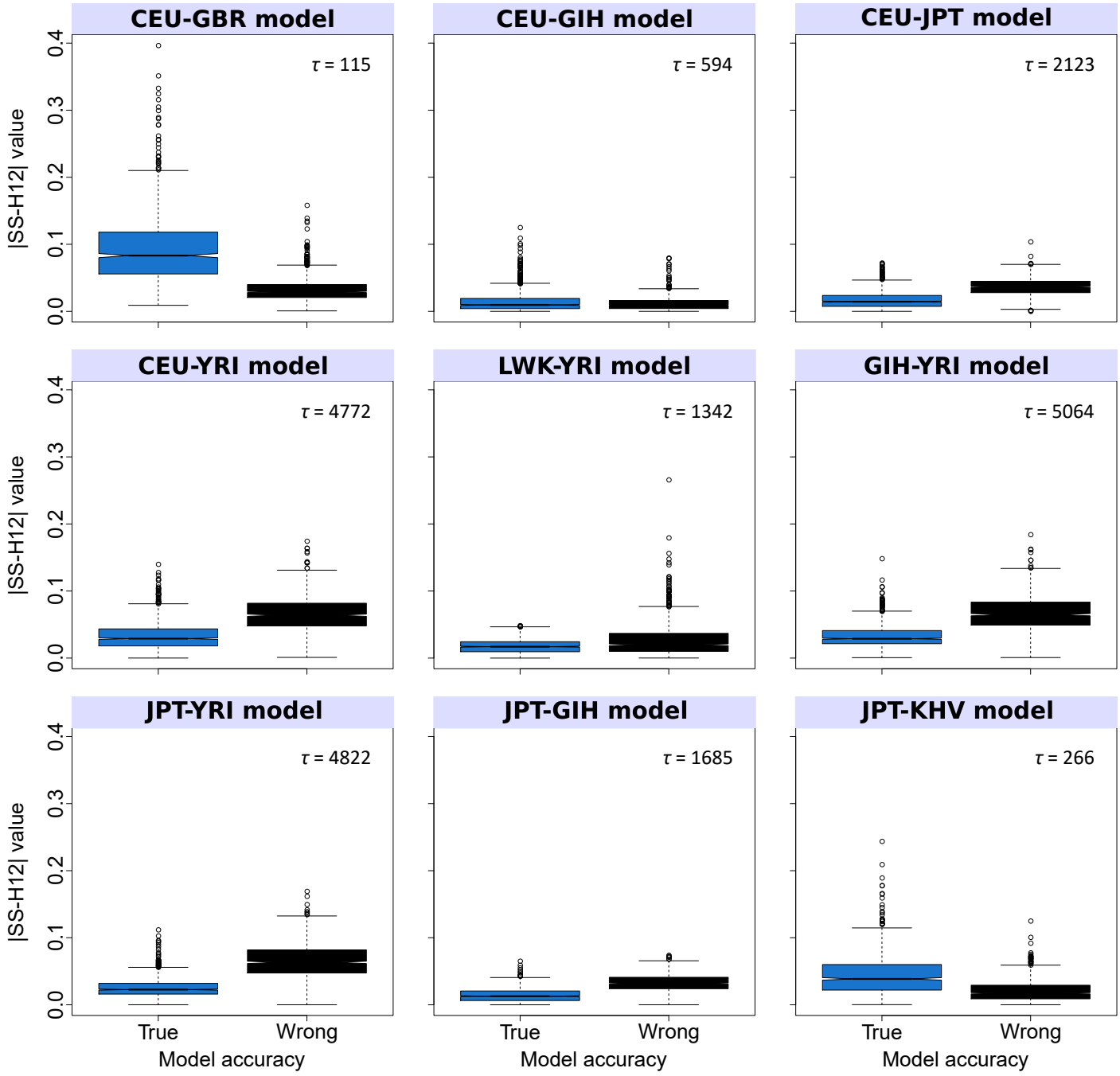

Figure S45 Box plots illustrating the effect on |SS-H12| of using a misspecified ("Wrong") simulated demographic model for each empirical comparison we performed. The misspecified model had equivalent mean F_{ST} to the `smc++`-derived ("True") model, but assumed a constant-size history of $N = 10^4$ diploids per population and τ as specified in each panel.

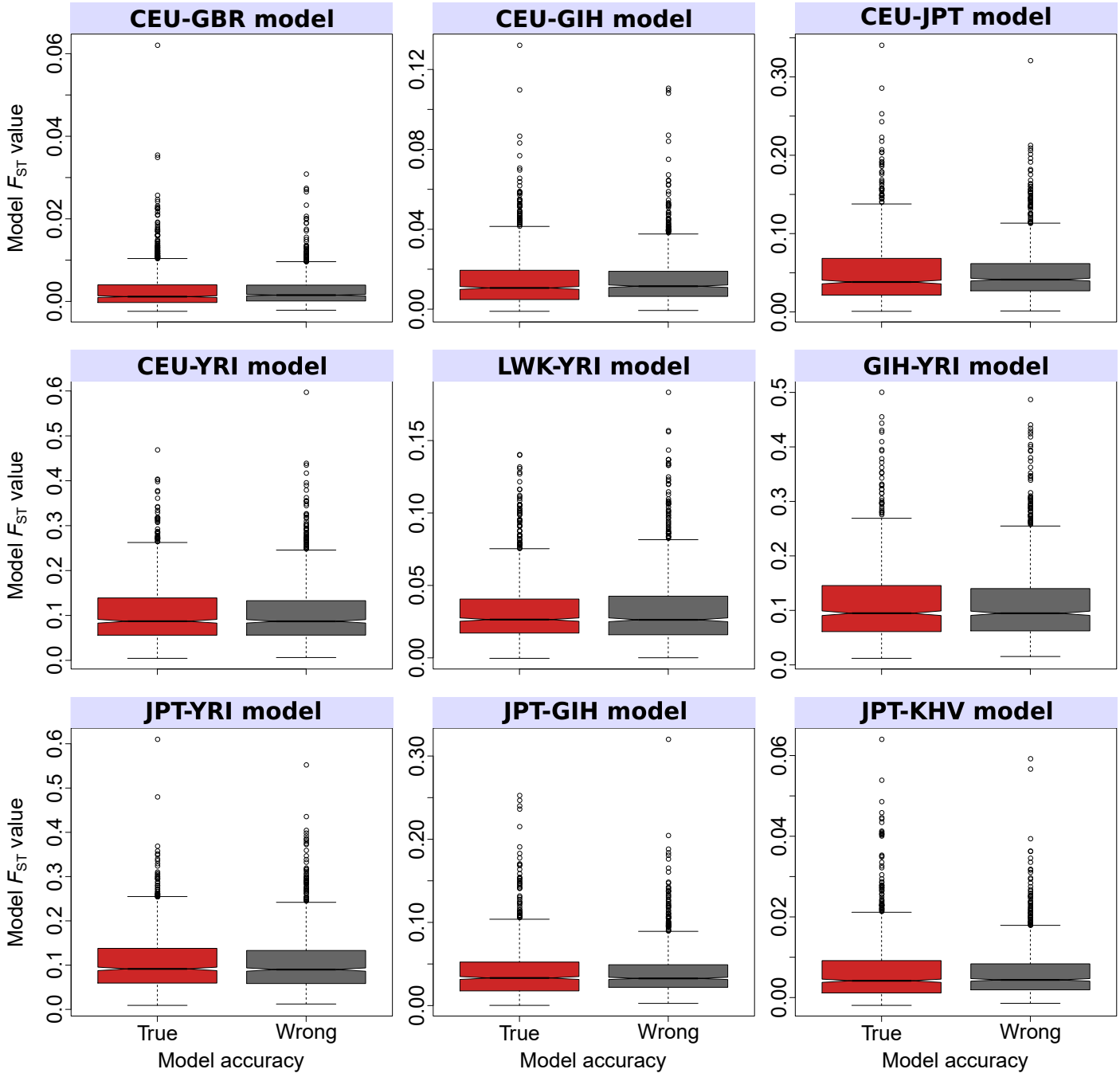

Figure S46 Box plots confirming comparable F_{ST} values between simulated misspecified ("Wrong") and `smc++`-derived ("True") demographic models for each empirical comparison we performed. See Figure S45 for effect of misspecification on |SS-H12| values.